

WANNIER90 v3.1.0: Solution booklet

Valerio Vitale

Contents

Preliminaries	3
About this booklet	3
Contact us	4
1 Gallium Arsenide — MLWFs for the valence bands	5
2 Lead — Wannier-interpolated Fermi surface	8
3 Silicon — Disentangled MLWFs	10
4 Copper — Fermi surface, orbital character of energy bands	13
5 Diamond — MLWFs for the valence bands	17
6 Copper — Fermi surface	19
7 Silane (SiH ₄) — Molecular MLWFs using Γ -point sampling	22
8 Iron — Spin-polarized WFs, DOS, projected WFs versus MLWFs	24
9 Cubic BaTiO ₃	31
10 Graphite	34
11 Silicon — valence and low lying conduction states	35
12 Benzene — valence and low lying conduction states	40
13 (5,5) Carbon Nanotube — Transport properties	44

14 Linear Sodium Chain — Transport properties	47
15 (5,0) Carbon Nanotube — Transport properties	49
16 Silicon — Boltzmann transport	50
17 Iron — Spin-orbit-coupled bands and Fermi-surface contours	55
18 Iron—Berry curvature, anomalous Hall conductivity and optical conductivity	58
19 Iron—Orbital magnetization	65
20 Disentanglement restricted inside spherical regions of k -space LaVO_3 .	68
21 Gallium Arsenide—Symmetry-adapted Wannier functions	72
22 Copper—Symmetry-adapted Wannier functions	79
23 Platinum—Spin Hall conductivity	83
24 Gallium Arsenide—Frequency-dependent spin Hall conductivity	87

Preliminaries

Welcome to WANNIER90! This is the solution booklet for the examples in the WANNIER90 v3.1.0 tutorial <http://www.wannier.org/doc/tutorial.pdf>. Info on the installation process and the theory of Maximally Localized Wannier Functions (MLWFs) is not reported here as they can be found elsewhere¹. The solutions in this booklet are for the v3.1.0 only! The following (open-source) programs are required to reproduce the plots and figures in this booklet:

- **gnuplot** is used to plot bandstructures. It is available for many operating systems and is often installed by default on Unix/Linux distributions. In particular, we used gnuplot 4.6 patchlevel 6. <http://www.gnuplot.info>
- **Grace** is another plotting tool to visualise bandstructures. <http://plasma-gate.weizmann.ac.il/Grace/>
- **Vesta** is the default 3D visualisation program[1] adopted in this booklet. It is used to visualise crystal structures, volumetric data (such as WFs and densities). Download is available for several OS here: <http://jp-minerals.org/vesta/en/>.
- **XCrySDen** is also used to visualise crystal structures and Fermi surfaces in particular. It is available for Unix/Linux, Windows (using cygwin), and OSX. To correctly display files from wannier90, version 1.4 or later must be used. <http://www.xcrysden.org>
- **VMD** may also be used to visualise crystal structures and 3D-fields. It can also read a great variety of input formats and it comes with handy postprocessing tools. <http://www.ks.uiuc.edu/Research/vmd>

Disclaimer: All the band structure interpolations have been carried out with `ws_distance = .false.`, which is the default value for the version 2.1. However, in the new WANNIER90 release, corresponding to version 3.0, the default value of `ws_distance` has been changed to `.true.`, as, to the best of our knowledge, the Wigner-Seitz interpolation scheme never lowers the quality of the interpolation and it is often superior to the default scheme.

About this booklet

This solution manual consists of 24 sections, each containing the solutions, in the form of plots, tabs, and texts, to the corresponding example in the WANNIER90 v3.1.0 tutorial! For each example, only the outline and key questions from the tutorial are reported here. All of the WANNIER90 input files have been provided. From example 5 onwards, input files for the pwscf interface (<http://www.quantum-espresso.org>) to WANNIER90 have also been provided. You will need a recent working version of the QUANTUM ESPRESSO package (v6.2 and above), to run these examples. In particular, you will need `pw.x` and `pw2wannier90.x`, as explained in the WANNIER90 v3.1.0 tutorial. Please visit <http://www.quantum-espresso.org> to download the package and follow the instruction on the website for installation. Further details on how to run the calculations for each example may be found in the corresponding section of the WANNIER90 v3.1.0 tutorial. There are interfaces to a number of other electronic structure codes including: ABINIT (<http://www.abinit.org>), FLEUR (<http://www.flapw.org>).

¹To install WANNIER90 you can follow the instructions in the README file of the WANNIER90 distribution. For an introduction to the theory, you can look at the WANNIER90 User guide http://www.wannier.org/user_guide.html, the WANNIER90 Tutorial and references therein.

de), OPENMX (<http://www.openmx-square.org/>), GPAW (<https://wiki.fysik.dtu.dk/gpaw/>), VASP (<http://www.vasp.at>), and WIEN2K (<http://www.wien2k.at>).

All the tests were performed on an x86_64 octa-core Intel(R) Xeon(R) CPU E5620 @2.40GHz. Two packages `intel-suite/2015.3.187` and `mk1/2015.3.187` were used for the compilation of WANNIER90. We expect some of the numerical results to depend on the architecture, the compiler distribution, e.g. `gcc` vs `gfortran`, the version of the compiler and the libraries. However, general trends should not be affected by these parameters and, in principle, it should be safe to ignore the differences between different set-ups. If you find that your results are significantly different from the one given in this booklet, please report it to the WANNIER90 developers team by opening an issue on the GitHub repository <https://github.com/wannier-developers/wannier90> or by writing an email to the forum at wannier@quantum-espresso.org (we strongly recommend the first option). Moreover, if you know how to solve the issue and you have a fix for it, you can open a pull-request on the GitHub repo.

Contact us

If you have any suggestions on how this solution manual may be improved and for any other issue, open an issue on the official repository of the WANNIER90 code on GitHub <https://github.com/wannier-developers/wannier90> or send an email on the forum at wannier@quantum-espresso.org (we strongly recommend the former). For the forum note that you will need to be registered. Emails from non-registered users will be deleted automatically. You can register by following the links at <http://www.wannier.org/forum.html>.

1: Gallium Arsenide — MLWFs for the valence bands

- Outline: *Obtain and plot MLWFs for the four valence bands of GaAs.*

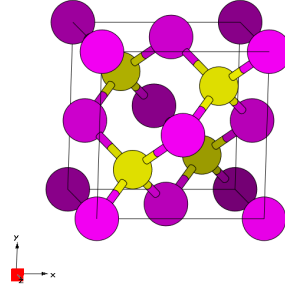


Figure 1: Unit cell of GaAs crystal plotted with the XCRYSDEN program.

1. *Inspect the output file `gaas.wout`.*

Tab. 1 shows the converged values (after 20 iterations) for a $2 \times 2 \times 2$ \mathbf{k} -point mesh of the total spread functional Ω and its three components, i.e. the gauge-invariant component Ω_I , the off-diagonal component of the gauge-dependent part Ω_{OD} , and the diagonal component of the gauge-dependent part Ω_D , respectively. These can be found at the end of the `gaas.wout` file, from the line starting with `Final State`. You will find the MLWF centres and their spreads together with the information on the spread functional components as reported below, and summarized in tab.1.

Final State				
WF centre and spread	1	(-0.866253, 1.973841, 1.973841)		1.11672024
WF centre and spread	2	(-0.866253, 0.866253, 0.866253)		1.11672024
WF centre and spread	3	(-1.973841, 1.973841, 0.866253)		1.11672024
WF centre and spread	4	(-1.973841, 0.866253, 1.973841)		1.11672024
Sum of centres and spreads		(-5.680188, 5.680188, 5.680188)		4.46688098
Spreads (Ang ²)			Omega I =	3.956862958
=====			Omega D =	0.008030049
			Omega OD =	0.501987969
Final Spread (Ang ²)			Omega Total =	4.466880976

The geometric centre lies along the Ga-As bond, slightly closer to As than Ga. To see this, we introduce a measure β defined as

$$\beta \triangleq \frac{d_{\text{Ga-MLWF}}}{d_{\text{Ga-As}}},$$

where $d_{\text{Ga-MLWF}}$ is the distance of the Ga atom placed in the origin and the MLWF centre (along the Ga-As bond), and $d_{\text{Ga-As}}$ is the Ga-As bond length, cf. Ref. [2]. A value of 0.5 corresponds to the MLWF centre being equidistant from the Ga atom and As atom. In our case, we find:

$$\beta = \frac{d_{\text{Ga-MLWF}(2)}}{d_{\text{Ga-As}}} = \frac{0.866253\sqrt{3}}{1.4200\sqrt{3}} \approx 0.61.$$

Maximum RAM allocated for the wannierisation was 0.06Mb.

Table 1: Converged values of the components of spread functional and their sum, given in \AA^2 . Here β is the distance of the Ga atom placed in the origin and the MLWF centre (along the Ga-As bond) as a fraction of the Ga-As bond length 2.4595\AA .

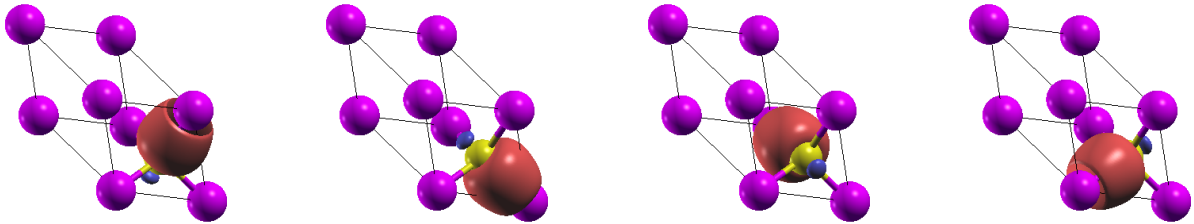
MP mesh	Ω	Ω_I	Ω_{OD}	Ω_D	β
$2 \times 2 \times 2$	4.467	3.957	0.502	0.008	0.610

2. Plot the MLWFs.

In Fig. 2 are shown the four valence MLWFs as plotted by XCRYSDEN, where we used the following parameters in the Tools \mapsto Data Grid section:

Xcrysden: Tools \mapsto Data Grid

Degree of triCubic Spline = 3; Isovolume = 0.95; Render +/- isovalue = yes



(a) 1st valence MLWF

(b) 2nd valence MLWF

(c) 3rd valence MLWF

(d) 4th valence MLWF

Figure 2: Four valence MLWFs for the Ga-As system plotted using the XCRYSDEN visualisation program.

Extra : Plot the 3rd MLWFs in a supercell of size 3. Choose a low value for the isosurface (say 0.5). Can you explain what you see?

With XCRYSDEN we can also plot the 3rd MLWF to check its periodicity. The period in each direction is given by the spacing used to sample the first irreducible Brillouin zone, i.e. the \mathbf{k} -point mesh. We used a $2 \times 2 \times 2$ \mathbf{k} -point mesh, hence we expect to find a periodic image of our MLWF in a supercell which is 2 times larger than the unit cell along each direction. This is shown in Fig. 3, where the 3rd has been plotted using both the XCRYSDEN program and the VESTA program.

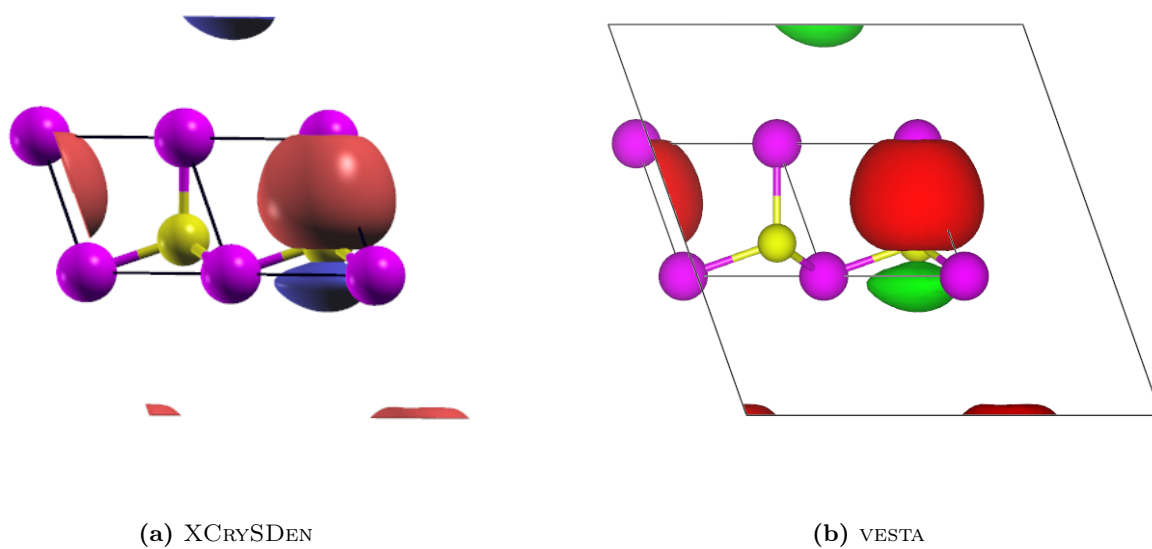


Figure 3: 3rd MLWF with a supercell value of 3 and for an isovalue of 0.5 using (a) XCrySDEN and (b) VESTA.

2: Lead — Wannier-interpolated Fermi surface

- Outline: Obtain MLWFs for the four lowest states in lead. Use Wannier interpolation to plot the Fermi surface.

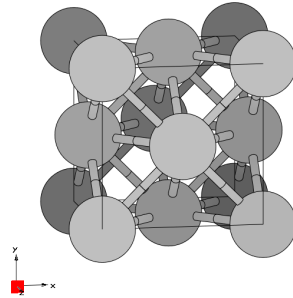


Figure 4: Unit cell of lead crystal plotted with the XCrySDen program.

1. Inspect the output file `lead.wout`.

A summary of the wannierisation is given in tab.2. At the end of the `.wout` file you should find the info on the final state of the minimization as

Final State			
WF centre and spread	1	(0.397070, 0.397070, 0.397070)	1.93781315
WF centre and spread	2	(0.397070, -0.397070, -0.397070)	1.93781315
WF centre and spread	3	(-0.397070, 0.397070, -0.397070)	1.93781315
WF centre and spread	4	(-0.397070, -0.397070, 0.397070)	1.93781315
Sum of centres and spreads		(0.000000, -0.000000, -0.000000)	7.75125261
Spreads (Ang ²)		Omega I =	6.039099038
=====		Omega D =	0.007065754
		Omega OD =	1.705087819
Final Spread (Ang ²)		Omega Total =	7.751252611

Table 2: Converged values of the components of spread functional and their sum, given in \AA^2 .

MP mesh	Ω	Ω_I	Ω_{OD}	Ω_D
$4 \times 4 \times 4$	7.751	6.039	0.007	1.705

2. Use Wannier interpolation to generate the Fermi surface of lead.

As can be seen from the bandstructure plot in the WANNIER90 tutorial, that we report here, cf. Fig. 5, the four lower valence bands are separated in energy from the higher conduction states (there is however an indirect band gap). The Fermi level lies somewhere in the middle of the manifold making crystalline lead a metal. As a result, the states belonging to these manifold will have partial occupancy. We can see that 2 bands are entirely below and above the Fermi level, respectively. Hence, no Fermi surface can be plotted from these bands. On the other hand,

the two central bands do cross the Fermi energy level and the corresponding Fermi surfaces are shown in Fig. 6.

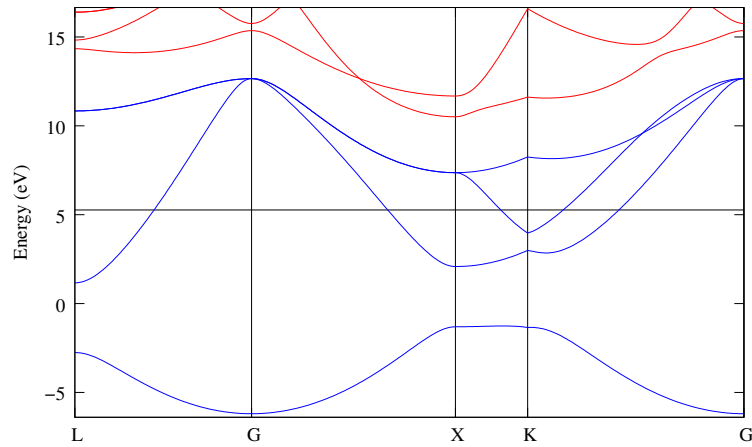
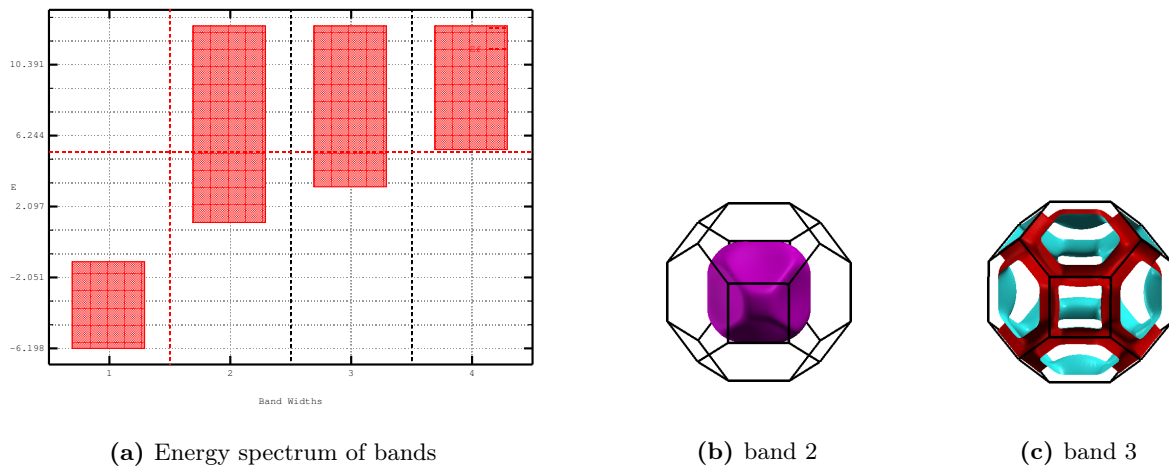


Figure 5: Bandstructure of lead showing the position of the Fermi level. Only the lowest four bands are included in the calculation.



(a) Energy spectrum of bands

(b) band 2

(c) band 3

Figure 6: Fermi surfaces for band 2 and band 3 in lead. The value of the Fermi energy is 5.2676eV, and it was obtained from the first principle calculation, with a $4 \times 4 \times 4$ \mathbf{k} -point mesh. To calculate the band energies and to plot Fermi surfaces, Wannier interpolation was employed on a dense mesh in the Brillouin zone consisting of 50^3 points.

3: Silicon — Disentangled MLWFs

- Outline: Obtain disentangled MLWFs for the valence and low-lying conduction states of Si. Plot the interpolated bandstructure.

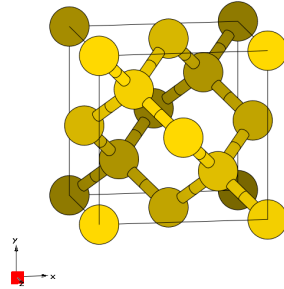


Figure 7: Unit cell of Silicon crystal plotted with the XCrySDen program.

1. Inspect the output file `silicon.wout`.

Starting from 4 sp^3 orbitals on each Silicon atom we obtain two sets of 4 WFs, all with the same spread, that show the sp^3 character one would expect from symmetry considerations. A summary of the wannierisation is given in tab.3. At the end of the `.wout` file you should find the info on the final state of the minimization, here we show an extract of the output file

Final State			
WF centre and spread	1	(-0.460754, -0.460711, -0.460767)	1.81241746
WF centre and spread	2	(-0.460743, 0.460722, 0.460718)	1.81246400
WF centre and spread	3	(0.460703, -0.460761, 0.460685)	1.81248774
WF centre and spread	4	(0.460704, 0.460724, -0.460764)	1.81244947
WF centre and spread	5	(1.810128, 1.810112, 1.810113)	1.81247628
WF centre and spread	6	(1.810097, 0.888662, 0.888617)	1.81242110
WF centre and spread	7	(0.888640, 1.810140, 0.888660)	1.81240614
WF centre and spread	8	(0.888643, 0.888652, 1.810090)	1.81245230
Sum of centres and spreads	(5.397417, 5.397539, 5.397353)	14.49957450
Spreads (Ang ²)	Omega I	=	11.849193709
=====	Omega D	=	0.105470243
	Omega OD	=	2.544910550
Final Spread (Ang ²)	Omega Total	=	14.499574503

2. Plot the energy bands.

Table 3: Converged values of the components of spread functional and their sum, given in \AA^2 .

MP mesh	Ω	Ω_I	Ω_{OD}	Ω_D
$4 \times 4 \times 4$	14.5	11.849	2.545	0.105

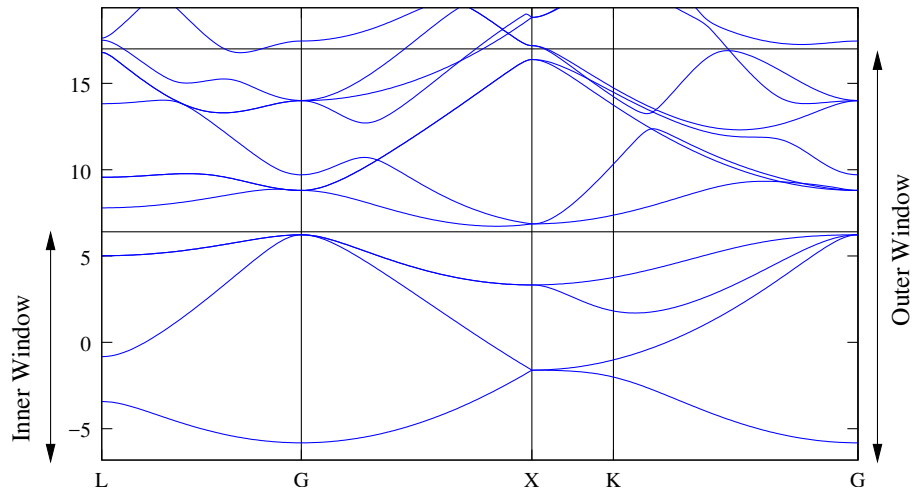


Figure 8: Bandstructure of Silicon showing the position of the Fermi level and of the inner and outer windows. Both the 4 valence bands and the 4 low-lying conduction bands are included in the calculation.

As can be seen from DFT bandstructure plot in the WANNIER90 tutorial, that we report here, cf. Fig. 8, the four lower valence bands are separated in energy from the higher conduction states (there is however an indirect band gap). The Fermi level lies inside the gap, making crystalline Silicon a semiconductor.

The path in \mathbf{k} -space given in the tutorial (L- Γ -X-K- Γ) and shown in Fig. 9-(a)-top is the following

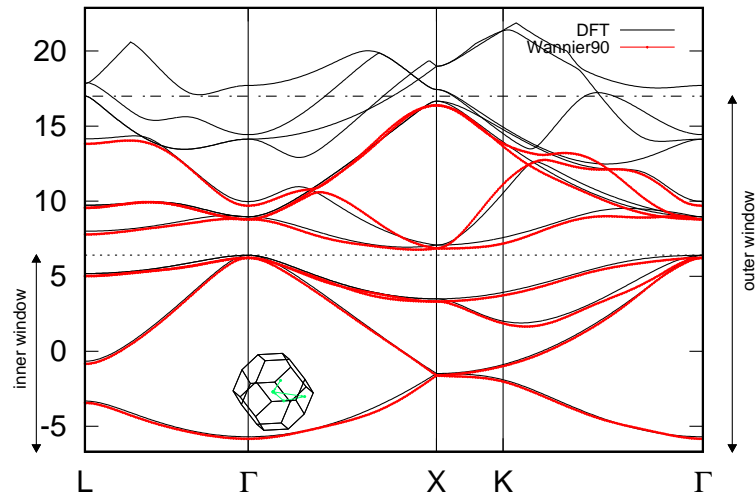
```
begin kpoint_path
L 0.50000 0.50000 0.50000 G 0.00000 0.00000 0.00000
G 0.00000 0.00000 0.00000 X 0.50000 0.00000 0.50000
X 0.50000 -0.50000 0.00000 K 0.37500 -0.37500 0.00000
K 0.37500 -0.37500 0.00000 G 0.00000 0.00000 0.00000
end kpoint_path
```

which gives the bandstructure shown in Fig. 9-(a)-bottom.

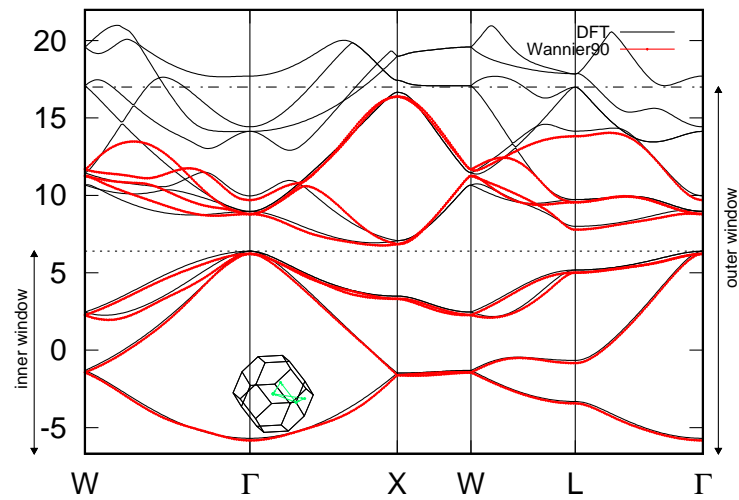
Extra : *Try plotting along different paths.*

Another path usually used for Silicon is W- Γ -X-W-L- Γ shown in Fig. 8-(b)-top and the corresponding bands are shown in Fig. 9-(b)-bottom. To obtain this path you need to replace the previous `kpoint_path` block with the following block

```
begin kpoint_path
W 0.25000 0.75000 0.50000 G 0.00000 0.00000 0.00000
G 0.00000 0.00000 0.00000 X 0.50000 0.50000 0.00000
X 0.50000 0.50000 0.00000 W -0.25000 0.25000 -0.25000
W -0.25000 0.25000 -0.25000 L 0.00000 0.50000 0.00000
L 0.00000 0.50000 0.00000 G 0.00000 0.00000 0.00000
end kpoint_path
```



(a)



(b)

Figure 9: Bandstructure of Silicon showing the position of the Fermi level and of both the inner and outer windows. The 4 valence bands together with the 4 low-lying conduction bands are included in the calculation. Panel a) Interpolation with Wannier90 on the L- Γ -X-K- Γ path in \mathbf{k} space (red dots) and DFT reference bandstructure (solid black). Panel b) Interpolation with Wannier90 on the W- Γ -X-W-L- Γ path in \mathbf{k} space (red dots) and DFT reference bandstructure (solid black).

4: Copper — Fermi surface, orbital character of energy bands

- Outline: Obtain MLWFs to describe the states around the Fermi-level in copper

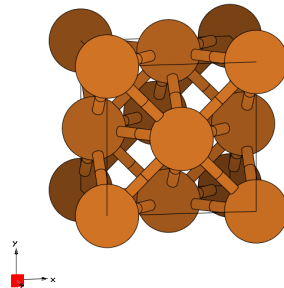


Figure 10: Unit cell of Copper crystal plotted with the XCRYSDEN program.

1. Run WANNIER90 to minimise the MLWFs spread. Inspect the output file `copper.wout`.

Starting from 5 d orbitals centred on the Copper atom and 2 s orbitals in the interstitial regions of the FCC, we obtain the following spreads and centres after 200 iterations (extract from the `copper.wout`, a summary of the wannierisation is given in tab.4.):

Final State			
WF centre and spread	1	(-0.000000, 0.000000, -0.000000)	0.40838932
WF centre and spread	2	(-0.000000, -0.000000, -0.000000)	0.30784969
WF centre and spread	3	(-0.000000, -0.000000, 0.000000)	0.30784979
WF centre and spread	4	(-0.000000, -0.000000, 0.000000)	0.40838973
WF centre and spread	5	(0.000000, -0.000000, -0.000000)	0.30784886
WF centre and spread	6	(-0.902512, 0.902512, 0.902512)	1.14385632
WF centre and spread	7	(0.902512, -0.902512, -0.902512)	1.14385635
Sum of centres and spreads	(0.000000, -0.000000, -0.000000)	4.02804006
Spreads (Ang ²)	Omega I	=	3.662691490
=====	Omega D	=	0.001894482
	Omega OD	=	0.363454087
Final Spread (Ang ²)	Omega Total	=	4.028040058

We can readily see that looking at the individual spreads we find two groups of MLWFs, a group of 5 d -like MLWFs centred on the Copper atom, whose spreads are 0.4084\AA^2 and 0.3078\AA^2 respectively, and a group of 2 s -like MLWFs centred on two opposite (with respect to the origin) interstitial points, whose spread is 1.1439\AA^2 . The 3+2 d -like MLWFs are the basis of two representations of the O_h group, with character t_{2g} and e_g respectively.

2. Plot the Fermi surface, it should look familiar! The Fermi energy is at 12.2103 eV.

As explained in example 2 of the tutorial, we need to add the following lines to the input file (`copper.win`):

```
restart = plot
fermi_energy = 12.2103
fermi_surface_plot = true
fermi_surface_num_points = 50
```

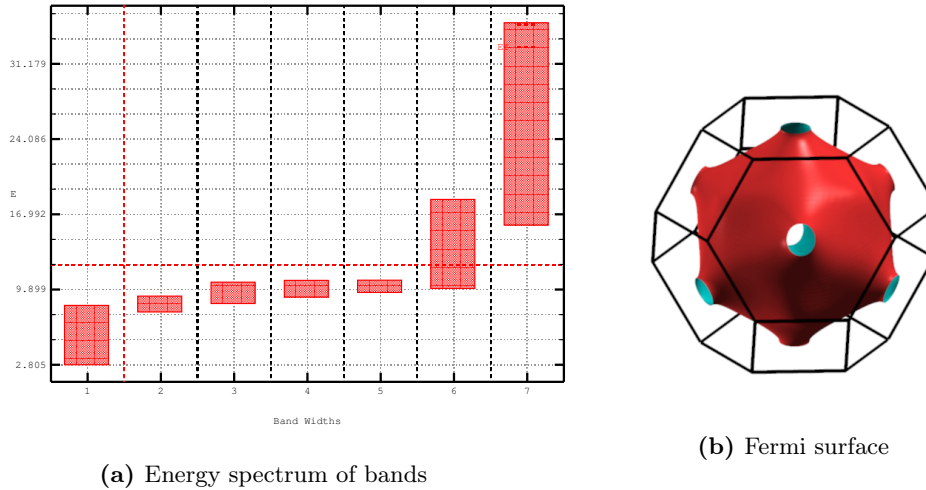


Figure 11: Fermi surfaces for band 6 in copper. The value of the Fermi energy is 12.2103eV, and it was obtained from DFT calculation, with a $4 \times 4 \times 4$ \mathbf{k} -point mesh. To calculate the band energies and to plot Fermi surfaces, Wannier interpolation was employed on a dense mesh in the Brillouin zone consisting of 50^3 points.

and re-run the WANNIER90 executable. The result will be a file named `copper.bxsf`, which contains volumetric data in a format suitable for `xcrysden`. There is only one band that crosses the Fermi level (12.2103eV), i.e. band 6, as shown in Fig. 11-(a). The corresponding Fermi surface is shown in Fig. 11-(b)

3. Plot the interpolated bandstructure.

Interpolated bandstructure, with path in \mathbf{k} -space given in the tutorial, is shown in Fig. 12.

4. Plot the contribution of the interstitial WF to the bandstructure.

The contribution of the 2 s -like MLWFs to the band structure is shown in Fig. 13

Extra : Investigate the effect of the outer and inner energy window on the interpolated bands.

From now on, we will refer to the inner window energy level as ε_{in} and to the outer window energy level as ε_{out} . The reference values are in this case $\varepsilon_{\text{in}}^0 = 13\text{eV}$ and $\varepsilon_{\text{out}}^0 = 38\text{eV}$. Hereafter, we will use ε_{min} to refer to the minimum energy eigenvalue (for the chosen path). The value of $\varepsilon_{\text{out}}^0$ must be chosen such that there are at least N_{wannier} (7 in this case) states inside the outer energy window for each \mathbf{k} -point. This means that for a given path in the BZ there exists a lower bound to $\varepsilon_{\text{out}}^0$. The actual value depends on the path in the BZ and on the choice of the zero for the pseudopotential. The result for several values of ε_{in} and ε_{out} are shown in Fig. 14.

Table 4: Converged values of the components of spread functional and their sum, given in \AA^2 .

MP mesh	Ω	Ω_{I}	Ω_{OD}	Ω_{D}
$4 \times 4 \times 4$	4.028	3.66	0.363	0.002

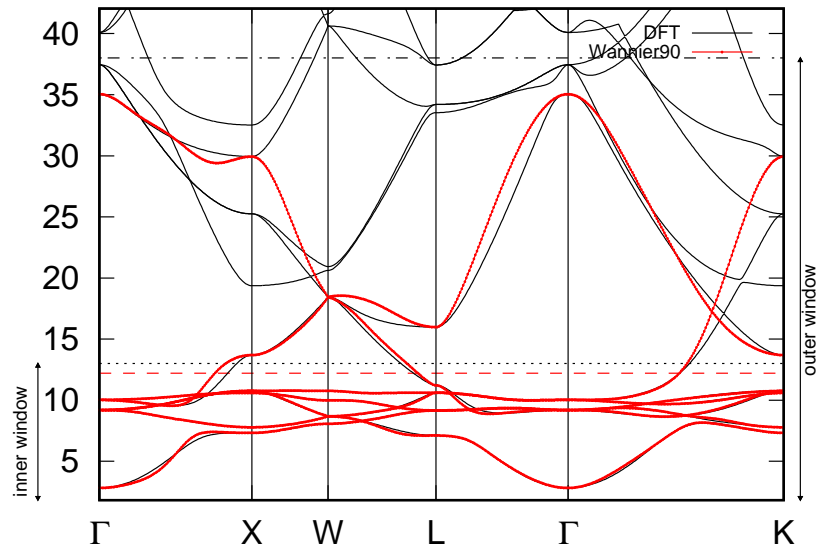


Figure 12: Interpolated bandstructure of Copper (solid red) showing the position of the Fermi level (dashed red) and both inner and outer windows (dotted and dashed-dotted respectively). The reference DFT bandstructure (solid black) was obtained with Quantum ESPRESSO, see procedure in Example 6.

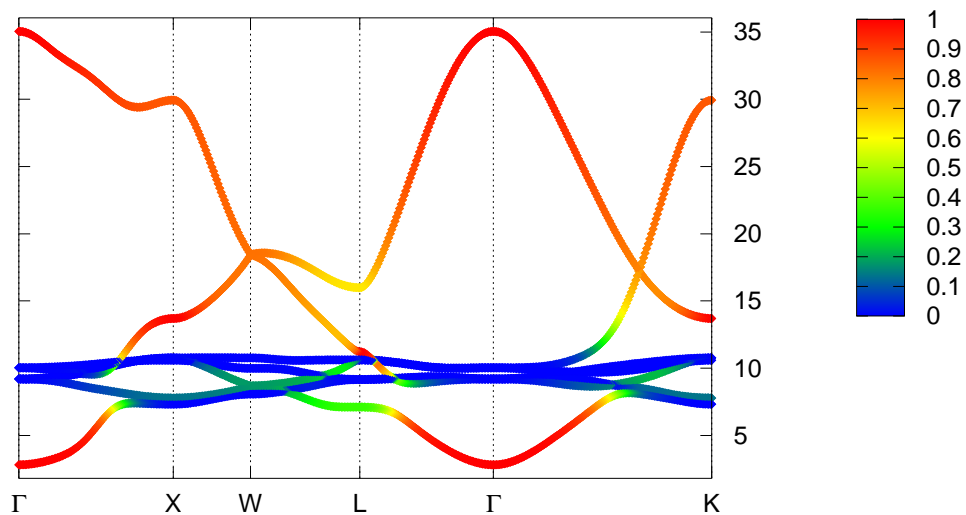


Figure 13: Bandstructure of Copper showing the contribution from the 2 *s*-like MLWFs in red.

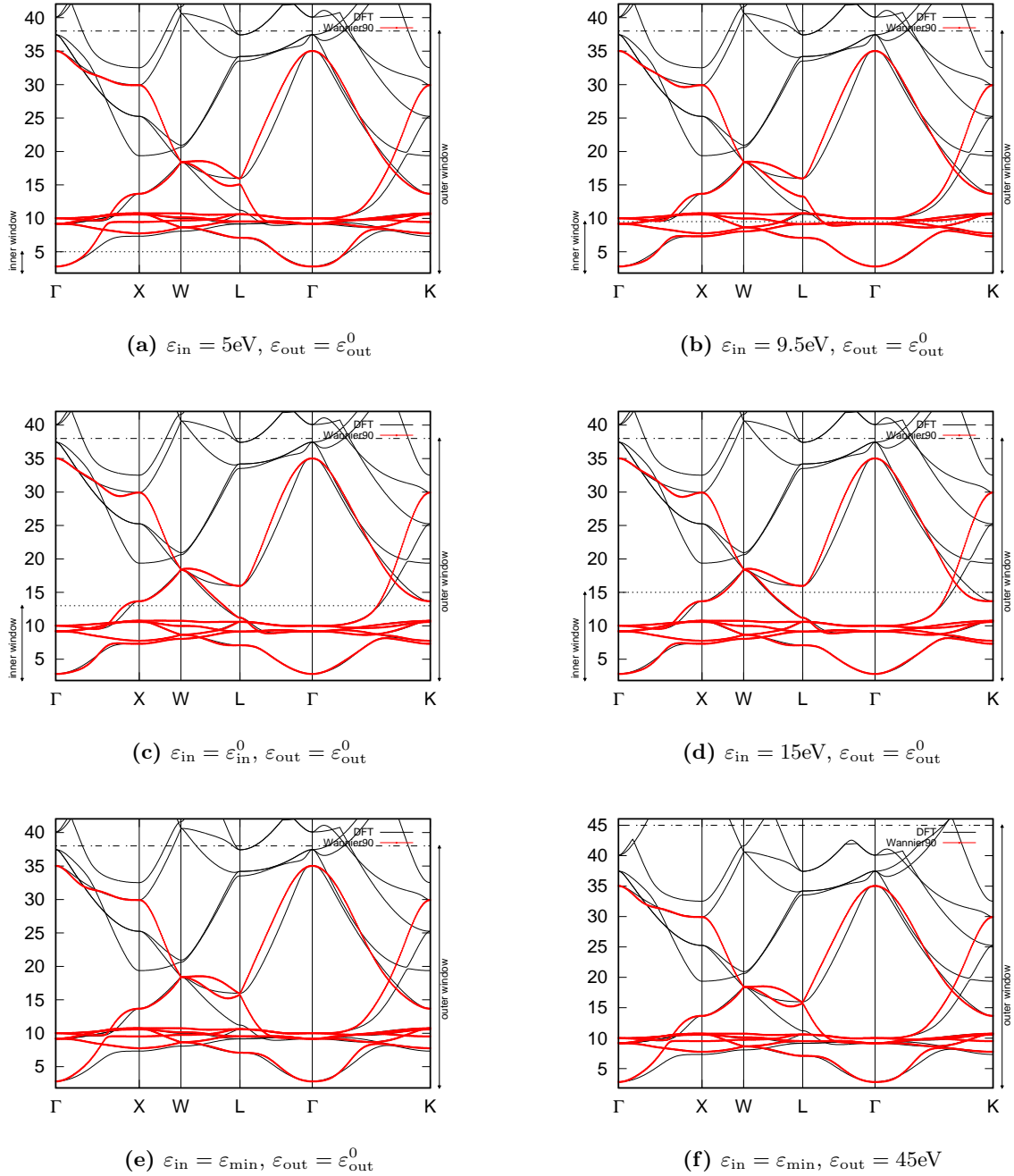


Figure 14: Interpolated bandstructure of Copper (solid red) with DFT reference (solid black) and different values of the inner window. Panel a) ...

5: Diamond — MLWFs for the valence bands

- Outline: *Obtain MLWFs for the valence bands of diamond.*

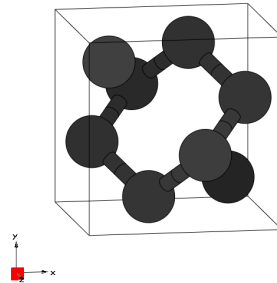


Figure 15: Unit cell of Diamond crystal plotted with the XCRYSDEN program.

1. *Run pwscf to obtain the ground state of diamond.*

Convergence of the self-consistent field calculation in Quantum Espresso can be checked at the end of the `scf.out` file. At the very end of the file one should find the line confirming that the job has finished without crashing, e.g.

```
=====
JOB DONE.
=====
```

Depending on the output verbosity one may or may not find info about WALL times for the calls to the different routines. Just above this block, if present, one may find the info about the convergence of the SCF loop, such as the `scf` accuracy and the number of iterations to required to achieve it:

```
! total energy           = -22.58128615 Ry
  Harris-Foulkes estimate = -22.58128615 Ry
  estimated scf accuracy  <  1.0E-14 Ry
```

The total energy is the sum of the following terms:

```
one-electron contribution =  11.69117931 Ry
hartree contribution      =   1.57036314 Ry
xc contribution           =  -7.58421586 Ry
ewald contribution       = -28.25861274 Ry
```

```
convergence has been achieved in  9 iterations
```

2. *Run pwscf to obtain the Bloch states on a uniform k-point grid.*

Similarly for the non-scfc calculation one can check that the calculation has been carried out without crashing by looking at the last three line of the `nscf.out` file. A useful information to check is the value of the highest eigenvalue (for insulators and semiconductors) or the value of the Fermi level (for metals). In the diamond we case, we find:

```
highest occupied level (ev): 19.3978
```

5 Run WANNIER90 to compute the MLWFs.

The result of the wannierisation, after 20 iterations, may be found at the end of `diamond.wout` file:

```
Final State
WF centre and spread  1 ( -0.000000,  0.000000, -0.000000 )  0.58022623
WF centre and spread  2 ( -0.806995,  0.806995,  0.000000 )  0.58022623
WF centre and spread  3 ( -0.000000,  0.806995,  0.806995 )  0.58022623
WF centre and spread  4 ( -0.806995, -0.000000,  0.806995 )  0.58022623
Sum of centres and spreads ( -1.613990,  1.613990,  1.613990 )  2.32090491

      Spreads (Ang^2)      Omega I      =      1.954619859
      =====            Omega D      =      0.000000000
                                Omega OD     =      0.366285054
      Final Spread (Ang^2)  Omega Total =      2.320904912
-----
```

Extra : Plot the 4 MLWFs.

The resulting 4 σ -bonding MLWFs are shown in Fig. 16

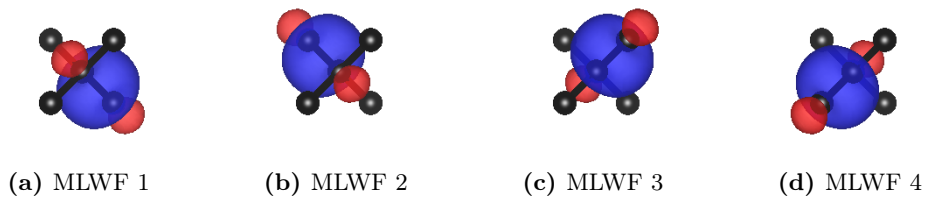


Figure 16: 4 MLWFs in diamond describing the valence bands plotted using VESTA.

6: Copper — Fermi surface

- Outline: *Obtain MLWFs to describe the states around the Fermi-level in copper.*

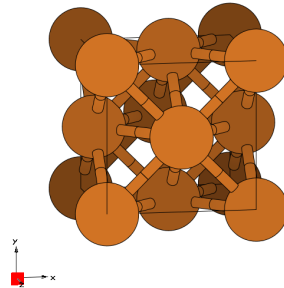


Figure 17: Unit cell of Copper crystal plotted with the XCRYSDEN program.

After checking that the calculations have converged as shown in Example 5, one can proceed with other points in the example.

1. *Use Wannier interpolation to obtain the Fermi surface of copper.*

To obtain the value of the Fermi energy we can use the `grep` command (only for Linux/Unix systems) as:

```
$ > grep Fermi nscf.out
```

The output should be:

```
the Fermi energy is 12.9344 ev
```

Alternatively, one can open the `nscf.out` file with the editor of choice and search for "Fermi" inside the file. We can then use this value in the `.win` file to compute the Fermi surface as done in Example 2. The interpolated Fermi surface is shown in Fig. 18-(a).

2. *Plot the interpolated bandstructure.*

Bandstructure is shown in Fig. 18-(b). One way to obtain the DFT bandstructure on exactly the same path as the one in the `.win` input file, is given by the `bands.x` program available at <http://www.tcm.phy.cam.ac.uk/~jry20/bands.html>.

Extra 1: *Compare the Wannier interpolated bandstructure with the full `pwscf` bandstructure. Obtain MLWFs using a denser k -point grid.*

Extra 2: *Investigate the effects of the outer and inner energy windows on the interpolated bands.*

The effect of different energy windows has already been discussed in the Example 4, so it won't be repeated here.

Extra 2: *Instead of extracting a subspace of seven states, we could extract a nine dimensional space (i.e., with s , p and d character). Examine this case and compare the interpolated bandstructures.*

Using s , p , and d orbitals as initial guesses for the MLWFs of Copper, yields the bandstructure (solid blue) shown in Fig. 19 (with reference values for the inner and outer windows). The

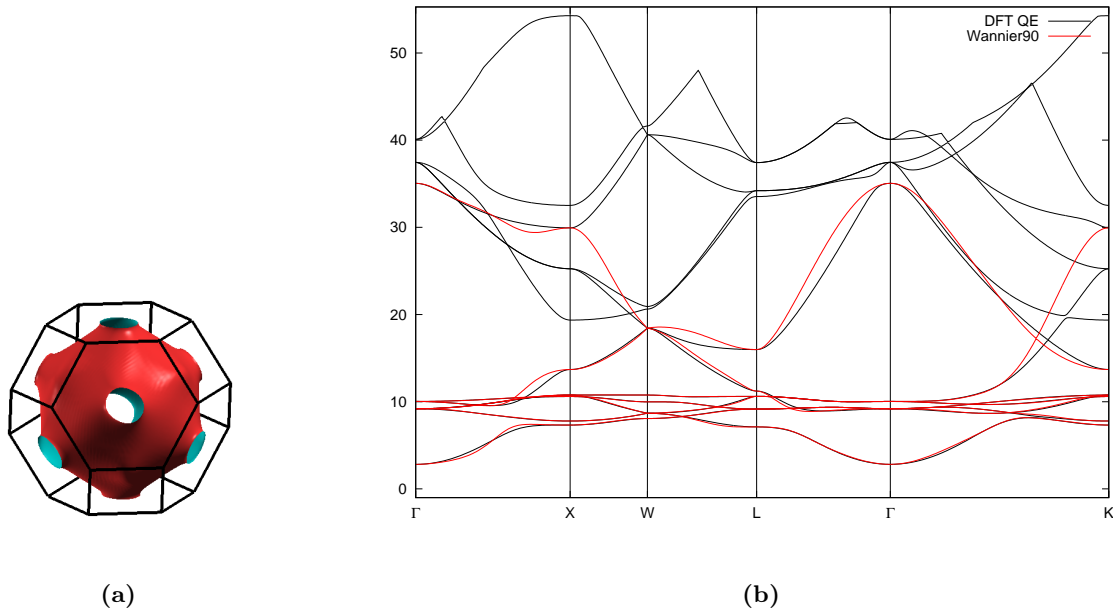


Figure 18: a) Fermi surface of Copper. b) Band structure of Copper along the Γ -X-W-L- Γ -K computed from a non-scf DFT calculation (solid black) and via Wannier interpolation (solid red).

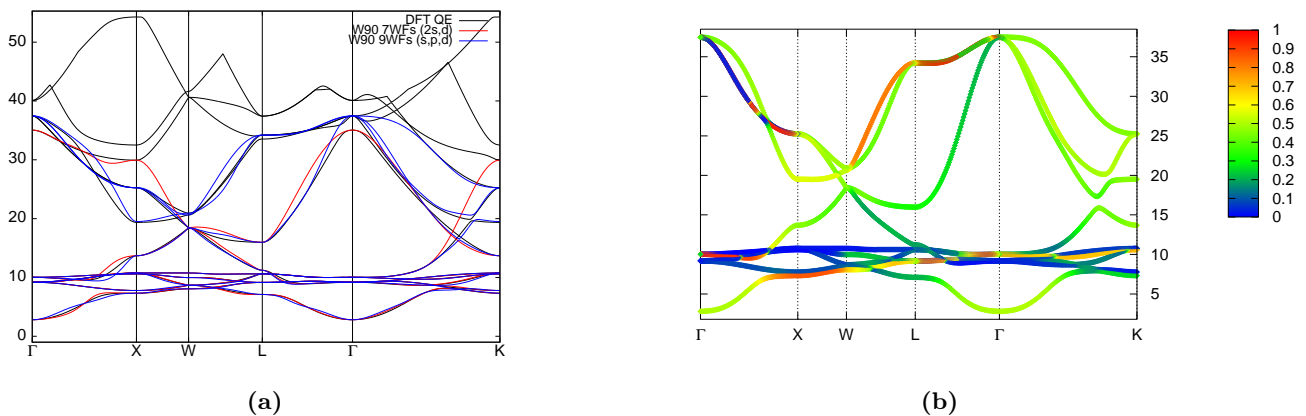


Figure 19: a) Bandstructure of Copper along the Γ -X-W-L- Γ -K from a non-scf DFT calculation (solid black) and via Wannier interpolation using two different sets of initial projections, namely 2s and 5d ($N_w = 7$) (solid red) and 1s 3p and 5d ($N_w = 9$) (solid blue). b) p character of bands computed using `bands_plot_project = 2,3,4` in the input file. A color scheme is used to measure the p character of the bands.

bandstructure obtained starting from 2s and 5d orbitals is shown in red, whereas the DFT reference bandstructure, computed with the procedure described above, is in black. It is clear from Fig. 19(a), and Fig. 19(b) that the bands of interest have very little p character, particularly the 5 flat bands, which are well very described by d states.

BANDS.X MINITUTORIAL

Here we summarize the main steps to produce the bandstructure with the `bands.x` code:

- Compilation:

```
eg. g95 -o bands.x bands.F90
ifort -o bands.x bands.F90
for NAG
f95 -o bands.x bands.F90 -DNAG
```

- Usage: First you need to generate an `copper.inp` file, with the following structure

```
! Input file for Copper
!
! First the unit cell (in atomic units = Bohr)
-3.411 0.000 3.411
 0.000 3.411 3.411
-3.411 3.411 0.000

!then the number of points along the 1st special path
100

! then the special kpoints and their labels
G 0.00 0.00 0.00 X 0.50 0.50 0.00
X 0.50 0.50 0.00 W 0.50 0.75 0.25
W 0.50 0.75 0.25 L 0.00 0.50 0.00
L 0.00 0.50 0.00 G 0.00 0.00 0.00
G 0.00 0.00 0.00 K 0.00 0.50 -0.50
```

Then you need to generate the kpoint list by running the `bands.x` program with the `-pp` flag

```
$ > ./bands.x -pp copper
```

This will read data from `copper.inp` and write kpoints into `copper_band.kpt`.

WARNING: if you already have a `copper_band.kpt` file from a previous Wannier90 calculation, running the above command will overwrite it.

Now you need to calculate a non-scf or bands calculation with Quantum ESPRESSO on the k-points given in `copper_band.kpt`. To do so, copy the `copper.nscf` to `copper.bands` and modify it accordingly. Run a non-scf calculation

```
$ > pw.x < copper.bands > copper.pwscf
```

WARNING: the output file must terminate with `.pwscf` in order to be read by `bands.x`.

Now extract the bands from the `copper.pwscf` file

```
$ > bands.x copper
```

The bands are written into `copper_band.dat`. **WARNING:** if you already have a `copper_band.dat` file and a `copper_band.gnu` file from a previous Wannier90 calculation, running the above command will overwrite them.

Plot with gnuplot

```
$ > gnuplot -persist copper_band.gnu
```

7: Silane (SiH₄) — Molecular MLWFs using Γ -point sampling

- Outline: *Obtain MLWFs for the valence bands of silane.*

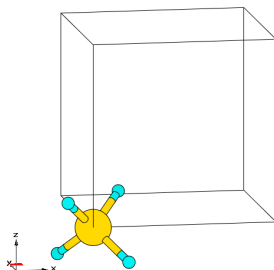


Figure 20: Silane molecule in a periodic cell plotted with the XCrySDen program.

1. Convergence of the self-consistent field calculation in Quantum Espresso can be checked at the end of the `scf.out` file. At the very end of the file one should find the line confirming that the job has finished without crashing, e.g.

```

=====
JOB DONE.
=====

```

Just above the block reporting the info about WALL times, if present, one may find the info about the convergence of the SCF loop, such as the scf accuracy and the number of iterations to required to achieve it:

```

!   total energy           =   -12.25602944 Ry
!   Harris-Foulkes estimate =   -12.25602944 Ry
!   estimated scf accuracy <    7.0E-11 Ry

      The total energy is the sum of the following terms:

      one-electron contribution =    11.69117931 Ry
      hartree contribution     =    1.57036314 Ry
      xc contribution          =   -7.58421586 Ry
      ewald contribution       =  -28.25861274 Ry

      convergence has been achieved in   9 iterations

```

2. Similarly for the non-scf calculation one can check that the calculation has been carried out without crashing by looking at the last three line of the `nscf.out` file. A useful information to check is the value of the highest eigenvalue (for insulators and semiconductors) or the value of the Fermi level (for metals). In the diamond we case, we find:

```

highest occupied level (ev):   -6.5316

```

- 5 The result of the wannierisation, after 20 iterations, may be found at the end of `silane.wout` file:

Final State

WF centre and spread	1	(0.762490, 0.762490, 0.762490)	1.01124580
WF centre and spread	2	(0.762491, -0.762492, -0.762491)	1.01124445
WF centre and spread	3	(-0.762491, 0.762490, -0.762491)	1.01124473
WF centre and spread	4	(-0.762491, -0.762491, 0.762491)	1.01124420
Sum of centres and spreads		(-0.000002, -0.000003, -0.000001)	4.04497917

Spreads (Ang ²)	Omega I	=	3.920639090
=====	Omega D	=	0.000000000
	Omega OD	=	0.124340085
Final Spread (Ang ²)	Omega Total	=	4.044979175

8: Iron — Spin-polarized WFs, DOS, projected WFs versus MLWFs

- Outline : *Generate both maximally-localized and projected Wannier functions for ferromagnetic bcc Fe. Calculate the total and orbital-projected density of states by Wannier interpolation.*

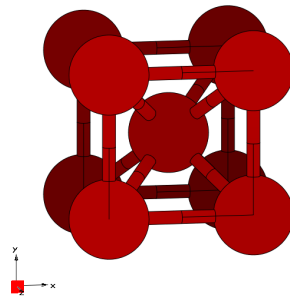


Figure 21: Unit cell of Iron crystal plotted with the XCrySDen program.

1-5 *Converged values for the total spread functional and its components for both spin channels are shown in Tab. 5. The final state for spin-up MLWFs is*

Final State			
WF centre and spread	1	(0.709852, 0.000108, 0.000131)	1.08935224
WF centre and spread	2	(0.000131, 0.000053, -0.709852)	1.08935218
WF centre and spread	3	(-0.709852, -0.000108, -0.000131)	1.08935221
WF centre and spread	4	(0.000108, -0.709852, -0.000053)	1.08935218
WF centre and spread	5	(-0.000131, -0.000053, 0.709852)	1.08935226
WF centre and spread	6	(0.000000, 0.000000, 0.000000)	0.43234428
WF centre and spread	7	(-0.000000, 0.000000, 0.000000)	0.43234429
WF centre and spread	8	(-0.000108, 0.709852, 0.000053)	1.08935225
WF centre and spread	9	(0.000000, 0.000000, -0.000000)	0.43234428
Sum of centres and spreads		(0.000000, -0.000000, -0.000000)	7.83314616
Spreads (Ang ²)		Omega I =	5.948424630
=====		Omega D =	0.017027691
		Omega OD =	1.867693841
Final Spread (Ang ²)		Omega Total =	7.833146162

and for spin-down MLWFs is

Table 5: Converged values of the components of spread functional and their sums for both spin channels for ferromagnetic bcc Fe, given in \AA^2 .

spin	Ω	Ω_I	Ω_{OD}	Ω_D	N_{iter}
up	7.8331	5.9484	1.8677	0.0170	400
down	7.8496	5.9467	1.8884	0.0145	400

```
[sharp corners,boxrule=0.5pt]
```

```
Final State
```

```
WF centre and spread 1 ( -0.685467, -0.000123,  0.000259 ) 1.10268580
WF centre and spread 2 ( -0.000259, -0.000207, -0.685467 ) 1.10268617
WF centre and spread 3 (  0.685468,  0.000123, -0.000259 ) 1.10268605
WF centre and spread 4 ( -0.000123,  0.685467, -0.000207 ) 1.10268595
WF centre and spread 5 (  0.000259,  0.000207,  0.685467 ) 1.10268552
WF centre and spread 6 (  0.000000,  0.000000, -0.000000 ) 0.41116646
WF centre and spread 7 ( -0.000000,  0.000000, -0.000000 ) 0.41116648
WF centre and spread 8 (  0.000123, -0.685467,  0.000207 ) 1.10268572
WF centre and spread 9 (  0.000000,  0.000000,  0.000000 ) 0.41116644
Sum of centres and spreads (  0.000000, -0.000000,  0.000000 ) 7.84961460
```

```

      Spreads (Ang^2)      Omega I      =      5.946718376
=====
                               Omega D      =      0.014524283
                               Omega OD     =      1.888371944
Final Spread (Ang^2)      Omega Total   =      7.849614603
-----
```

As it is clear from the output file snippets above, the s, p and d orbitals hybridize to give rise to two groups of functions for both spin channels. A first group made of 6 MLWFs coming from the hybridisation of sp^3 and d_{e_g} MLWFs, with a total spread of $1.089(1.103)\text{\AA}^2$ for spin-up(down). A second group made of 3 MLWFs with a $d_{t_{2g}}$ character, with a total spread of $0.432(0.4112)\text{\AA}^2$ for spin-up(down). Two sample MLWFs, one for each group, are shown in Fig. 22.

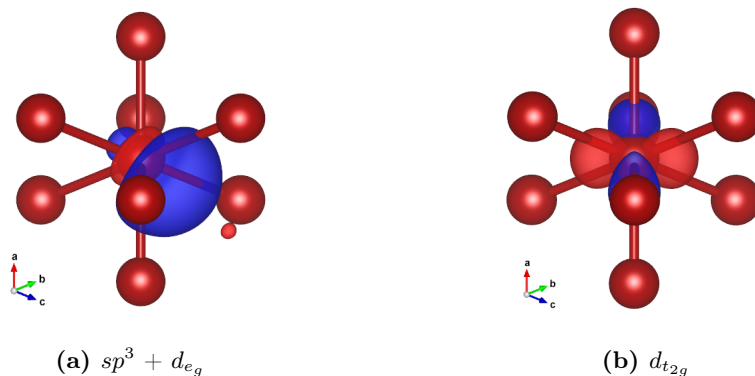


Figure 22: 2 representative MLWFs from the wannierisation of 9 spin-up bands of iron. a) A representative of the hybrid (sp^3 and d_{e_g}) group of MLWFs. b) A representative of the $d_{t_{2g}}$ group of MLWFs.

Density of states

- run `postw90` and plot the DOS with `gnuplot`

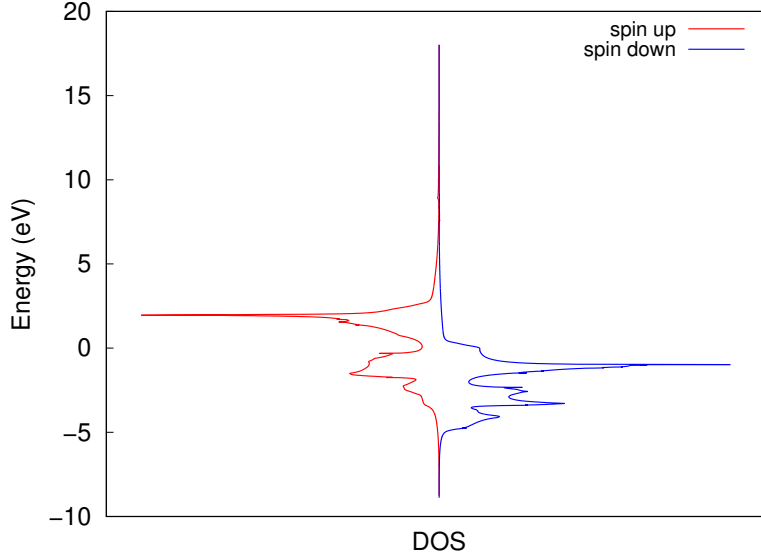


Figure 23: Interpolated DOS of bcc iron on a $25 \times 25 \times 25$ \mathbf{k} -mesh. Up-spin channel (solid red). Down-spin channel (solid blue).

- Check the convergence by repeating the DOS calculations with more \mathbf{k} -points.

Plots of the DOS calculated with different \mathbf{k} -point mesh densities for the spin-down channel are shown in Fig. 24-(a). In Fig. 24-(b)-(c) and (d) we show the convergence of the DOS for the spin-down channel, spin-up channel and both spin channels respectively. The convergence is assessed by looking at the number of states N computed by integrating the DOS up to the Fermi level using the formula

$$N_{\uparrow/\downarrow} = \int_{-\infty}^{\epsilon_F} d\epsilon f_{\text{MV}}(\epsilon, \uparrow / \downarrow) g(\epsilon, \uparrow / \downarrow), \quad (1)$$

where $f_{\text{MV}}(\epsilon, \uparrow) = \int_{-\infty}^{\epsilon} d\epsilon' \tilde{\delta}(\epsilon')$ is the Marzari-Vanderbilt occupation number function, with

$$\tilde{\delta}(x) = \frac{2}{\sqrt{\pi}} e^{-[x-(1/\sqrt{2})]^2} (2 - \sqrt{2}x), \quad x = \frac{\mu - \epsilon}{\sigma},$$

where ϵ_F is the Fermi energy (12.6256 eV) and σ is the smearing (0.02 eV). $g(\epsilon, \uparrow)$ is the DOS from WANNIER90 interpolation.

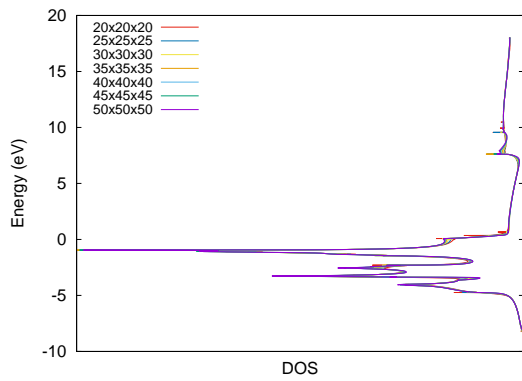
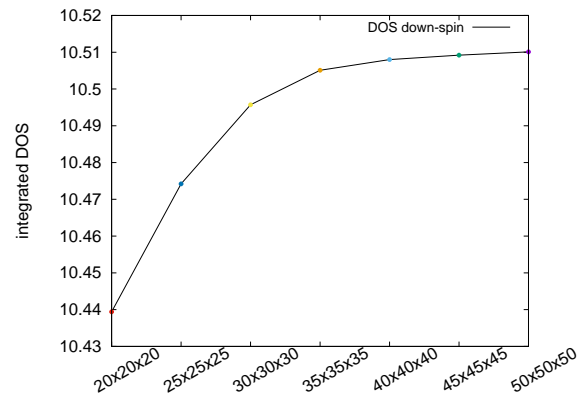
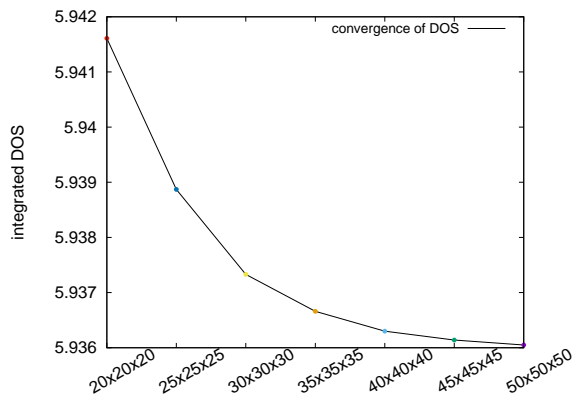
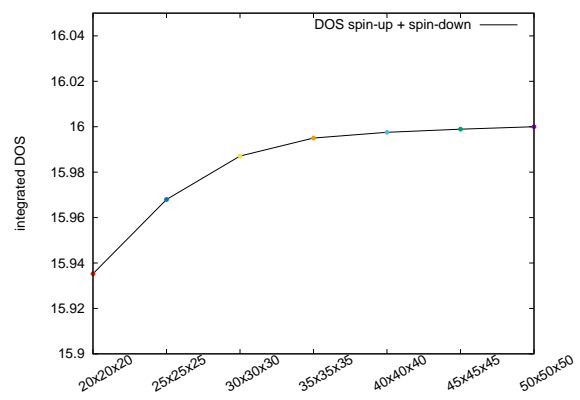
(a) DOS spin \downarrow (b) N_{\downarrow} (c) N_{\uparrow} (d) $N_{\uparrow+\downarrow}$

Figure 24: Panel (a) interpolated DOS for the up-spin channel of bcc iron for different \mathbf{k} -mesh sizes. Panel (b) corresponding integrated DOS. The integral of the DOS is used as a convergence criterion. $N_{\uparrow+\downarrow}$ has been scaled such as the final value is equal to the total number of electrons.

Projected versus maximally-localized Wannier functions

- Open one of the .wout files and search for “Initial state”; those are the projected WFs.

For the spin-up channel one finds

Initial State			
WF centre and spread	1	(-0.000000, -0.000000, -0.000000)	2.25930561
WF centre and spread	2	(-0.000000, 0.000000, -0.000000)	2.32454089
WF centre and spread	3	(0.000000, 0.000000, -0.000000)	2.32428592
WF centre and spread	4	(0.000000, -0.000000, -0.000000)	2.32428592
WF centre and spread	5	(-0.000000, 0.000000, -0.000000)	0.54443303
WF centre and spread	6	(0.000000, -0.000000, -0.000000)	0.51353680
WF centre and spread	7	(0.000000, 0.000000, -0.000000)	0.51353680
WF centre and spread	8	(0.000000, 0.000000, -0.000000)	0.54447716
WF centre and spread	9	(0.000000, 0.000000, 0.000000)	0.51347734
Sum of centres and spreads		(0.000000, -0.000000, -0.000000)	11.86187946

It is clear from the spreads and the centres that these are the projected WFs. In particular, WF 1 is the s -projected WF. WF 2-4 are the p -projected WFs and WF 5-9 are the d -projected WF, with e_g (5,8) and t_{2g} (6,7,9) character, respectively (see Fig. 25).

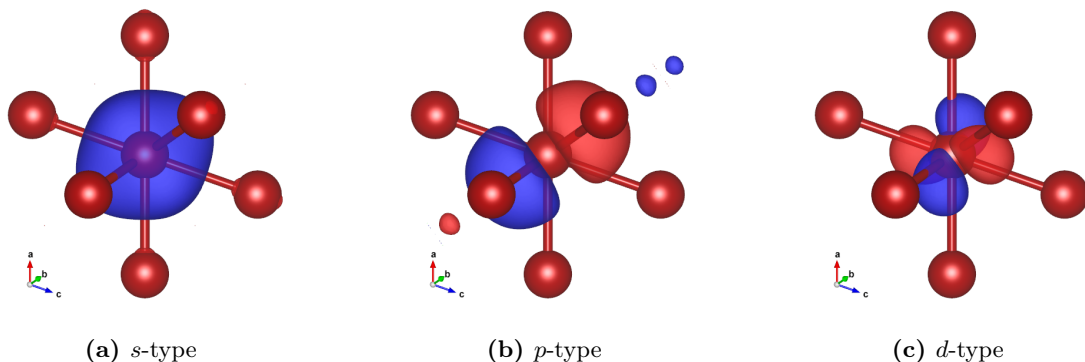


Figure 25: 3 representative MLWFs from the wannierisation via projections of 9 spin-up bands of iron. a) MLWF from projection onto 1 s orbital. b) A representative of the MLWFs from projection onto p orbitals. c) A representative of the MLWFs from projection onto d orbitals.

- The Wannier spreads have re-organized in two groups, 6+3; moreover, the six more diffuse WFs are off-centred: the initial atomic-like orbitals hybridized with one another, becoming more localized in the process.

Final State				
WF centre and spread	1	(-0.709852, 0.000191, 0.000015)		1.08935227
WF centre and spread	2	(-0.000015, -0.000041, -0.709852)		1.08935223
WF centre and spread	3	(0.709852, -0.000191, -0.000015)		1.08935227
WF centre and spread	4	(-0.000191, -0.709852, 0.000041)		1.08935226
WF centre and spread	5	(0.000015, 0.000041, 0.709852)		1.08935227
WF centre and spread	6	(-0.000000, -0.000000, 0.000000)		0.43234437
WF centre and spread	7	(0.000000, 0.000000, 0.000000)		0.43234440
WF centre and spread	8	(0.000191, 0.709852, -0.000041)		1.08935228
WF centre and spread	9	(-0.000000, 0.000000, 0.000000)		0.43234438
Sum of centres and spreads		(-0.000000, -0.000000, -0.000000)		7.83314672

- The first plateau corresponds to atom-centred WFs of separate s , p , and d character, and the sharp drop signals the onset of the hybridization. With hindsight, we can redo steps 4 and 5 more efficiently using trial orbitals with the same character as the final MLWFs,

Fe : $sp_3d_2; d_{xy}; d_{xz}; d_{yz}$

With this choice the minimization converges much more rapidly as can be seen in Fig. 26-(a).

- Let us recompute the DOS using, instead of MLWFs, the WFs obtained by projecting onto s , p , and d -type trial orbitals.

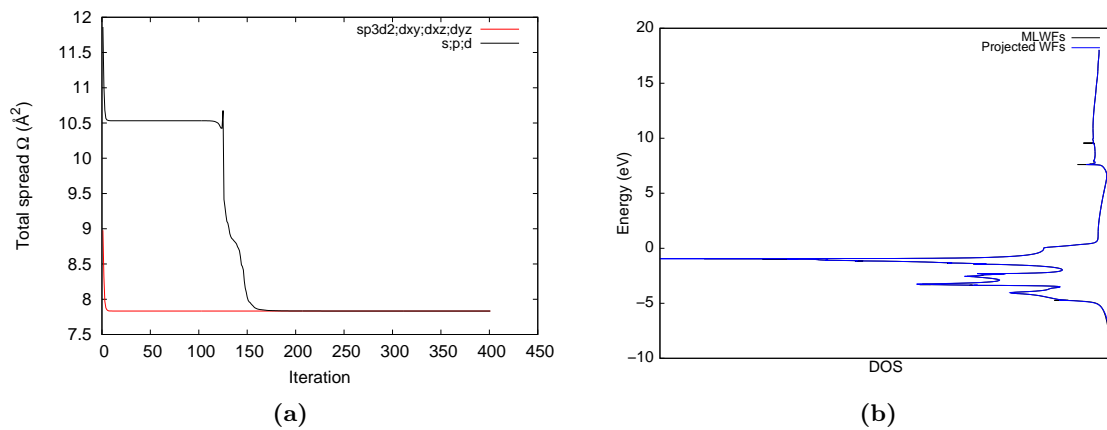


Figure 26: a) Convergence of Ω for two different sets of initial projections: $s; p; d$ (solid black) and $sp_3d_2; d_{xy}; d_{xz}; d_{yz}$ (solid red). b) DOS with MLWFs (solid black) and projected $s; p; d$ Wannier functions (solid blue).

Orbital-projected DOS and exchange splitting

In order to obtain the partial DOS projected onto the p -type WFs, add to the `.win` files

```
dos_project = 2,3,4
```

and re-run `postw90`.

- Plot the projected DOS for both up- and down-spin bands. Repeat for the s and d projections. Results are shown in figure below (Fig. 27).

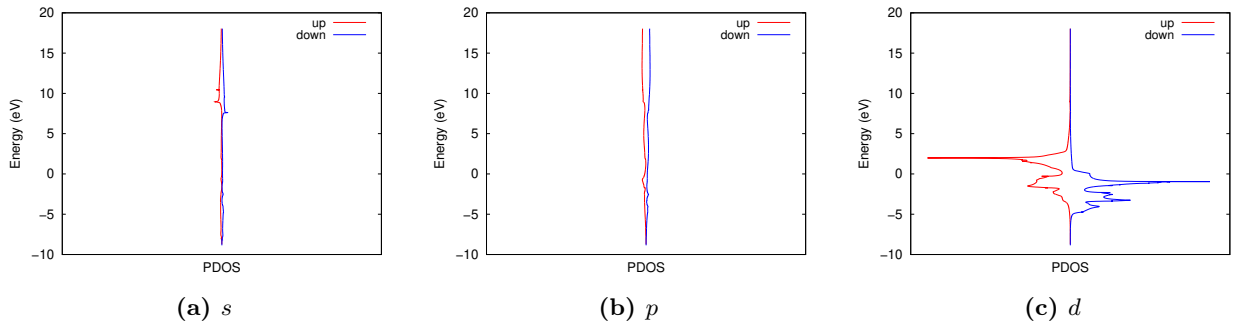


Figure 27: Partial DOS projected onto a) 1 s -like WF, b) 3 p -like WFs and c) 5 d -like WFs.

- The difference between corresponding values of the on-site energies the on-site energies $\langle \mathbf{0}n | H | \mathbf{0}n \rangle$ in `iron_up.wout` and in `iron_dn.wout` gives the exchange splittings for the individual orbitals. Results are shown in Tab. 6.

Table 6: Exchange splittings for individual orbitals in eV.

n	character	$\langle \mathbf{0}n H \mathbf{0}n \rangle$ for \downarrow [eV]	$\langle \mathbf{0}n H \mathbf{0}n \rangle$ for \uparrow [eV]	Δ [eV]
1	s	21.307132	22.074648	0.767516
2	p	26.353088	26.817526	0.464438
3	p	26.352956	26.817207	0.464251
4	p	26.352956	26.817207	0.464251
5	d	10.531720	13.206631	2.67491
6	d	10.775917	12.808277	2.03236
7	d	10.775917	12.808277	2.03236
8	d	10.532108	13.207139	2.67503
9	d	10.775177	12.807388	2.03221

- Compare their magnitudes with the splittings displayed by the orbital-projected DOS plots

9: Cubic BaTiO₃

- Outline : *Obtain MLWFs for a perovskite.*

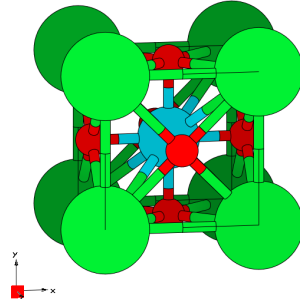


Figure 28: Unit cell of cubic BaTiO₃ crystal plotted with the XCRYSDEN program.

1-5 *Compute the MLWFs.*

Converged values for the total spread functional and its components are shown in Tab. 7.

- *Plot the second MLWF.*

The result is shown in Fig. 29-(a) and -(b).

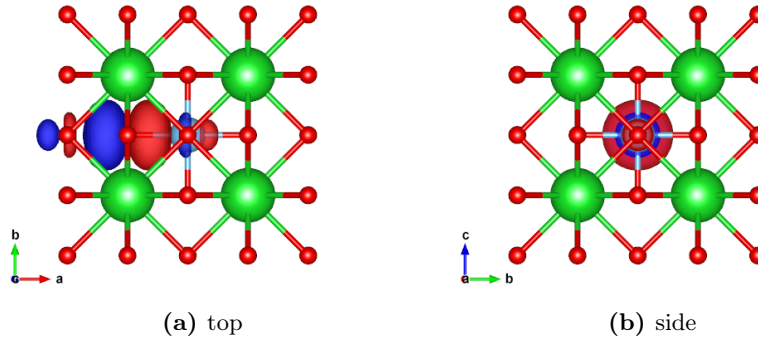


Figure 29: Top-view (a) and side-view (b) of the second MLWF in BaTiO₃

- *We can now simulate the ferroelectric phase by displacing the Ti atom. Regenerate the MLWFs (i.e., compute the ground-state charge density and Bloch states using pwscf, etc.) and look at the change in the second MLWF.*

The result is shown in Fig. 30-(a) and -(b).

Table 7: Converged values of the components of spread functional and their sums for cubic BaTiO₃ in Å².

Ω	Ω_I	Ω_{OD}	Ω_D	N_{iter}
12.7187	12.5662	0.1525	0.000	50

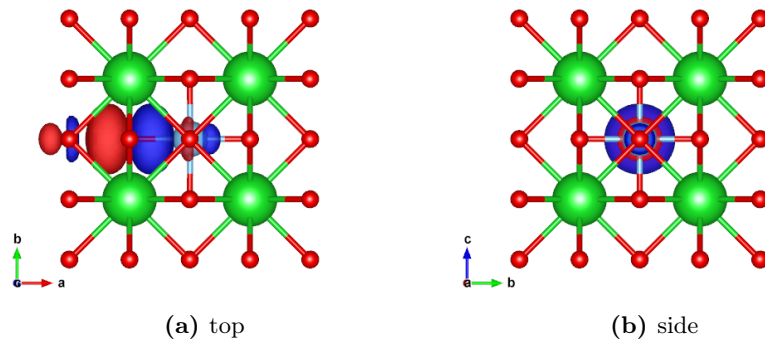


Figure 30: Top-view (a) and side-view (b) of the second MLWF in BaTiO_3 with the Ti atom displaced.

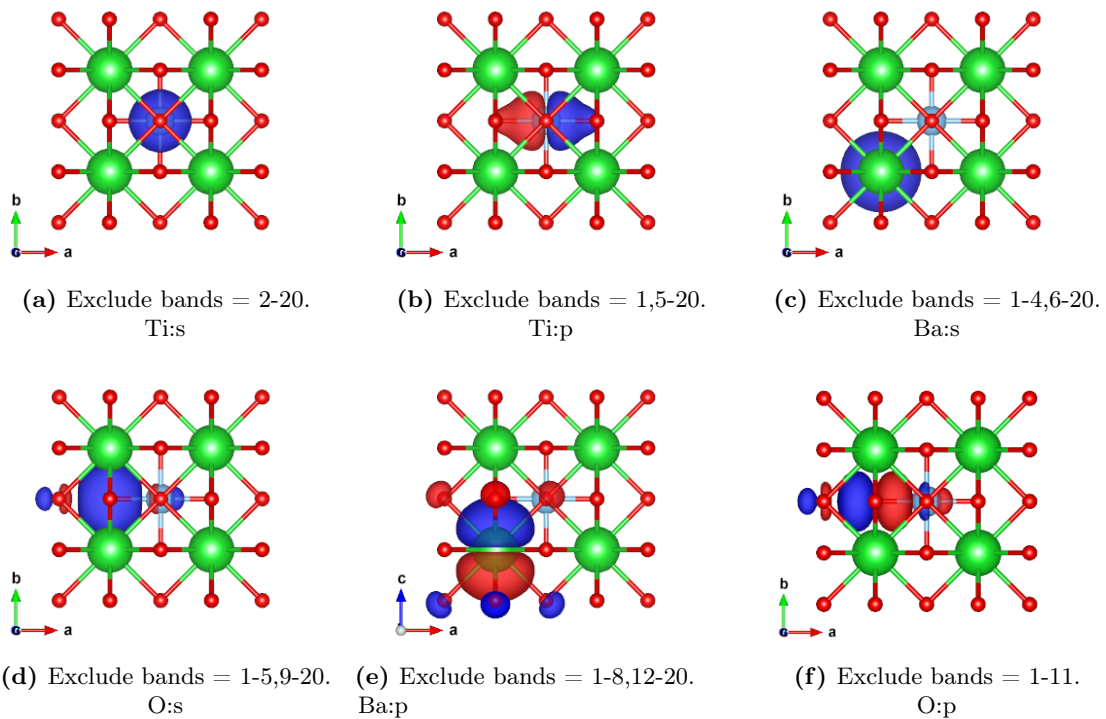


Figure 31: MLWFs for other group of bands.

Further ideas

- Look at MLWFs for other groups of bands.

Plots of MLWFs for other group of bands are shown in Fig. 31-(a)-(b)-(c)-(d)-(e) and -(f).

- What happens if you form MLWFs for the whole valence manifold?

Some representative MLWFs from the wannierisation of the whole valence bands are shown in Fig. 32.

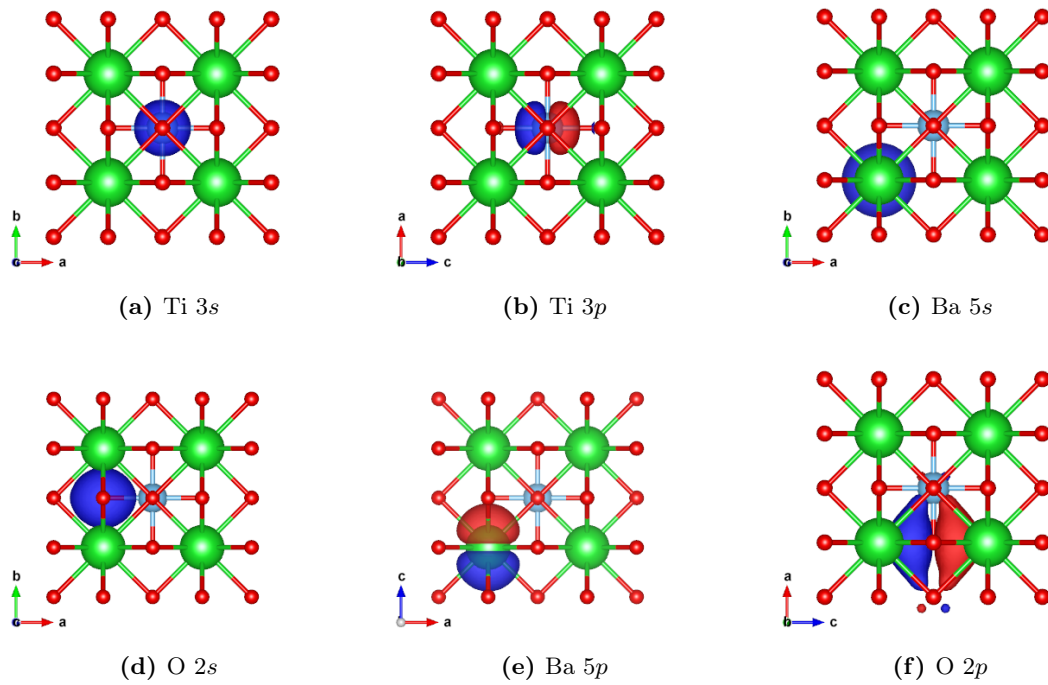


Figure 32: MLWFs formed from the whole valence manifold, i.e. from 20 bands.

10: Graphite

- Outline: *Obtain MLWFs for the graphite (AB, Bernal).*

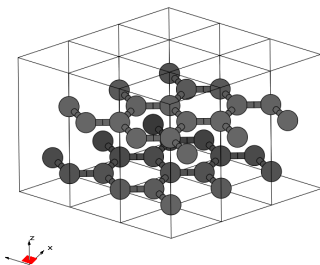


Figure 33: Unit cell of Graphite plotted with the XCRYSDEN program.

1-5 *Compute the MLWFs.*

Converged values for the total spread functional and its components are shown in Tab. 8. Three MLWFs, one σ and two p_z on different layers are shown in Fig. 34(a),(b) and (c) respectively.

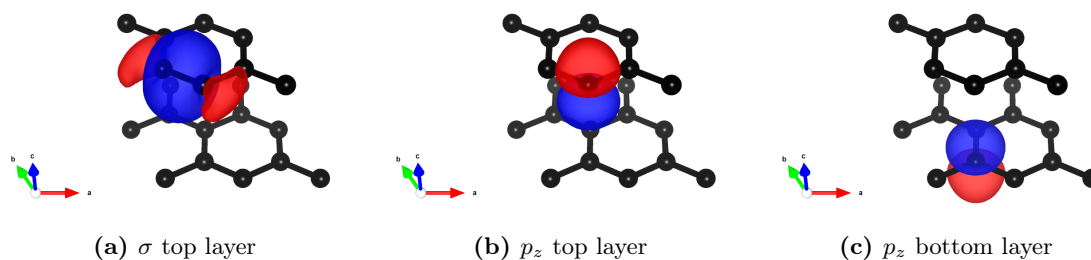


Figure 34: MLWFs for graphite. (a) σ -like MLWF centred on a C–C bond. (b) p_z -like MLWF on the top layer. (c) p_z -like MLWF on the bottom layer.

Table 8: Converged values of the components of spread functional and their sums for graphite (AB, Bernal) in \AA^2 .

Ω	Ω_I	Ω_{OD}	Ω_D	N_{iter}
7.3809	5.7641	1.5874	0.0293	100

11: Silicon — valence and low lying conduction states

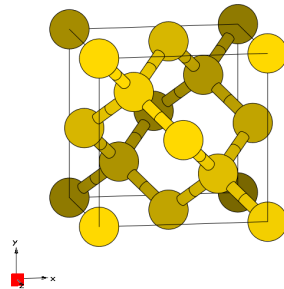


Figure 35: Unit cell of Silicon crystal plotted with the XCRYSDEN program.

Valence States

- Outline: *Obtain MLWFs for the valence bands of silicon.*

1-5 *Inspect the output file silicon.wout. The total spread converges to its minimum value after just a few iterations. Note that the geometric centre of each MLWF lies at the centre of the Si–Si bond. Note also that the memory requirement for the minimisation of the spread is very low as the MLWFs are defined by just the 4×4 unitary matrices $U(\mathbf{k})$.*

Below a snippet from the silicon.wout output file

Final State			
WF centre and spread	1	(-0.674701, 0.674701, -0.674701)	1.59185520
WF centre and spread	2	(-0.674701, -0.674701, 0.674701)	1.59185520
WF centre and spread	3	(0.674701, 0.674701, 0.674701)	1.59185520
WF centre and spread	4	(0.674701, -0.674701, -0.674701)	1.59185520
Sum of centres and spreads		(-0.000000, 0.000000, 0.000000)	6.36742081
Spreads (Ang ²)	Omega I	=	5.801375426
=====	Omega D	=	0.000000000
	Omega OD	=	0.566045385
Final Spread (Ang ²)	Omega Total	=	6.367420811

Memory estimates may be found in the MEMORY ESTIMATE section of the silicon.wout file.

=====			
MEMORY ESTIMATE			
Maximum RAM allocated during each phase of the calculation			
=====			
Disentanglement		1.57 Mb	
Wannierise:		0.47 Mb	

Converged values for the total spread functional and its components are shown in Tab. 9.

- *Plot the MLWFs* The four MLWFs with σ character describing the valence manifold of Si are shown in Fig. 36(a),(b) and (c) respectively.

Table 9: Converged values of the components of spread functional and their sum, given in \AA^2 .

MP mesh	Ω	Ω_I	Ω_{OD}	Ω_D
$4 \times 4 \times 4$	6.3674	5.8014	0.5660	0.0000

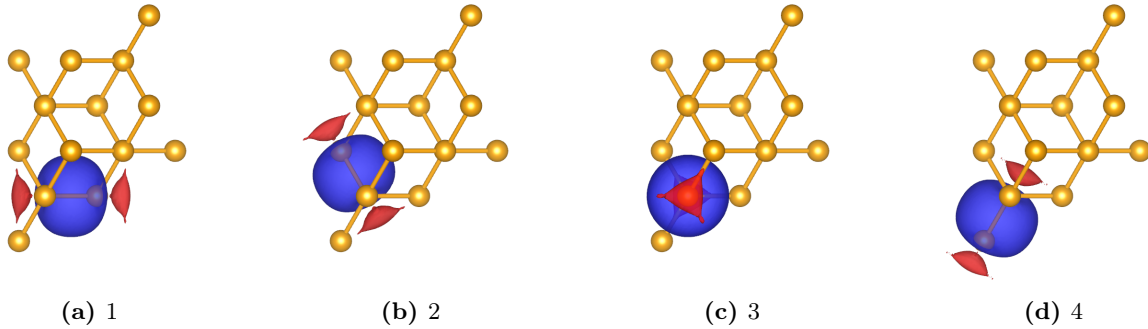


Figure 36: Four MLWFs for the valence manifold of Si.

Valence + Conduction States

- Outline: Obtain MLWFs for the valence and low-lying conduction-band states of Si. Plot the interpolated bandstructure. Apply a scissors correction to the conduction bands.
- Inspect the output file `silicon.wout`. The minimisation of the spread occurs in a two-step procedure. First, we minimise Ω_I – this is the extraction of the optimal subspace in the disentanglement procedure. Then, we minimise $\Omega_D + \Omega_{OD}$.

Converged values for the total spread functional and its components are shown in Tab. 10. The two groups of four MLWFs with sp^3 character are shown in Fig. 37

Extraction of optimally-connected subspace					
+-----					+<-- DIS
Iter	Omega_I(i-1)	Omega_I(i)	Delta (frac.)	Time	<-- DIS
+-----					+<-- DIS
1	12.97640155	12.44630235	4.259E-02	0.00	<-- DIS
.					
79	12.33580893	12.33580893	-6.531E-11	0.23	<-- DIS
80	12.33580893	12.33580893	-5.241E-11	0.23	<-- DIS
<<< Delta < 1.000E-10 over 3 iterations >>>					
<<< Disentanglement convergence criteria satisfied >>>					
Final Omega_I	12.33580893 (Ang^2)				
+-----					+-----

Table 10: Converged values of the components of spread functional and their sum, given in \AA^2 .

MP mesh	Ω	Ω_I	Ω_{OD}	Ω_D
$4 \times 4 \times 4$	17.54841	12.3358	5.03501	0.17759

Final State				
WF centre and spread	1	(1.807167, 1.807167, 1.807167)		2.01695824
WF centre and spread	2	(1.807167, 0.891636, 0.891636)		2.01695823
WF centre and spread	3	(0.891636, 1.807167, 0.891636)		2.01695823
WF centre and spread	4	(0.891636, 0.891636, 1.807167)		2.01695824
WF centre and spread	5	(0.226733, 0.226733, 0.226733)		2.37014516
WF centre and spread	6	(0.226733, -0.226733, -0.226733)		2.37014508
WF centre and spread	7	(-0.226733, 0.226733, -0.226733)		2.37014515
WF centre and spread	8	(-0.226733, -0.226733, 0.226733)		2.37014514
Sum of centres and spreads		(5.397608, 5.397608, 5.397608)		17.54841346
Spreads (Ang ²)	Omega I	=	12.335808933	
=====	Omega D	=	0.177593840	
	Omega OD	=	5.035010692	
Final Spread (Ang ²)	Omega Total	=	17.548413465	

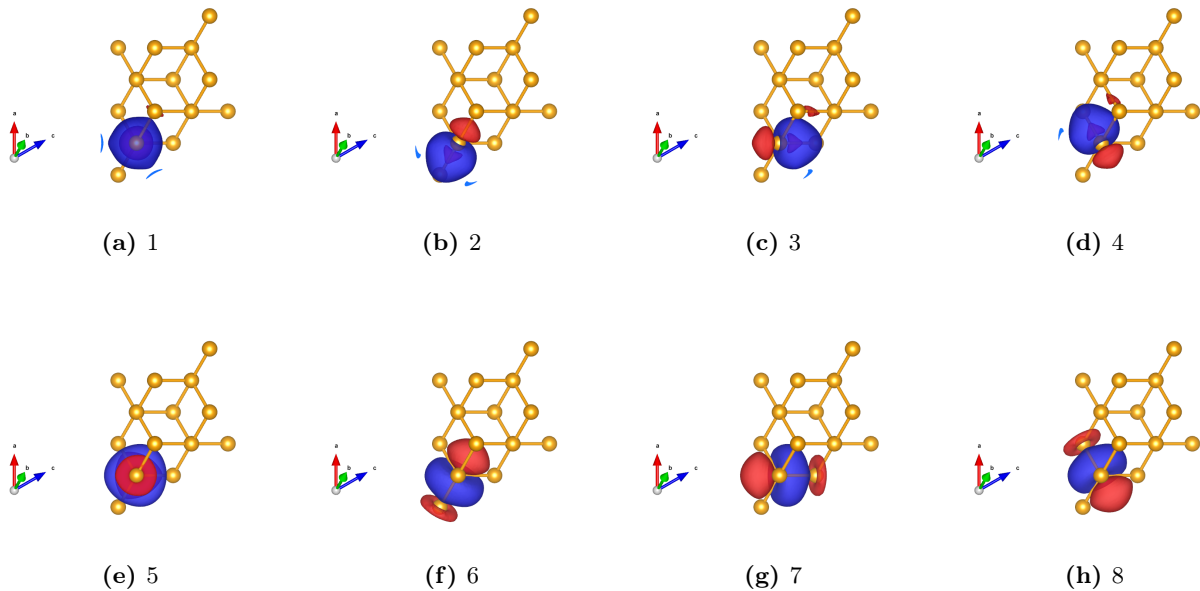


Figure 37: Eight MLWFs with sp^3 character, four on each Si atom in the unit cell.

- Plot the bandstructure.

The interpolated bandstructure is given in Fig. 38.

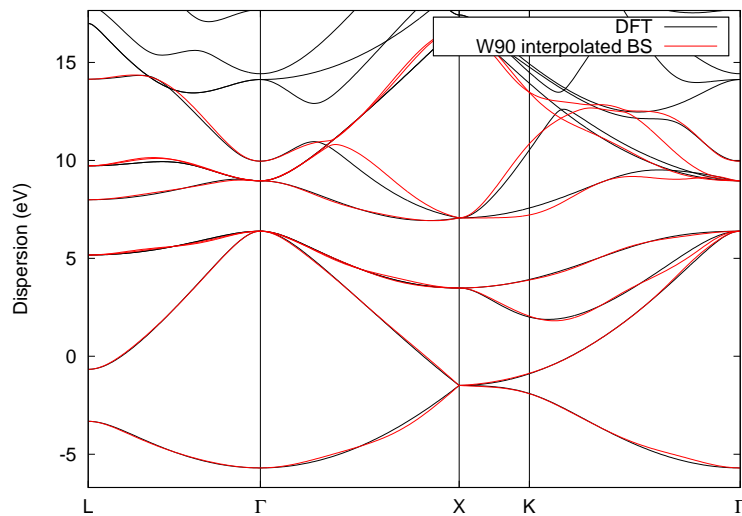


Figure 38: Bandstructure of silicon from DFT calculation (solid black) and from Wannier interpolation (solid red).

Further ideas

- Compare the Wannier-interpolated bandstructure with the full pwscf bandstructure with a finer k -point grid.

Result for a $8 \times 8 \times 8$ mesh is shown in Fig. 39.

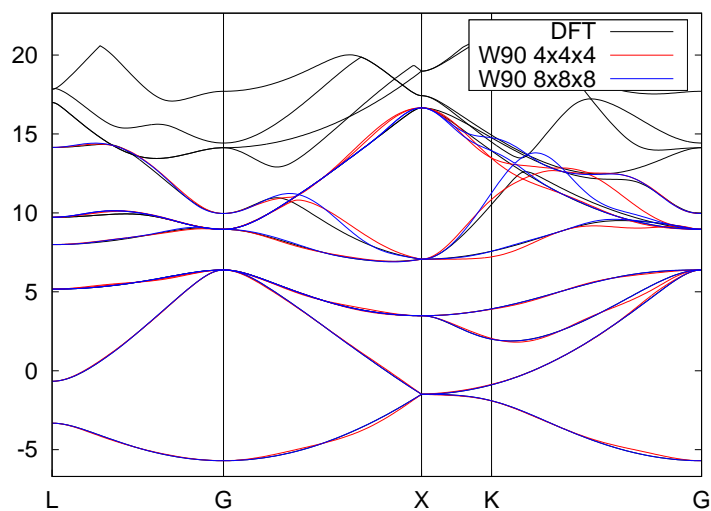


Figure 39: Bandstructure of silicon from DFT calculation (solid black) and from Wannier interpolation with a $4 \times 4 \times 4$ mesh (solid red) and $8 \times 8 \times 8$ mesh (solid blue).

- Compute four MLWFs spanning the low-lying conduction states.

The MLWFs spanning the 4 low-lying conduction states are shown in Fig. 40. The initial projections were 4 sp^3 on the Si atom at (0,0,0).

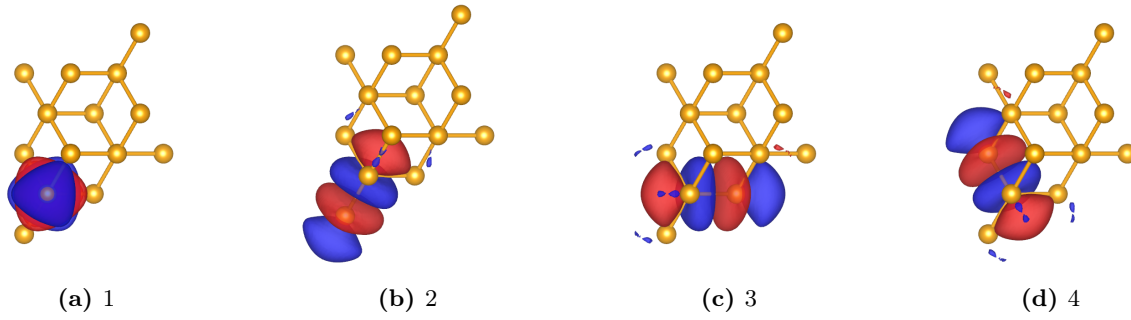


Figure 40

12: Benzene — valence and low lying conduction states

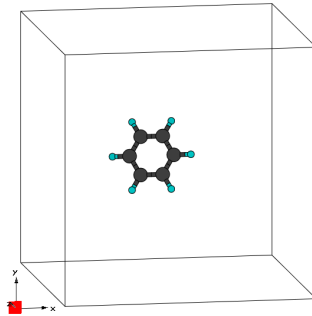


Figure 41: Benzene molecule in periodic cell plotted with the XCRYSDEN program.

Valence States

- Outline: *Obtain MLWFs for the valence bands of benzene.*

1-4 *Inspect the output file benzene.wout. The total spread converges to its minimum value after just a few iterations.*

Convergence of total spread Ω is shown in Fig. 43. The spread converges very quickly, and after only 15 iterations the $|\Delta\Omega|$ is already below 10^{-8} . Below is shown the final state of the minimization, after 22 iterations:

Final State				
WF centre and spread	1	(-6.875141, 7.935472, 7.937658)		0.65233309
WF centre and spread	2	(4.748245, 7.935472, 7.937658)		0.65234300
WF centre and spread	3	(5.809324, 6.097678, 7.937658)		0.65186298
WF centre and spread	4	(7.816785, -7.396927, 7.648002)		1.20135958
WF centre and spread	5	(7.816785, -7.396927, -7.648002)		1.20135948
WF centre and spread	6	(7.936083, 7.324218, -7.937658)		0.60992987
WF centre and spread	7	(7.935073, -6.095184, 7.937658)		0.65161009
WF centre and spread	8	(6.874208, -6.712573, 7.937658)		0.61134798
WF centre and spread	9	(6.874224, 6.850489, -7.648754)		1.20500764
WF centre and spread	10	(-7.936214, 6.097679, 7.937658)		0.65186256
WF centre and spread	11	(5.813353, -6.095183, 7.937658)		0.65160955
WF centre and spread	12	(6.874224, 6.850489, 7.648754)		1.20500766
WF centre and spread	13	(5.812342, 7.324217, 7.937658)		0.60993084
WF centre and spread	14	(5.931632, -7.396946, 7.648001)		1.20136423
WF centre and spread	15	(5.931632, -7.396946, -7.648001)		1.20136424
Sum of centres and spreads		(71.362557, 7.925029, 55.563607)		12.95829277
Spreads (Ang ²)		Omega I	=	10.455434168
=====		Omega D	=	0.000000000
		Omega OD	=	2.502858604
Final Spread (Ang ²)		Omega Total	=	12.958292772

5 *Plot the MLWFs 2-4*

MLWFs are shown in Fig. 42.

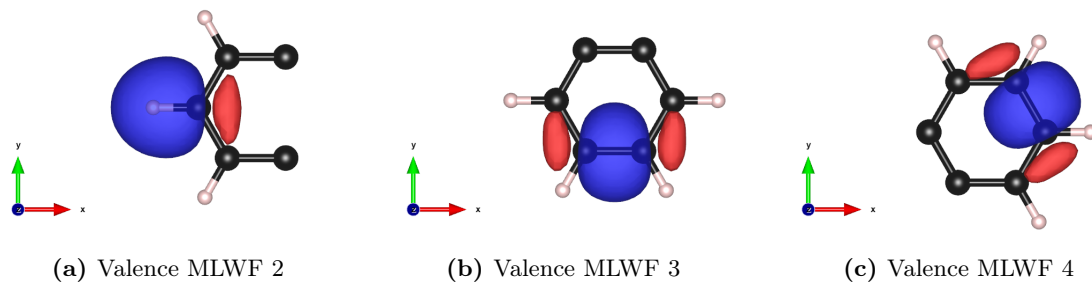


Figure 42: MLWFs 2, 3 and 4, with Vesta from cube format.

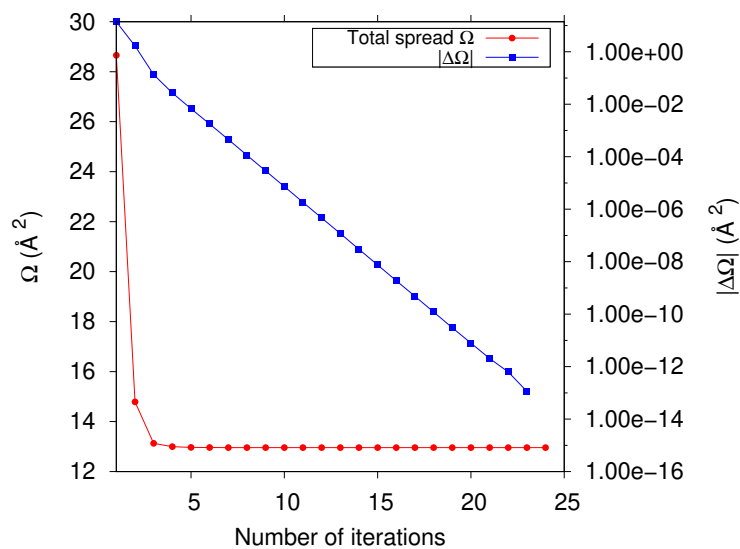


Figure 43: Convergence of total spread Ω . The red curve refers to the left y-axis, i.e. the actual value of the total spread at each iteration. The blue curve refers to the right y-axis, i.e. the absolute difference between between the spread functional at iteration i and $i - 1$, i.e. $\Delta\Omega$.

Valence + Conduction States

- Outline: *Obtain MLWFs for the valence and low-lying conduction states of benzene.*

1 *First, we minimise Ω_I . Then, we minimise $\Omega_D + \Omega_{OD}$.*

Extract from the `.wout` output file for the disentanglement procedure with initial and final value of Ω_I

Below a snippet from the `.wout` output file, showing the finale state of the minimisation of Ω_D and Ω_{OD} .

2 *Plot the MLWFs 1, 7 and 13.*

MLWFs are shown in Fig. 44.

```

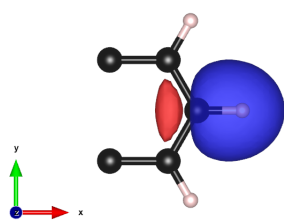
                                Extraction of optimally-connected subspace
                                -----
+-----+-----+-----+-----+-----+-----+<-- DIS
| Iter   Omega_I(i-1)   Omega_I(i)   Delta (frac.)   Time   |<-- DIS
+-----+-----+-----+-----+-----+-----+<-- DIS
      1     14.77292507     14.36793746     2.819E-02     0.06   <-- DIS
      . . . . .
      . . . . .
     76     14.26979011     14.26979011     7.234E-11     0.34   <-- DIS

      <<<      Delta < 1.000E-10 over 3 iterations      >>>
      <<< Disentanglement convergence criteria satisfied >>>

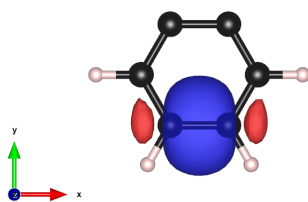
      Final Omega_I   14.26979011 (Ang^2)

+-----+-----+-----+-----+-----+-----+

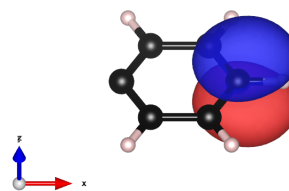
```



(a) Valence MLWF 1



(b) Valence MLWF 7



(c) Conduction MLWF 13

Figure 44: MLWFs 1, 3 and 13 with Vesta from cube format.

Final State

WF centre and spread	1	(-6.872991, -7.937658, 7.937657)	0.64685210
WF centre and spread	2	(-7.937084, -6.094542, -7.937656)	0.64620663
WF centre and spread	3	(5.810194, -6.094542, 7.937654)	0.64620672
WF centre and spread	4	(4.746097, -7.937658, 7.937657)	0.64685949
WF centre and spread	5	(5.810193, 6.094541, -7.937657)	0.64620720
WF centre and spread	6	(-7.937083, 6.094541, 7.937655)	0.64620743
WF centre and spread	7	(6.874209, 6.725491, 7.937658)	0.58709128
WF centre and spread	8	(6.874209, -6.725491, 7.937657)	0.58709059
WF centre and spread	9	(5.824168, -7.331141, 7.937657)	0.58581741
WF centre and spread	10	(5.824168, 7.331141, -7.937658)	0.58581778
WF centre and spread	11	(7.924257, 7.331142, 7.937657)	0.58581692
WF centre and spread	12	(7.924257, -7.331141, -7.937658)	0.58581674
WF centre and spread	13	(-7.514755, 7.937658, -7.937656)	1.57077288
WF centre and spread	14	(7.622957, -6.642249, 7.937655)	1.58413409
WF centre and spread	15	(6.125499, -6.642276, -7.937651)	1.58406298
WF centre and spread	16	(5.387848, -7.937658, -7.937656)	1.57079972
WF centre and spread	17	(6.125498, 6.642275, 7.937656)	1.58407213
WF centre and spread	18	(7.622957, 6.642249, -7.937653)	1.58414266
Sum of centres and spreads		(60.234596, -15.875317, 15.875317)	16.87397474

Spreads (Ang ²)	Omega I	=	14.269790106
=====	Omega D	=	0.000000000
	Omega OD	=	2.604184635
Final Spread (Ang ²)	Omega Total	=	16.873974742

13: (5,5) Carbon Nanotube — Transport properties

- Outline: Obtain the bandstructure, quantum conductance and density of states of a metallic (5,5) carbon nanotube.

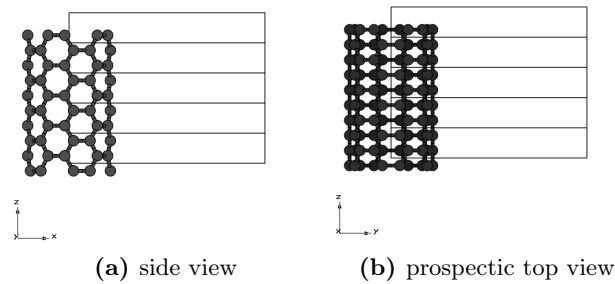


Figure 45: 5 unit cells for the carbon nanotube system from a) side view and b) prospective top view plotted with the XCRYSDEN program.

- 1 Run `pwscf` and `wannier90`. Inspect the output file `cnt55.wout`. The minimisation of the spread occurs in a two-step procedure. First, we minimise Ω_I . Then, we minimise $\Omega_D + \Omega_{OD}$.

Below, an extract from the `.wout` file showing a summary of the disentanglement procedure (minimisation of Ω_I)

```

                                Extraction of optimally-connected subspace
                                -----
+-----+-----+-----+-----+-----+-----+-----+-----+
| Iter   Omega_I(i-1)   Omega_I(i)   Delta (frac.)   Time   |<-- DIS
+-----+-----+-----+-----+-----+-----+-----+-----+
|   1    33.96797815    33.91073784    1.688E-03    0.00   |<-- DIS
|   2    33.92937273    33.90274574    7.854E-04    0.02   |<-- DIS
|   . . . . .
|   . . . . .
|  45    33.89889125    33.89889125    4.172E-11    0.50   |<-- DIS
|  46    33.89889125    33.89889125    1.626E-11    0.51   |<-- DIS
|
|          <<<   Delta < 1.000E-10 over 3 iterations   >>>
|          <<< Disentanglement convergence criteria satisfied >>>
|
|          Final Omega_I   33.89889125 (Ang^2)
+-----+-----+-----+-----+-----+-----+-----+-----+

```

Below, an extract from the `.wout` file showing the final state for the minimisation of $\Omega_D + \Omega_{ODs}$

```

Final State
WF centre and spread  1 ( -6.875141,  7.935472,  7.937658 )    0.65233309
WF centre and spread  2 (  4.748245,  7.935472,  7.937658 )    0.65234300
WF centre and spread  3 (  5.809324,  6.097678,  7.937658 )    0.65186298
WF centre and spread  4 (  7.816785, -7.396927,  7.648002 )    1.20135958
WF centre and spread  5 (  7.816785, -7.396927, -7.648002 )   1.20135948
WF centre and spread  6 (  7.936083,  7.324218, -7.937658 )    0.60992987
WF centre and spread  7 (  7.935073, -6.095184,  7.937658 )    0.65161009
WF centre and spread  8 (  6.874208, -6.712573,  7.937658 )    0.61134798
WF centre and spread  9 (  6.874224,  6.850489, -7.648754 )    1.20500764
WF centre and spread 10 ( -7.936214,  6.097679,  7.937658 )    0.65186256
WF centre and spread 11 (  5.813353, -6.095183,  7.937658 )    0.65160955
WF centre and spread 12 (  6.874224,  6.850489,  7.648754 )    1.20500766
WF centre and spread 13 (  5.812342,  7.324217,  7.937658 )    0.60993084
WF centre and spread 14 (  5.931632, -7.396946,  7.648001 )    1.20136423
WF centre and spread 15 (  5.931632, -7.396946, -7.648001 )   1.20136424
Sum of centres and spreads ( 71.362557,  7.925029, 55.563607 ) 12.95829277

      Spreads (Ang^2)      Omega I      =      10.455434168
=====
                          Omega D      =      0.000000000
                          Omega OD     =      2.502858604
Final Spread (Ang^2)      Omega Total  =      12.958292772
-----

```

2. Note that the initial p_z projections on the carbon atoms are oriented in the radial direction with respect to the nanotube axis.

Begin Projections

Ang

c= 3.3780, -0.7128, -0.6157 :pz :z= 3.3780, -0.7128, 0.0000 :x=0,0,1

3. The interpolated bandstructure is written to `cnt55_band.agr`

To plot the interpolated bands, the quantum conductance and the Density of States as shown in Fig. 6 in the WANNIER90 tutorial, one can use the `xmgrace` program.

XMGRACE TUTORIAL

Run the `xmgrace` plotting program from command line as

```
$ > xmgrace
```

Before importing the data to be plotted, we have to reorganize the layout by selecting

```
Edit ↪ Arrange graphs...
```

here we can generate a grid of graphs by selecting the number of columns and rows from the drop menus. For this particular example, we want to increase the number of columns to 3, i.e. **Cols: 3** and leave the number of rows to 1 in the **Matrix** section. Moreover, we don't want any gap between the graphs so we also need to modify the value of **Hgap/width** in the bottom **Spacing** section, i.e. **Hgap/width 0**. Once we have generated the three graphs we need to import the data. This can be achieved by

```
Data ↪ Import ↪ ASCII...
```

The three files to import are `cnt_band.agr`, `cnt_qc.dat` and `cnt_dos.dat`, respectively. For each file we need to select the graph in the **Read to graph:** section, i.e. **G(0)**, **G(1)** and **G(2)**, respectively.

In order to flip the x-axis with the y-axis, one need to perform the following

```
Data ↪ Transformations ↪ Evaluate expressions...
```

In the **Formula:** section write

```
s1.x=s0.y; s1.y=s0.x
```

and then click apply.

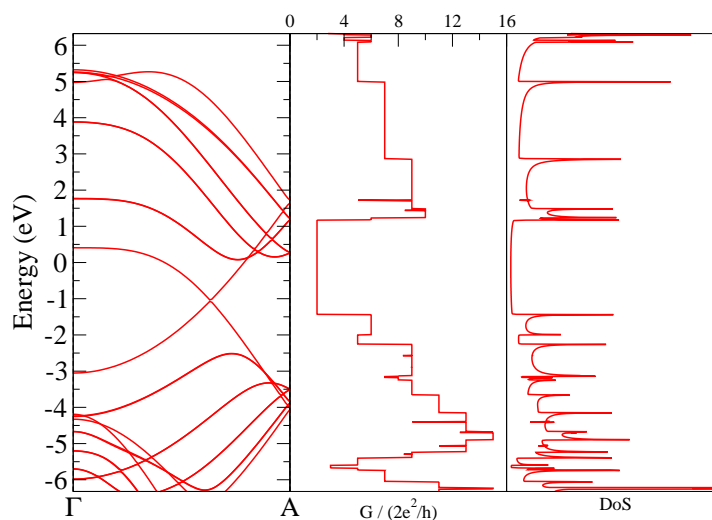
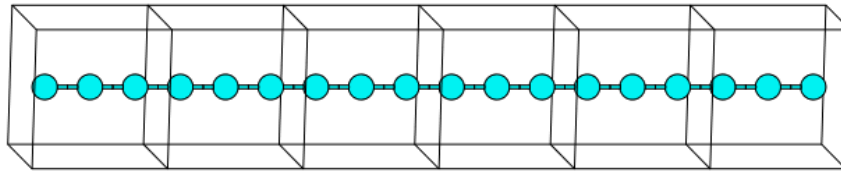


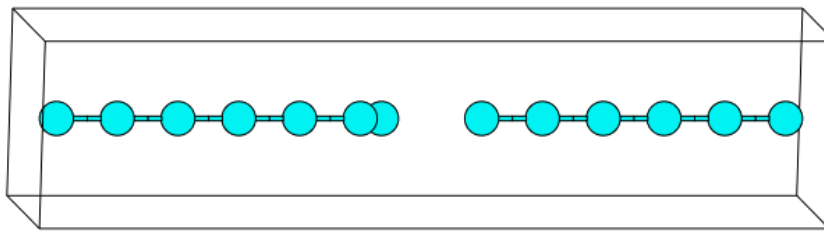
Figure 46: Reproduction of Fig. 6 in the WANNIER90 tutorial.

14: Linear Sodium Chain — Transport properties

- Outline: Compare the quantum conductance of a periodic linear chain of Sodium atoms with that of a defected chain



(a) periodic



(b) defected

Figure 47: Unit cell of a periodic linear Sodium chain (left panel) and of a defected linear Sodium chain (right panel) plotted with the XCRYSDEN program. The former consists of 2 Na atom per unit cell (6 unit cells have been drawn for comparison with the defected system). The latter consists of 13 Na atoms per unit cell.

1-2 Run *pwscf* and *wannier90* for the periodic and defected systems.

- 3 Compare the quantum conductance of the periodic (bulk) calculation with the defected (LCR) calculation.

The quantum conductance and the DOS are shown in Fig. 48.

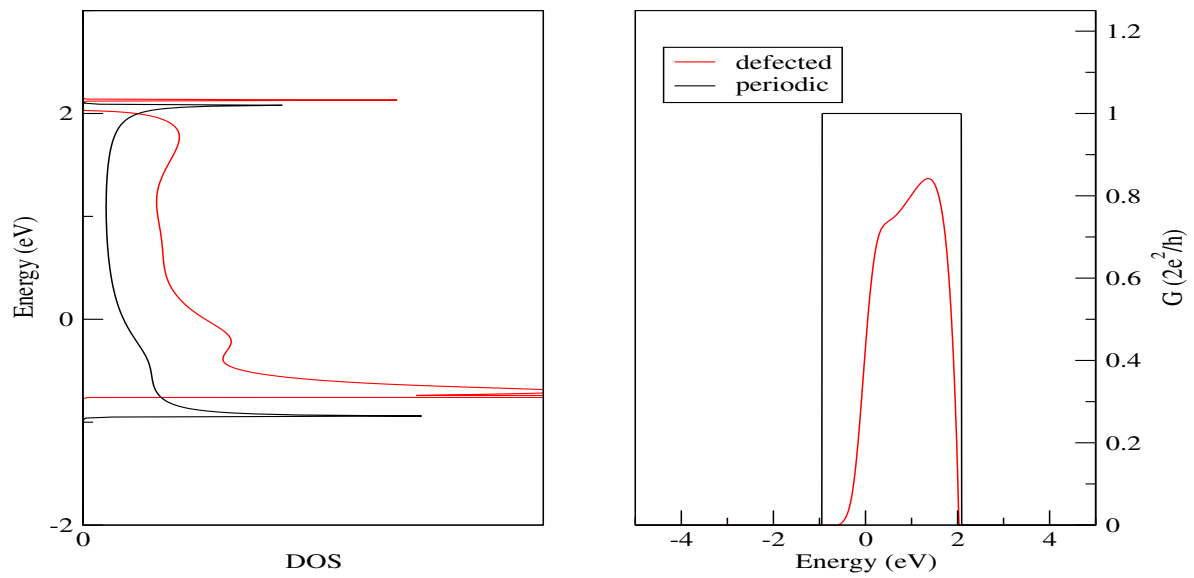


Figure 48: DOS (left) and quantum conductance (right) of periodic (solid black) and defected (solid red) Sodium linear chain.

15: (5,0) Carbon Nanotube — Transport properties

16: Silicon — Boltzmann transport

- Outline: *Obtain MLWFs for the valence and low-lying conduction states of Si. Calculate the electrical conductivity, the Seebeck coefficient and the thermal conductivity in the constant relaxation time approximation using the BoltzWann module.*

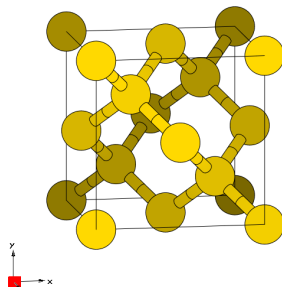


Figure 49: Unit cell of Silicon crystal plotted with the XCRYSDEN program.

1-5 For this example we are only going to show the solutions from point 6 onwards, as the first 5 steps are the usual steps to obtain MLWFs.

6 Run `postw90` to calculate the transport coefficients.

- Inspect the output file `Si.wpout`. Check if no warnings are issued. Note that if no special flags are passed to `BOLTZWANN`, it assumes that the *ab initio* calculation did not include magnetization effects, and thus it sets to 2 the number of electrons per state.

Below the section in the `Si.wpout` relative to the Boltzmann transport, where it reports the number of electrons per state and the relaxation time in fs.

```

*-----*
|           Boltzmann Transport (BoltzWann module)           |
*-----*
| Please cite the following paper when publishing results obtained using |
| the BoltzWann module:                                             |
| G. Pizzi, D. Volja, B. Kozinsky, M. Fornari, and N. Marzari,    |
| Comp. Phys. Comm. 185, 422 (2014); DOI:10.1016/j.cpc.2013.09.015 |
*-----*

Calculating Transport Distribution function (TDF) and DOS...
  k-grid used for band interpolation in BoltzWann: 40x40x40
  Number of electrons per state: 2
  Relaxation time (fs):    10.00000000
TDF and DOS calculated.

Transport properties calculated.

*-----*
|           End of the BoltzWann module           |
*-----*

```

Using your favourite plotting program, plot the `Si_boltzdos.dat` file to inspect the DOS.

Plot shown in Fig. 50-(a).

Using your favourite plotting program, plot columns 1 and 3 of the `Si_seebeck.dat` file to inspect the S_{xx} component of the Seebeck coefficient as a function of the chemical potential μ , at $T = 300$ K.

Plot shown in Fig. 50-(b).

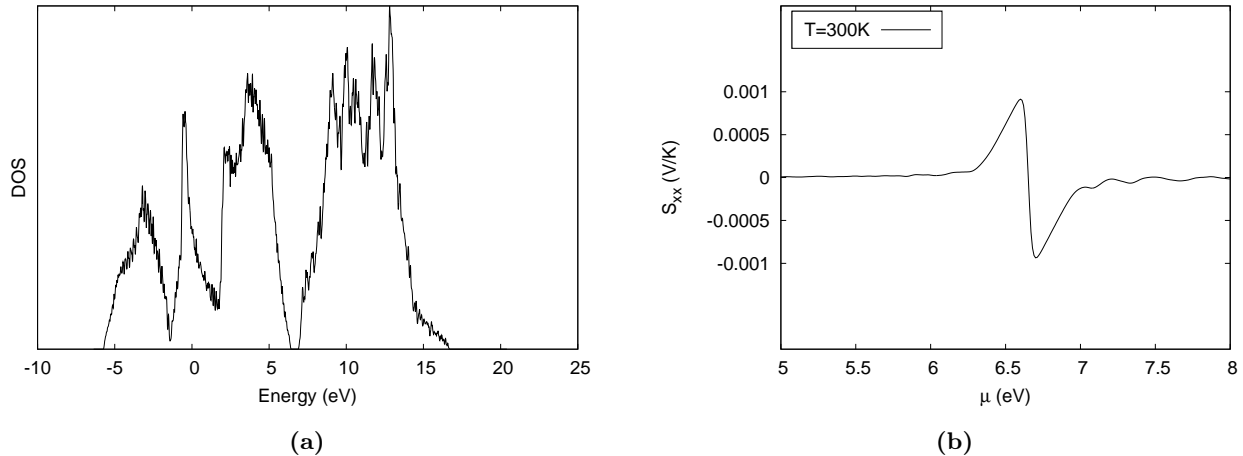


Figure 50: Panel (a) DOS of Silicon computed with BOLTZWANN. Panel (b) S_{xx} component of the Seebeck tensor as function of the chemical potential μ computed with BOLTZWANN at $T = 300$ K.

Further ideas

- Change the interpolation to a $60 \times 60 \times 60$ mesh and run again `postw90` to check if the results for the transport properties are converged.

Plot of the two DOS with $40 \times 40 \times 40$ (red line) and $60 \times 60 \times 60$ (blue line) are shown in Fig. 51. We can see that all the peaks for the valence and conduction states in the $60 \times 60 \times 60$ DOS are also reproduced in the $40 \times 40 \times 40$ DOS (even though there is some noise, which however does not affect the qualitative description.)

- Change the `Si.win` input file so that it calculates the transport coefficients for temperatures from 300 to 700 K, with steps of 200 K. Rerun `postw90` and verify that the increase in execution time is negligible (in fact, most of the time is spent to interpolate the band structure on the k mesh). Plot the Seebeck coefficient for the three temperatures $T = 300$ K, $T = 500$ K and $T = 700$ K. To do this, you have to filter the `Si_seebeck.dat` to select only those lines where the second column is equal to the required temperature. A possible script to select the S_{xx} component of the Seebeck coefficient for $T = 500$ K using the `awk/gawk` command line program is the following:

```
awk 'if ($2 == 500) print $1, $3;' < Si_seebeck.dat > Si_seebeck_xx_500K.dat
```

Below is shown the total wall-time for the two calculations done with the original set up, i.e. $T_{min} = T_{max} = 300$ K and $T_{min} = 300$ K, $T_{max} = 700$ K, $\Delta T = 200$ K.

Total Execution Time	16.356 (sec)
----------------------	--------------

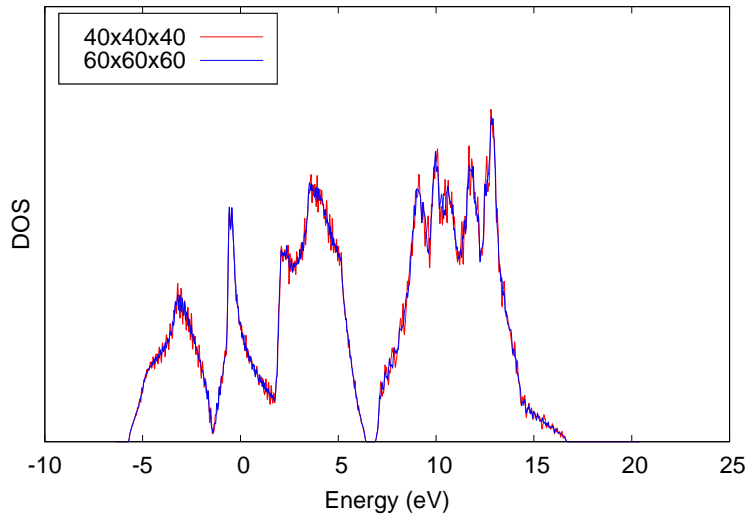


Figure 51: Convergence of DOS

Total Execution Time	16.108 (sec)
----------------------	--------------

The plot of $S_{xx}(\mu)$ for different values of T is shown in Fig. 52

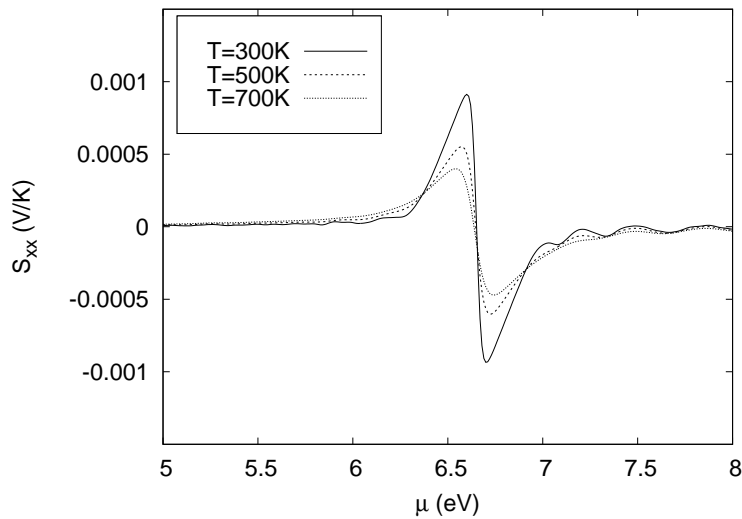


Figure 52: S_{xx} component of the Seebeck tensor as function of the chemical potential μ for different values of the temperature: $T = 300$ K (solid purple), $T = 500$ K (solid green) and $T = 700$ K (solid blue).

- Try to calculate the Seebeck coefficient as a function of the temperature, for a n -doped sample with, e.g., $n = 10^{18} \text{ cm}^{-3}$. Note that to this aim, you need to calculate consistently the value $\mu(T)$

Table 11: Values of the chemical potential μ in eV as a function of T in K, computed by numerically solving Eq. 2.

T [K]	μ [eV]
300	6.839
400	6.798
500	6.752
600	6.707
700	6.677

of the chemical potential as a function of the temperature, so as to reproduce the given value of n . Then, you have to write a small program/script to interpolate the output of BOLTZWANN, that you should have run on a suitable grid of (μ, T) points.

ASSUMPTIONS: 1) The addition of a n -type dopant does not modify the electronic structure, it only moves the Fermi level up; 2) The density of states is temperature-independent. $\mu(T)$ is a decreasing monotonic function of T .

To obtain a $\mu(T)$ in a consistent way we use the above assumptions and the following equation:

$$N_c + N_v = \int_{-\infty}^{+\infty} d\varepsilon g(\varepsilon, T = 0) f(\varepsilon, \mu(T)), \quad (2)$$

where $N_v = 8$, number of valence electrons per unit cell when no dopants are considered, $N_c = nV_{cell}$ is the number of carriers per unit cell (V_{cell} is the volume of the unit cell in cm^{-3}). $g(\varepsilon, T = 0)$ is the density of states at $T = 0\text{K}$ and by assumption it does not change with T . Finally, $f(\varepsilon, \mu(T))$ is the Fermi-Dirac distribution as a function of ε and T

$$f(\varepsilon, \mu(T)) = \frac{1}{1 + \exp\left[\frac{\varepsilon - \mu(T)}{\kappa_B T}\right]} \quad (3)$$

For each T we find the value of the $\mu(T)$ such as the integral is (approximately) $N_c + N_v$.² The values of μ for T in the range [300 K-700 K] are shown in Tab. 11

In practice we do not perform an interpolation but we run a single calculation with $\Delta\mu = 0.001$ eV since these are not expensive and then we filter out the result from `Si_seebeck.dat` with the following simple script

```
mulist='cat mu.dat | awk 'printf "i4" $1''; i=0; for mu in $mulist; do i='echo
$i+1|bc' ; cat Si_seebeck.dat | awk -v "mu=$mu" 'if($1==mu) print $1,$2,$3,$7,$11'
| awk -v "Tcol=$i" 'if(NR==Tcol) print $1, $2, $3, $4, $5' » Si_seebeck_vs_T.dat;done
```

where `mu.dat` is a data file containing the second column of Tab. 11. Fig. 53 shows the plots of the diagonal coefficients of the Seebeck tensor with respect to T generated by the above script and stored in `Si_seebeck_vs_T.dat`.

²This can be easily achieved with any code, e.g. Python, MATLAB or even bash.

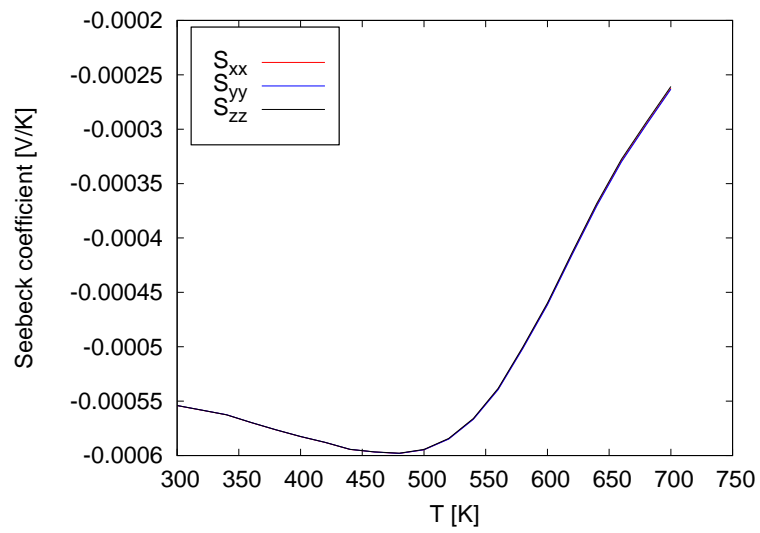


Figure 53

17: Iron — Spin-orbit-coupled bands and Fermi-surface contours

- Outline: *Plot the spin-orbit-coupled bands of ferromagnetic bcc Fe. Plot the Fermi-surface contours on a plane in the Brillouin zone.*

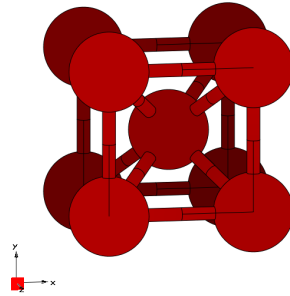


Figure 54: Unit cell of Iron crystal plotted with the XCRYSDEN program.

1-6 Compute the MLWFs and compute the energy eigenvalues and spin expectation values.

The final state for all the 18 MLWFs is

Final State			
WF centre and spread	1	(-0.709848, 0.000000, 0.000000)	1.08973288
WF centre and spread	2	(-0.685480, -0.000000, 0.000000)	1.10285536
WF centre and spread	3	(0.709848, -0.000000, 0.000000)	1.08973288
WF centre and spread	4	(0.685480, -0.000000, 0.000000)	1.10285536
WF centre and spread	5	(-0.000000, -0.709848, 0.000000)	1.08973287
WF centre and spread	6	(0.000000, -0.685480, 0.000000)	1.10285536
WF centre and spread	7	(0.000000, 0.709848, 0.000000)	1.08973288
WF centre and spread	8	(0.000000, 0.685480, 0.000000)	1.10285536
WF centre and spread	9	(0.000000, -0.000000, -0.709835)	1.08977307
WF centre and spread	10	(0.000000, -0.000000, -0.685503)	1.10302800
WF centre and spread	11	(-0.000000, -0.000000, 0.709835)	1.08977304
WF centre and spread	12	(0.000000, -0.000000, 0.685503)	1.10302800
WF centre and spread	13	(-0.000000, -0.000000, -0.000000)	0.43232470
WF centre and spread	14	(-0.000000, -0.000000, -0.000000)	0.41118748
WF centre and spread	15	(0.000000, 0.000000, -0.000000)	0.43232470
WF centre and spread	16	(0.000000, 0.000000, -0.000000)	0.41118748
WF centre and spread	17	(-0.000000, 0.000000, 0.000000)	0.43232866
WF centre and spread	18	(-0.000000, 0.000000, 0.000000)	0.41119649
Sum of centres and spreads		(0.000000, 0.000000, 0.000000)	15.68650457
Spreads (Ang ²)	Omega I	=	11.898334117
=====	Omega D	=	0.031570932
	Omega OD	=	3.756599523
Final Spread (Ang ²)	Omega Total	=	15.686504572

To plot the bands using python

```
$> python Fe-bands.py
```

The interpolated band structure of Fe with spin-orbit interaction using the module `kpath` is shown in Fig. 55. The color scheme is used to show the expectation value of the spin operator \hat{S}_z in units of $\hbar/2$.

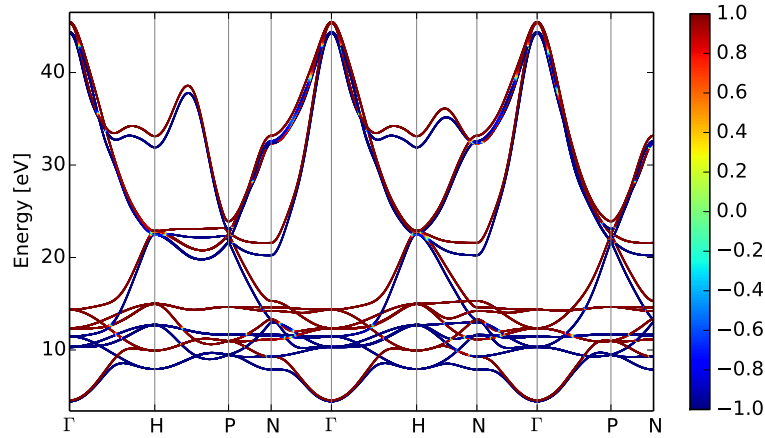


Figure 55: WANNIER90 interpolated bands of Fe computed from a DFT calculation with spin-orbit interaction. Colour-scheme shows the expectation value $\langle \hat{S}_z \rangle$ in units of $\hbar/2$.

Next we plot the Fermi-surface contours on the (010) plane $k_y = 0$, using the `kslice` module.

Further ideas

- Redraw the Fermi surface contours on the (010) plane starting from a calculation without spin-orbit coupling (SOC), by adding to the input files `iron_{up,down}.win` in Example 8. The Fermi surface contours on the (010) plane without SOC are shown in Fig. 57-(a).
- For a spinor calculation we can still spin-decompose the DOS.

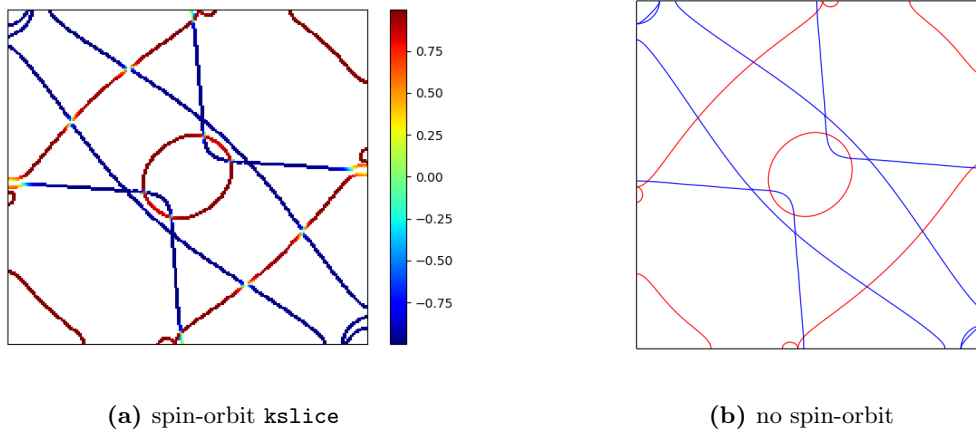


Figure 56

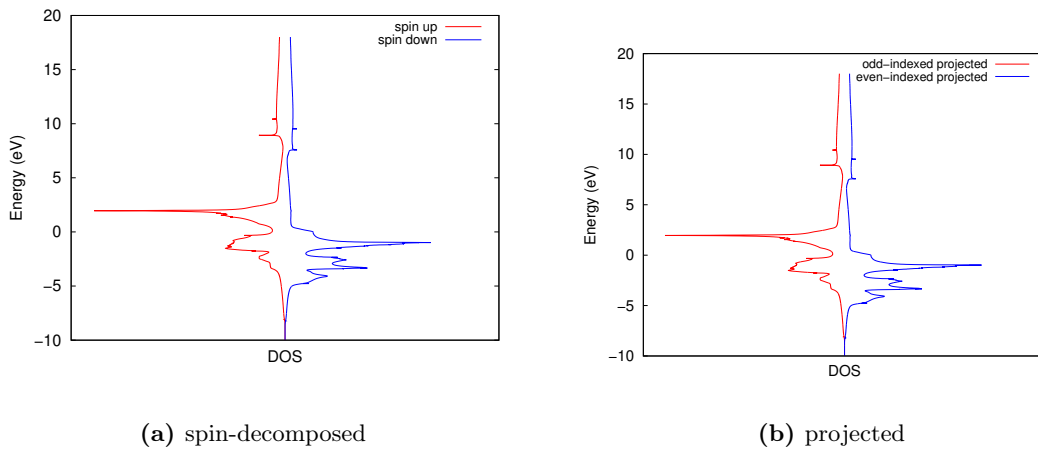


Figure 57: Spin-decomposed DOS (panel a) with spin-up (red) and spin-down (blue) components. Projected DOS on odd-indexed MLWFs (red) and even-indexed (blue).

18: Iron—Berry curvature, anomalous Hall conductivity and optical conductivity

- Outline: Calculate the Berry curvature, anomalous Hall conductivity, and (magneto)optical conductivity of ferromagnetic bcc Fe with spin-orbit coupling. In preparation for this example it may be useful to read Ref. 3 and Ch. 11 of the User Guide.

1-6 Compute the MLWFs and compute the energy eigenvalues and spin expectation values.

These are the same six steps of Ex. 17 and therefore the results are not going to be showed here again.

Berry curvature plots

- The Berry curvature $\Omega_{\alpha\beta}(\mathbf{k})$ of the occupied states is defined in Eq. (11.18) of the User Guide. Plot the Berry curvature component $\Omega_z(\mathbf{k}) = \Omega_{xy}(\mathbf{k})$ along the magnetization direction.

The Fermi energy should be 12.6283 eV. With this value we obtain the energy bands and the Berry curvature component $\Omega_z(\mathbf{k}) = \Omega_{xy}(\mathbf{k})$ along high-symmetry points shown in Fig. 58 and Fig. 59. Eq. (11.18) of the User Guide is reported below for completeness.

$$\Omega_{\alpha\beta}(\mathbf{k}) = \sum_n^{occ} f_{n\mathbf{k}} \Omega_{n,\alpha\beta}, \quad (4)$$

with

$$\Omega_{n,\alpha\beta} = \varepsilon_{\alpha\beta\gamma} \Omega_{n,\gamma} = -2 \operatorname{Im} \langle \nabla_{k\alpha} u_{n\mathbf{k}} | \nabla_{k\beta} u_{n\mathbf{k}} \rangle, \quad (5)$$

where the Greek letters indicate Cartesian coordinates, $\varepsilon_{\alpha\beta\gamma}$ is the Levi-Civita antisymmetric tensor, and $|u_{n\mathbf{k}}\rangle$ s are the cell-periodic Bloch functions.

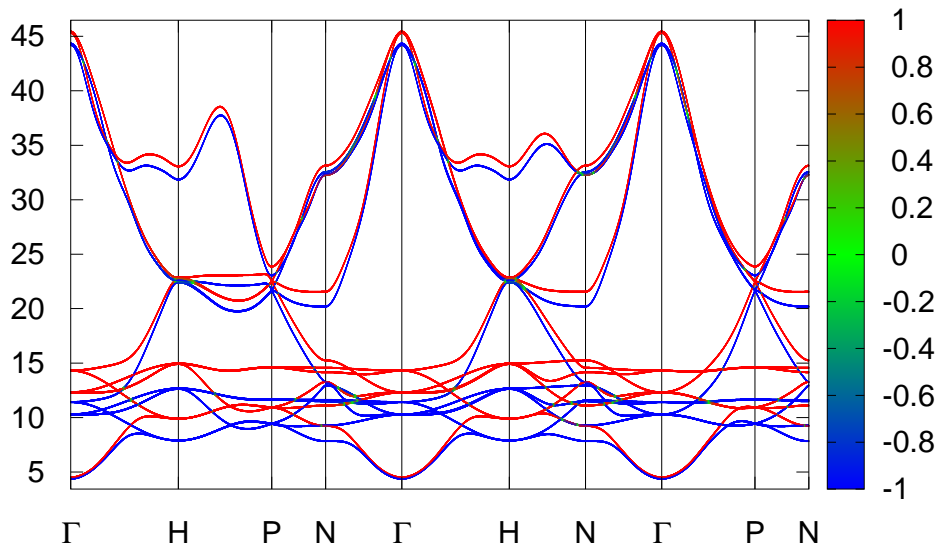


Figure 58: Band structure of Fe along symmetry lines Γ -H-P-N- Γ -H-N- Γ -P-N.

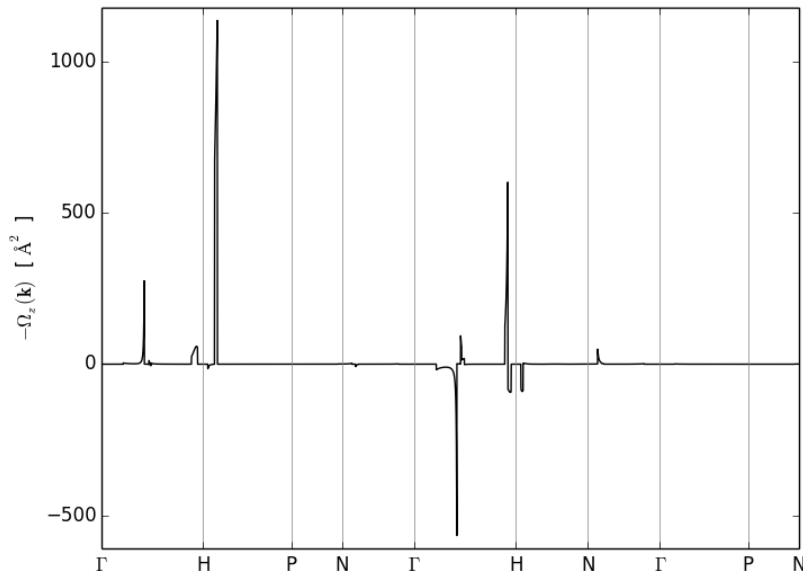


Figure 59: Berry curvature $\Omega_z(\mathbf{k})$ in Fe along symmetry lines.

- Combine the plot of the Fermi lines on the k_y plane with a heat-map plot of (minus) the Berry curvature

The plot of the Fermi lines with a colour-map of $-\Omega_z(k_x, 0, k_z)$ is shown in Fig. 59.

Anomalous Hall conductivity

- AHC converges rather slowly with k -point sampling, and a $25 \times 25 \times 25$ does not yield a well-converged value. Compare the converged AHC value with those obtained in Refs. 4 and 3.

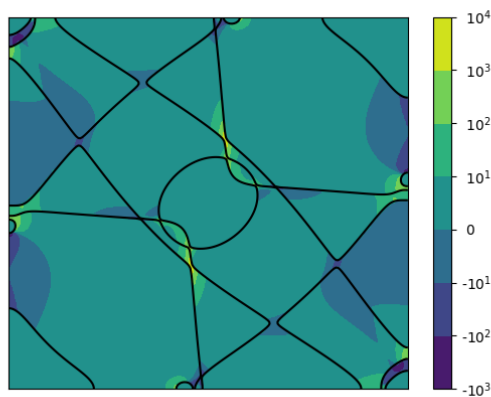


Figure 60: (Colour online) Calculated total Berry curvature $-\Omega_z(\mathbf{k})$ in the plane $k_y = 0$ (note log scale). Intersections of the Fermi surface with this plane are shown.

The x, y, z -components of the AHC for a $25 \times 25 \times 25$ BZ mesh are shown in the snippet below. The converged result reported in Refs. 4 and 3 for the z -component is $756.76 \text{ ((}\Omega\text{cm)}^{-1})$. Hence, a $25 \times 25 \times 25$ BZ mesh clearly gives a very inaccurate value ($\sim 36.4\%$ error). Even with adaptive refinement the error is still very large ($\sim 31.7\%$). It is worth to note that the adaptive refinement slightly breaks the symmetry and gives non-zero values for the x -component and y -component, although these are opposite in sign.

```

Without adaptive refinement

Properties calculated in module b e r r y
-----

* Anomalous Hall conductivity

Interpolation grid: 25 25 25

Fermi energy (ev): 12.6283

AHC (S/cm)      x      y      z
=====      -0.0000   0.0000  554.6437

Total Execution Time      59.112 (sec)

```

```

With adaptive refinement

Properties calculated in module b e r r y
-----

* Anomalous Hall conductivity

Regular interpolation grid: 25 25 25
Adaptive refinement grid: 5 5 5
  Refinement threshold: Berry curvature >100.00 bohr^2
Points triggering refinement: 42( 0.27%)

Fermi energy (ev): 12.6283

AHC (S/cm)      x      y      z
=====      2.4602  -2.4602  574.2950

```

Since these are quite demanding calculations, we only report the value of the AHC for a $125 \times 125 \times 125$ BZ mesh with a $5 \times 5 \times 5$ adaptive refinement grid (see snippet below). The value for the z -component is $729.8276 \text{ ((}\Omega\text{cm)}^{-1})$, which is in much closer agreement with the converged result from Refs. 4 and 3. Also, the magnitude of x, y -component is greatly reduced as expected.

```
125 x 125 x 125 BZ mesh with a 5 x 5 x 5 adaptive refinement grid
```

```
Properties calculated in module b e r r y
```

```
-----
* Anomalous Hall conductivity

Regular interpolation grid: 125 125 125
Adaptive refinement grid: 5 5 5
Refinement threshold: Berry curvature >100.00 Ang^2
Points triggering refinement: 1818( 0.09%)

Fermi energy (ev): 12.6283

AHC (S/cm)      x          y          z
=====
-0.2775         0.2775         729.8276
```

- The Wannier-interpolation formula for the Berry curvature comprises three terms, denoted J_0 , J_1 , and J_2 in Ref. 5.

From Ref. 4

$$-2 \operatorname{Im} G_{\alpha\beta} = J_0 + J_1 + J_2, \quad (6)$$

where

$$G_{\alpha\beta} = \operatorname{Tr}[(\partial_\alpha \hat{P}) \hat{Q} \hat{H} \hat{Q} (\partial_\beta \hat{P})] \quad (7)$$

The three components J_0 , J_1 and J_2 for the k -point sampling of $125 \times 125 \times 125$ and a $5 \times 5 \times 5$ adaptive refinement grid are shown in the snippet below

```
J0 term :      0.0002      -0.0002      2.8479
J1 term :      0.0004      -0.0004      18.4855
J2 term :     -0.2782       0.2782     708.4942
-----
```

Optical conductivity

- The optical conductivity tensor of bcc Fe with magnetization along $\hat{\mathbf{z}}$ has the form

$$\boldsymbol{\sigma} = \boldsymbol{\sigma}_S + \boldsymbol{\sigma}_A = \begin{pmatrix} \sigma_{xx} & 0 & 0 \\ 0 & \sigma_{yy} = \sigma_{xx} & 0 \\ 0 & 0 & \sigma_{zz} \end{pmatrix} + \begin{pmatrix} 0 & \sigma_{xy} & 0 \\ -\sigma_{yx} & 0 & 0 \\ 0 & 0 & 0 \end{pmatrix} \quad (8)$$

- The DC AHC calculated earlier corresponds to σ_{xy} in the limit $\omega \rightarrow 0$. At finite frequency $\sigma_{xy} = -\sigma_{yx}$ acquires an imaginary part which describes magnetic circular dichroism (MCD). Compute the complex optical conductivity for $\hbar\omega$ up to 7 eV

The plot for the ac AHC is shown in Fig. 61.

- Compare the $\omega \rightarrow 0$ limit of σ_{xy} with the result obtained earlier by integrating the Berry curvature.

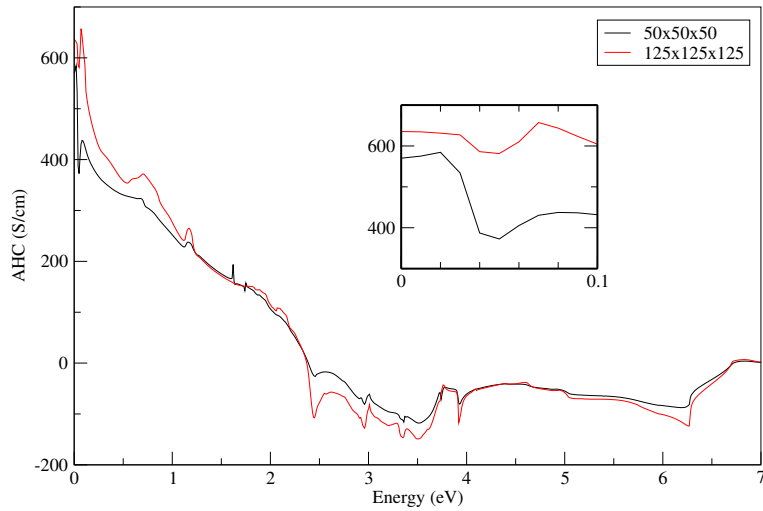


Figure 61: Plot of the real part of the complex optical conductivity with a $50 \times 50 \times 50$ k -point mesh (black) and $125 \times 125 \times 125$ k -point mesh (red). The inset is a magnification of the region $[0-0.1]$ eV.

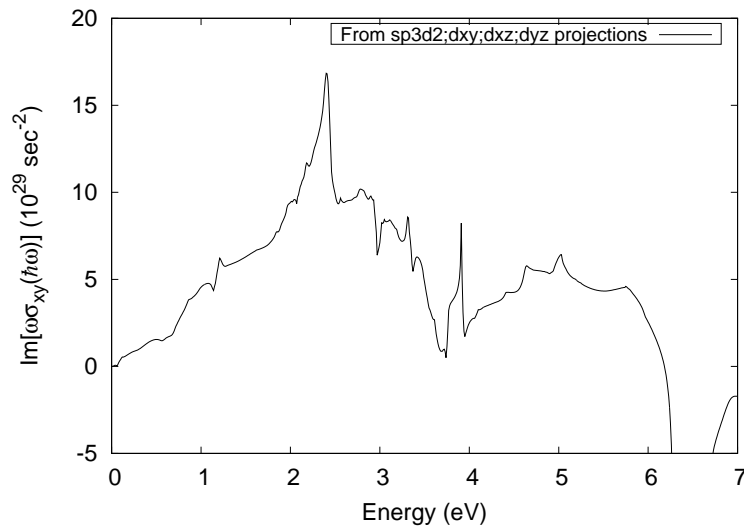


Figure 62: The magnetic circular dichroism from interpolation of the Kubo-Greenwood formula.

The result obtained by integrating the Berry curvature is $729.83 (\Omega\text{cm})^{-1}$ and the $\omega \rightarrow 0$ limit of the complex optical conductivity is $669.37 (\Omega\text{cm})^{-1}$.

Plot the MCD spectrum.

The plot of the magnetic circular dichroism is shown in Fig. 62.

Further ideas

- *Recompute the AHC and optical spectra of bcc Fe using projected s , p , and d -type Wannier functions instead of the hybridised MLWFs (see Example 8), and compare the results.*

First we have to modify the projection block in the input file `Fe.win` as did in Ex. 8

```
begin projections Fe:s;p;d end projections
```

Then we need to re-do points 3,4 and 6.

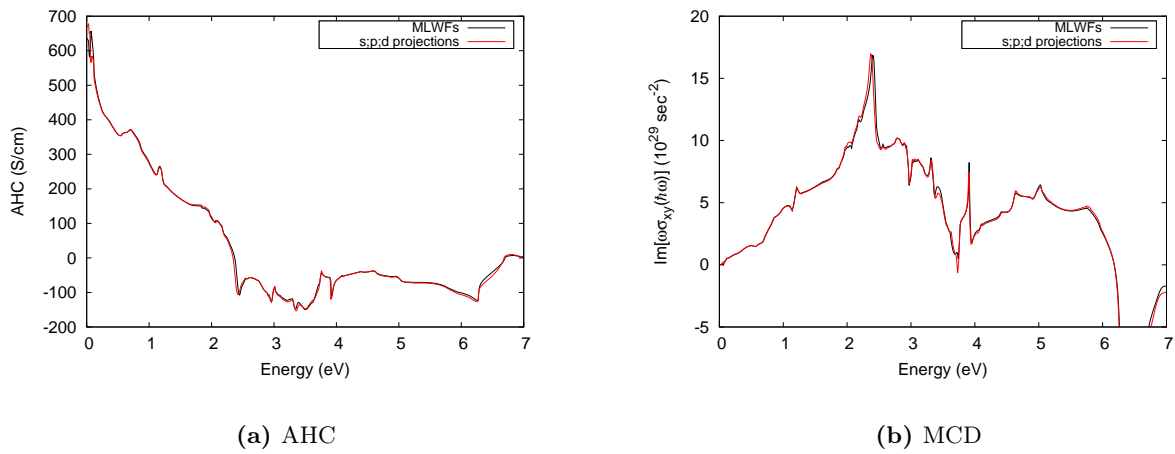
Below there is the extract from the output file `Fe.wpout`. The result obtained from s, p and d projections for the z component, i.e. σ_{xy} , of the AHC is exactly the same as the one obtained from sp_3d_2, d_{xy}, d_{xz} , and d_{yz} projections. Plot of AHC and MCD are shown in Fig. 63.

```
With adaptive refinement
Properties calculated in module b e r r y
-----
* Anomalous Hall conductivity

Regular interpolation grid: 25 25 25
Adaptive refinement grid: 5 5 5
  Refinement threshold: Berry curvature >100.00 bohr^2
Points triggering refinement: 42( 0.27%)

Fermi energy (ev): 12.6283

AHC (S/cm)      x          y          z
=====
J0 term :      0.0006    -0.0006    -2.9033
J1 term :      0.0032    -0.0032    10.0566
J2 term :      2.4564    -2.4564    567.1417
-----
Total   :      2.4602    -2.4602    574.2950
```



(a) AHC

(b) MCD

Figure 63: Left panel: Anomalous Hall conductivity. Right panel: Magnetic circular dichroism for $\hbar\omega$ up to 7 eV, starting from $s; p; d$ initial projections

19: Iron—Orbital magnetization

- Outline: Calculate the orbital magnetization of ferromagnetic bcc Fe by Wannier interpolation.

1-6 These are the same steps performed for Ex. 17 and Ex. 18. Hence, they are not repeated here.

- The orbital magnetization is computed as the BZ integral of the quantity $\mathbf{M}^{\text{orb}}(\mathbf{k})$ defined in Eq. (12.20) of the User Guide.

Below we report Eq. (11.20) from the User Guide, and the total orbital magnetization as the integral of $\mathbf{M}^{\text{orb}}(\mathbf{k})$ over the BZ

$$\mathbf{M}^{\text{orb}}(\mathbf{k}) = \sum_n \frac{1}{2} f_{n\mathbf{k}} \text{Im} \langle \nabla_{\mathbf{k}} u_{n\mathbf{k}} | \times (H_{\mathbf{k}} + \epsilon_{\mathbf{k}} - 2\epsilon_{\text{F}}) | \nabla_{\mathbf{k}} u_{n\mathbf{k}} \rangle \quad (9)$$

$$\mathbf{M}_{\text{tot}}^{\text{orb}} = V \int \frac{d\mathbf{k}}{(2\pi)^3} \mathbf{M}^{\text{orb}}(\mathbf{k}) \quad (10)$$

The two snippets below show the components of the total orbital magnetization computed according to Eq. (10), and the spin magnetisation from the DFT calculation respectively

From Fe.wpout			
Properties calculated in module b e r r y			

* Orbital magnetization			
Interpolation grid: 25 25 25			
Fermi energy (ev) = 12.628300			
M_orb (bohr magn/cell)	x	y	z
=====			
Local circulation :	0.0000	-0.0000	0.0935
Itinerant circulation:	0.0000	0.0000	-0.0180

Total :	0.0000	-0.0000	0.0755

From scf.out			
total magnetization	=	0.00 -0.00 -2.22 Bohr mag/cell	
absolute magnetization	=	2.34 Bohr mag/cell	

- Plot $\mathbf{M}^{\text{orb}}(\mathbf{k})$ along high-symmetry lines and compare the result with Fig. 2 of Ref. 5.

Before comparing the result of our calculation with the result in Fig. 2 of Ref. 5, we need to fix a unit-conversion problem in the python script `Fe-bands+morb_z.py`. In fact, the units of $\mathbf{M}^{\text{orb}}(\mathbf{k})$ are not $\text{Ry} \cdot \text{\AA}^2$ as stated in the python script but $\text{eV} \cdot \text{\AA}^2$ instead (as also stated in the User Guide). Moreover, in Ref. 5 $\mathbf{M}^{\text{orb}}(\mathbf{k})$ is given in atomic units, i.e. Hartree-bohr radii². In order to have a meaningful comparison we need to modify the python script accordingly. Open `Fe-bands+morb_z.py` and modify the following lines

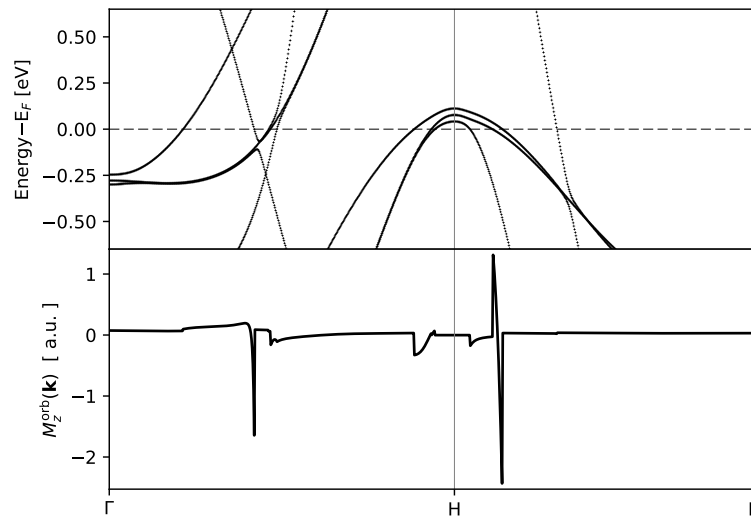


Figure 64: Plot of $M^{\text{orb}}(\mathbf{k})$ calculated by Wannier interpolation along the path Γ -H-P in the Brillouin zone.

```
data = np.loadtxt('Fe-morb.dat')
x=data[:,0]
y=data[:,3]
```

as

```
data = np.loadtxt('Fe-morb.dat')
x=data[:,0]
y=data[:,3] * 0.131234
```

where 0.131234 is the conversion factor from $\text{eV}\cdot\text{\AA}^2$ to a.u. We also need to modify the label for the y-axis from

```
pl.ylabel(r'$M^{\{\rm{orb}\}}_z(\mathbf{k})$ [ Ry$\cdot\text{\AA}^2$ ]')
```

to

```
pl.ylabel(r'$M^{\{\rm{orb}\}}_z(\mathbf{k})$ [ a.u. ]')
```

Now we can run the python script

```
$> python Fe-bands+morb_z.py
```

and look at the plot, here shown in Fig. 64. The difference between the quantities in the two plot is roughly the $-\frac{1}{2}$ factor due to the two different definitions of M^{orb} .

Plot $M^{\text{orb}}(\mathbf{k})$ together with the Fermi contours on the (010) BZ plane

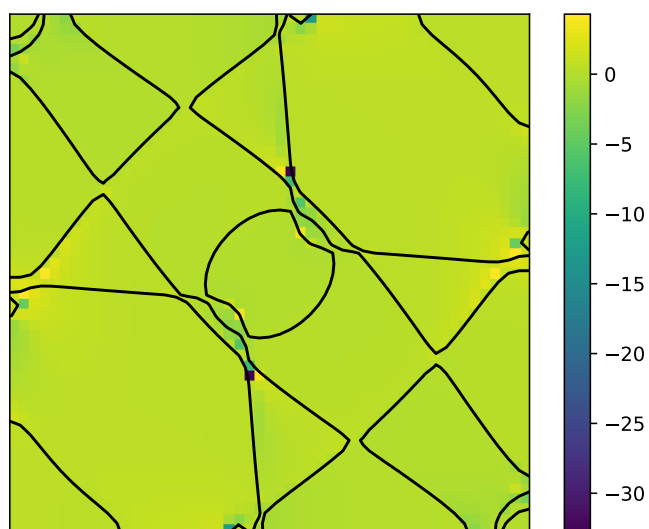


Figure 65: Plot of $\mathbf{M}^{\text{orb}}(\mathbf{k})$ together with the Fermi contours on the (010) BZ plane

20: Disentanglement restricted inside spherical regions of k -space LaVO_3 .

- Outline: *Obtain disentangled MLWFs for strained LaVO_3 .*

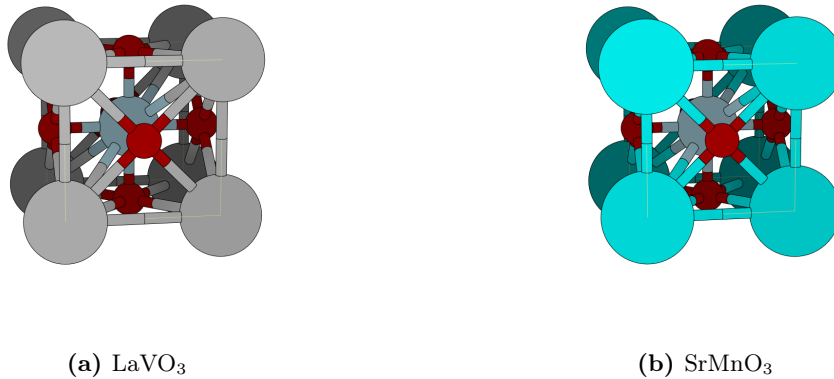


Figure 66: Left: atomic structure of epitaxially-strained (tetragonal) LaVO_3 . Right: atomic structure of epitaxially-strained (tetragonal) SrMnO_3 . Both structures have been plotted with the XCRYSDEN program.

1-5 These are the usual steps to generate MLWFs and are not reported here.

- *Inspect the output file `LaVO3.wout`. In the initial summary, you will see that the disentanglement was performed only within one sphere of radius 0.2 around the point $\mathbf{A} = (0.5, 0.5, 0.5)$ in reciprocal space:*

```

*----- DISENTANGLE -----*
| Using band disentanglement           :                               T           |
|
| ...
|
| Number of spheres in k-space           :                               1           |
| center n.  1 :   0.500  0.500  0.500,   radius = 0.200           |

```

- *Compare the band structure that WANNIER90 produced with the one obtained using Quantum ESPRESSO.*

To obtain the band structure from the Quantum ESPRESSO calculation we can use the `bands.x` program available at <http://www.tcm.phy.cam.ac.uk/~jry20/bands.html>, see mini-tutorial at the end of Ex. 6. Here, we only report the `.inp` file used to generate the k -point mesh for the non-scf calculation

```
bands.x input file LaVO3.inp
7.03 0.00 0.00
0.00 7.03 0.00
0.00 0.00 7.6627

30

G      0.00000  0.00000  0.00000  M      0.50000  0.50000  0.00000
M      0.50000  0.50000  0.00000  X      0.50000  0.00000  0.00000
X      0.50000  0.00000  0.00000  G      0.00000  0.00000  0.00000
G      0.00000  0.00000  0.00000  Z      0.00000  0.00000  0.50000
Z      0.00000  0.00000  0.50000  A      0.50000  0.50000  0.50000
A      0.50000  0.50000  0.50000  R      0.50000  0.00000  0.50000
R      0.50000  0.00000  0.50000  X      0.50000  0.00000  0.00000
```

Remember to add the following line to the `.bands` file in order to show the eigenvalues at each k-point.

```
verbosity = 'high'
```

Plot of the interpolated band structure is shown in Fig. (67). In the top panel, the full band structure is shown. In the bottom panel a magnification around the Fermi energy is shown (similar to Fig. 9 in the Tutorial).

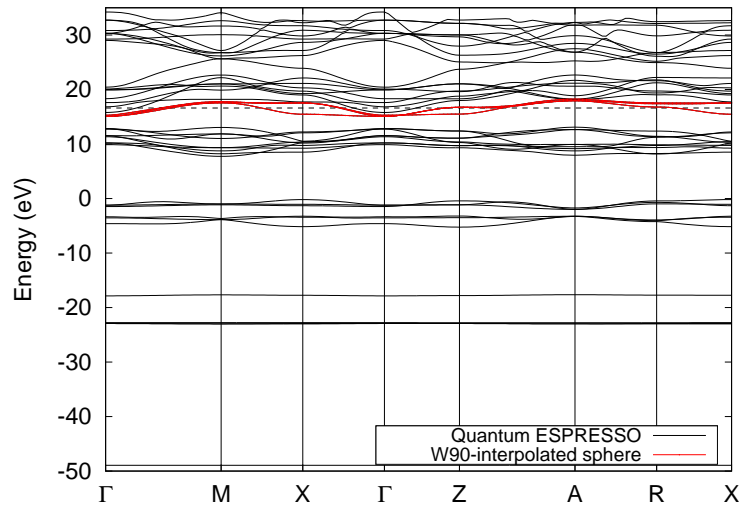
Further ideas

- *Try to obtain the Wannier functions using the standard disentanglement procedure ...*

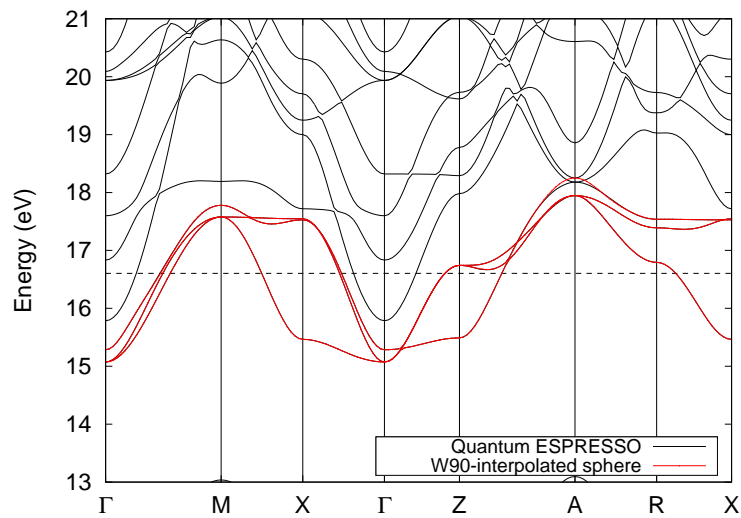
Plots of the band structure of LaVO_3 with full disentanglement and no disentanglement are shown in Fig. (68). These are plotted against the quantum ESPRESSO band structure (solid black lines) and the WANNIER90-interpolated one with disentanglement performed only within a sphere centred in A (red dots). We see that the other two methods diverge from the DFT calculation in region of k -space where the bands of interest are not entangled with other unwanted bands. For example, in the zone between Γ and M and Z and A the interpolated bands with full disentanglement and no disentanglement diverge substantially from the DFT calculation.

- *In order to illustrate all possible cases, it is instructive to apply this method to SrMnO_3 ...*

Plots of the interpolated bands for the different cases are shown in Fig. (69). In this case, the disentanglement for all the Mn-3d-derived states (empty red circles in Fig. (69)) is only necessary around the Γ point, as for all the other points and lines the bands of interest are well separated from other bands lower in energy. However, if we only consider the e_g states (solid blue circles in Fig. (69)) then the situation is different as these states are entangled with the t_{2g} states around X. Of course the t_{2g} states (solid green cones in Fig. (69)) are entangled with e_g states around X and with lower-lying states at Γ .



(a) Full BS



(b) BS around Fermi energy

Figure 67: Top panel: full band structure of epitaxially-strained (tetragonal) LaVO_3 along the Γ -M-X- Γ -Z-A-R-X from DFT calculation (solid black) and interpolation from WANNIER90 (red dots). Bottom panel: magnification around Fermi energy 16.6049 (dashed line). The disentanglement was performed only for k -points within a sphere of radius 0.2 \AA^{-1} centred in A.

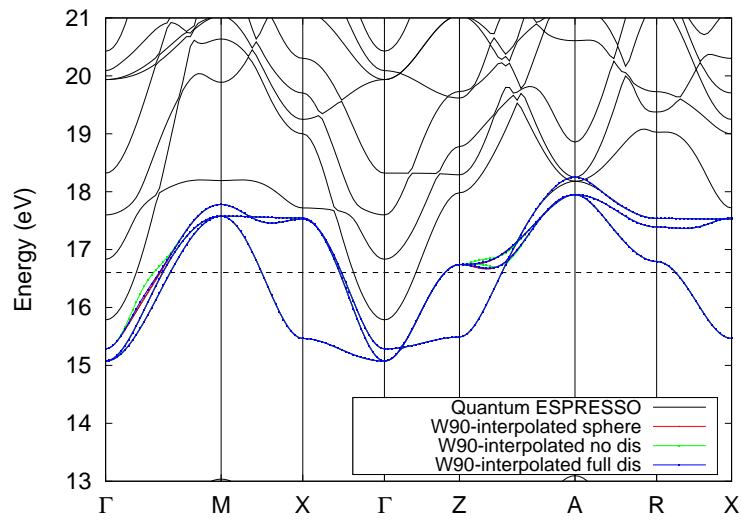


Figure 68: Comparison of interpolated band structure of epitaxially-strained (tetragonal) LaVO_3 with disentanglement on a sphere of radius 0.2 \AA^{-1} centred in A (red dots), full disentanglement (blue dots) and no disentanglement (green dots). Fermi energy is shown with a dashed line.

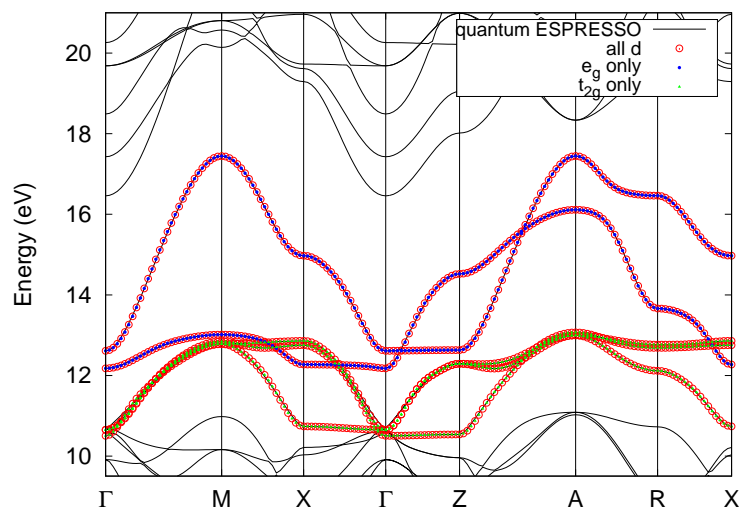


Figure 69: WANNIER90-interpolated bands of SrMnO_3 . From only t_{2g} states (solid green cones), from only e_g states (solid blue circles), or all Mn-3d-derived states ($t_{2g} + e_g$) (empty red circles).

21: Gallium Arsenide—Symmetry-adapted Wannier functions

- Outline: Obtain symmetry-adapted Wannier functions out of four valence bands of GaAs. For the theoretical background of the symmetry-adapted Wannier functions, see R. Sakuma, *Phys. Rev. B* **87**, 235109 (2013).

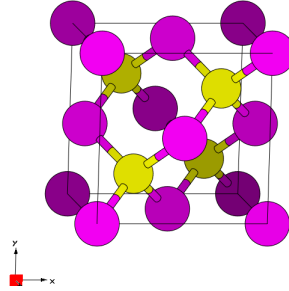


Figure 70: Unit cell of GaAs crystal plotted with the XCRYSDEN program.

1-3 These are common to all calculations, and they have already been performed in previous examples. Hence, no results are shown here.

The space group of GaAs is $F-43m$ (sequential number 276 in the International Tables for Crystallography, Vol. A). In our example the Ga atom is placed at the origin, whose Wyckoff letter is a and its multiplicity is 4. The site symmetry group of a is $-43m$, which is isomorphic to the full point group of the crystal, also known as T_d^2 . This is due to the fact that $F-43m$ is symmorphic. Hence, a contains 24 symmetry operations (see Tab. 12). The As atom is placed at $(0.25, 0.25, 0.25)$ in fractional coordinates, whose Wyckoff letter is c and its multiplicity is 4. It also contains 24 symmetry operations (see Tab. 13). The list of site-symmetry operations may be found in the `.sym` file and in the output file `pw2wan.out`. In the latter, the list is in the section relative to the computation of the D_{mn} matrix (see Ref. 7).

Table 12: 24 symmetry operations for the Wyckoff position $4a$ in $-43m$ [6].

x, y, z	$-x, -y, z$	$-x, y, -z$	$x, -y, -z$	z, x, y	$z, -x, -y$
$-z, -x, y$	$-z, x, -y$	y, z, x	$-y, z, -x$	$y, -z, -x$	$-y, -z, x$
y, x, z	$-y, -x, z$	$y, -x, -z$	$-y, x, -z$	x, z, y	$-x, z, -y$
$-x, -z, y$	$x, -z, -y$	z, y, x	$z, -y, -x$	$-z, y, -x$	$-z, -y, x$

Table 13: 24 symmetry operations for the Wyckoff position $4c$ in $-43m$ [6].

x, y, z	$-x+1/2, -y+1/2, z$	$-x+1/2, y, -z+1/2$	$x, -y+1/2, -z+1/2$
z, x, y	$z, -x+1/2, -y+1/2$	$-z+1/2, -x+1/2, y$	$-z+1/2, x, -y+1/2$
y, z, x	$-y+1/2, z, -x+1/2$	$y, -z+1/2, -x+1/2$	$-y+1/2, -z+1/2, x$
y, x, z	$-y+1/2, -x+1/2, z$	$y, -x+1/2, -z+1/2$	$-y+1/2, x, -z+1/2$
x, z, y	$-x+1/2, z, -y+1/2$	$-x+1/2, -z+1/2, y$	$x, -z+1/2, -y+1/2$
z, y, x	$z, -y+1/2, -x+1/2$	$-z+1/2, y, -x+1/2$	$-z+1/2, -y+1/2, x$

One s -like Wannier function centred at Ga

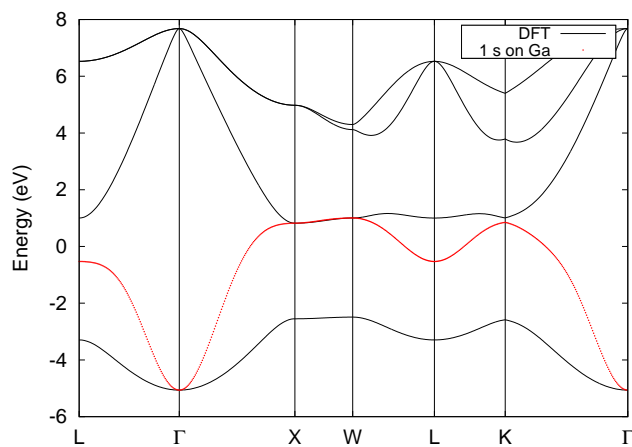
1-5 Compute the symmetry-adapted MLWF.

The $-43m$ site-symmetry group is isomorphic to T_d^2 . From the table of characters of T_d^2 we find 5 irreducible representations (*irrep*). The irrep with character A_1 is a one-dimensional representation, whose eigenfunction is spherically symmetric. Hence, a single s -like orbital in $(0,0,0)$ may be used. However, this is not enough as the choice of the initial guess must also be compatible with the symmetry of the bands. In fact, if we tried to wannierise only the lowest band, excluding all the other bands (this can be done by changing the input file as `num_wann = 1`, `num_bands = 1` and `exclude_bands = 1-5, 7-19`), the resulting $1 \times 1 U(\mathbf{k})$ could not fulfill Eq. 19 in Ref. 7. Similarly, if we tried to wannierise only the three top bands.

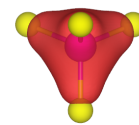
```
begin projections
f= 0.0, 0.0, 0.0 : s
end projections
```

```
-----
*** Compute DMN
-----
```

```
Number of symmetry operators = 24
```



(a) Wannier-interpolated band



(b) Sym.Ad. MLWF

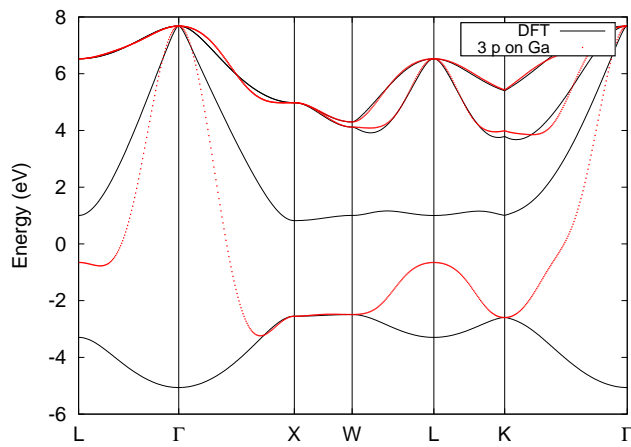
Figure 71: One s -like symmetry-adapted Wannier function centred on the Gallium atom in GaAs.

Three p -like Wannier functions centred at Ga

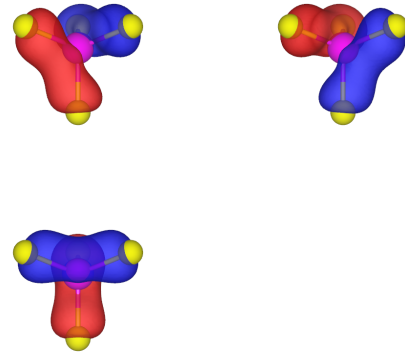
1-5 Compute the symmetry-adapted MLWFs.

Another representation of $-43m$, namely T_2 , has dimension 3. Its eigenfunctions are linear functions proportional to x, y, z . Hence, we can use three p -like orbitals (p_x, p_y, p_z) centred at $(0,0,0)$.

```
begin projections
f= 0.0, 0.0, 0.0 : p
end projections
```



(a) Wannier-interpolated band



(b) Sym.Ad. MLWFs

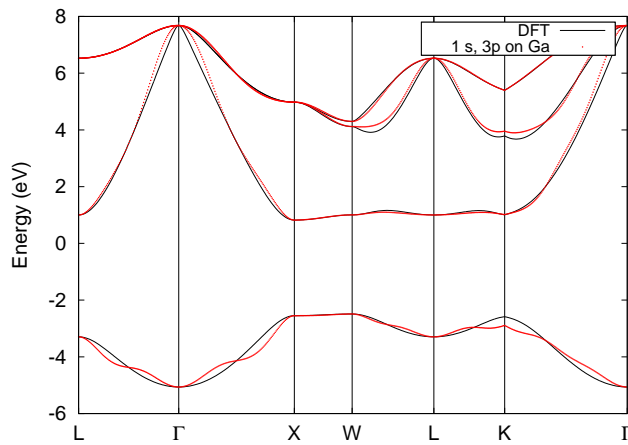
Figure 72: Three p -like symmetry-adapted Wannier functions centred on the Gallium atom in GaAs.

One s -like and three p -like Wannier functions centred at Ga

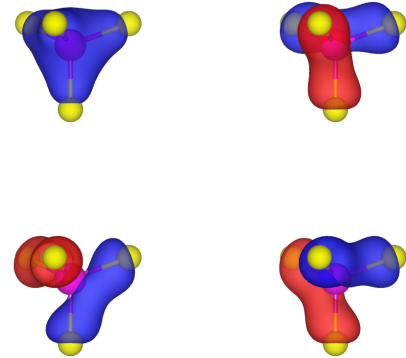
1-5 Compute the symmetry-adapted MLWFs.

We can also construct a representation of dimension $4 = 3 + 1$ for the 4 valence bands by specifying 1 s -like orbital and 3 p -like orbitals on Ga, which corresponds to the irreducible representations A_1 and T_2 respectively. However, it would not be possible to

```
begin projections
f= 0.0, 0.0, 0.0 : s
f= 0.0, 0.0, 0.0 : p
end projections
```



(a) Wannier-interpolated band



(b) Sym.Ad. MLWFs

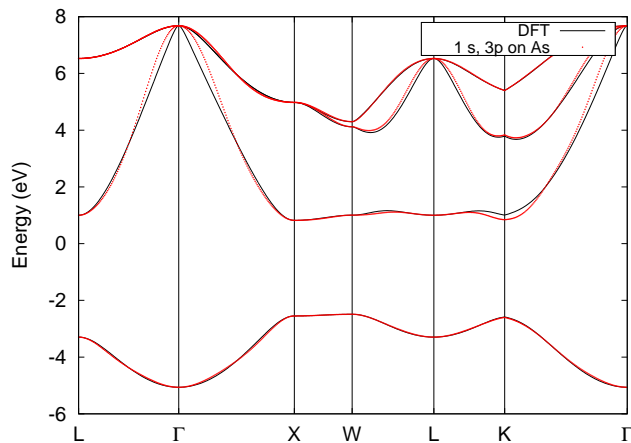
Figure 73: One s -like and three p -like Wannier functions centred on the Gallium atom in GaAs.

One s -like and three p -like Wannier functions centred at As

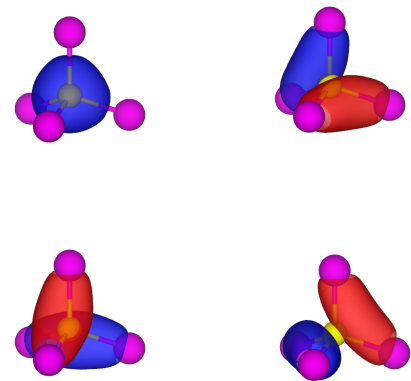
The site-symmetry group for the As anion centred at $(0.25, 0.25, 0.25)$ is $-43m$ as well and we can perform the same analysis done for the Ga cation. Contrary to the Ga case, for the As anion it is possible to wannierise the bottom band from one s -like orbital centred at $(0.25, 0.25, 0.25)$ and the top three bands from three p -like orbitals centred at $(0.25, 0.25, 0.25)$ (see Fig. 75).

1-5 Compute the symmetry-adapted MLWFs.

```
begin projections
f=0.25,0.25,0.25 : s
f=0.25,0.25,0.25 : p
end projections
```



(a) Wannier-interpolated band



(b) Sym.Ad. MLWFs

Figure 74: One s -like and three p -like Wannier functions centred on the Arsenic atom in GaAs.

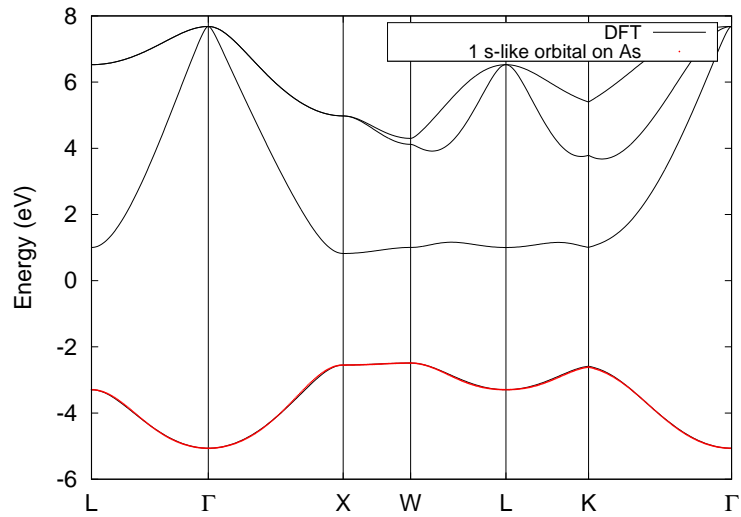
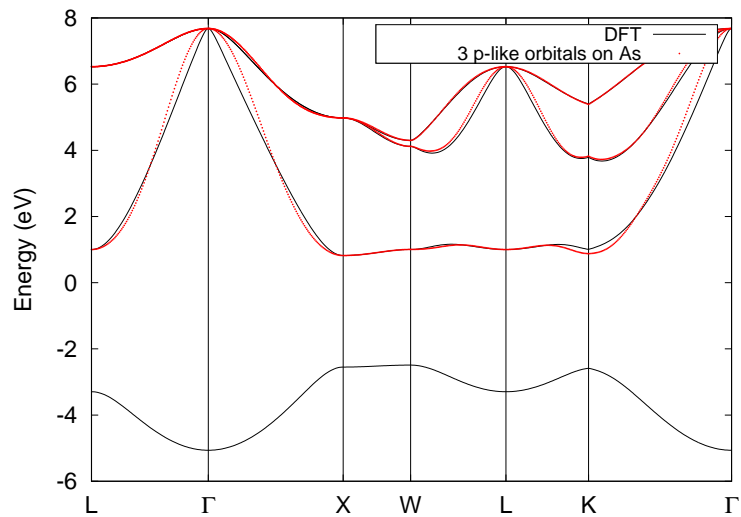
(a) *s*-like orbital on As(b) 3 *p*-like orbitals on As

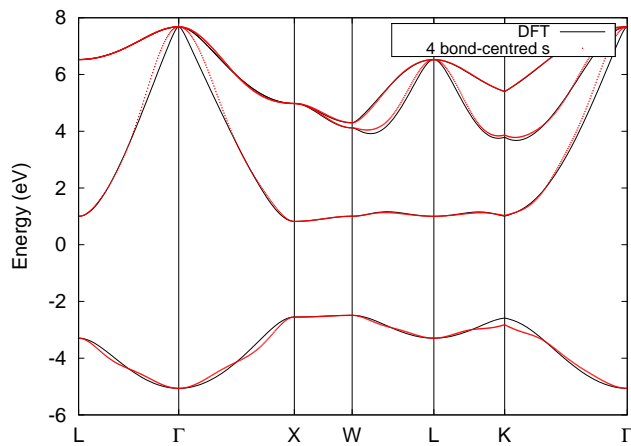
Figure 75: Interpolated WANNIER90 bands of GaAs starting from a) 1 *s*-like centred on the Arsenic anion and b) three *p*-like orbitals centred on the Arsenic anion, respectively.

Four s -like Wannier functions centred on the four Ga-As bonds

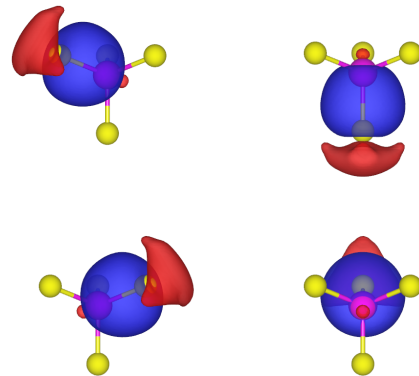
From a group-theoretical point of view, the case of four s -like functions centred on four covalent bonds, correspond to the *irrep* A_{1g} of the site-symmetry group $.3m$ of the Wyckoff position e . There are 6 symmetry operations for each equivalent position $(0.125, 0.125, 0.125)$, $(0.125, 0.125, -.375)$, $(-.375, 0.125, 0.125)$ and $(0.125, -.375, 0.125)$. The combined 24 symmetry operations turn out to be exactly that of the full $-43m$ group.

1-5 Compute the symmetry-adapted MLWFs.

```
begin projections
f= 0.125, 0.125, 0.125: s
f= 0.125, 0.125, -.375: s
f= -.375, 0.125, 0.125: s
f= 0.125, -.375, 0.125: s
end projections
```



(a) Wannier-interpolated band



(b) s, p_x, p_y, p_z

Figure 76: Four sp_3 -like symmetry-adapted Wannier functions centred on the Ga-As bonds in GaAs.

22: Copper—Symmetry-adapted Wannier functions

- Outline: Obtain symmetry-adapted Wannier functions for Cu. By symmetry-adapted mode, for example, we can make atomic centered s-like Wannier function, which is not possible in the usual procedure to create maximally localized Wannier functions. For the theoretical background of the symmetry-adapted Wannier functions, see R. Sakuma, *Phys. Rev. B* 87, 235109 (2013).

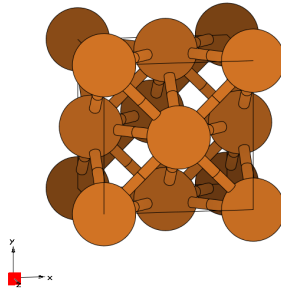


Figure 77: Unit cell of Copper crystal.

Each directory creates s-like symmetry-adapted Wannier function centered at different position on top of atomic centered d-like Wannier functions.

Below it is reported the README file from the example directory

```
# Symmetry-adapted mode

Additional input in Cu.win file
site_symmetry = .true.   (default value is .false.)
symmetrize_eps = 1d-9   (default value is 1d-3 )

Additional input in Cu.pw2wan file
write_dmn = .true.

Working directories
s_at_0.00 : s-like Wannier function centered at (0,0,0)      + atomic-centered d-like WFs
s_at_0.25 : s-like Wannier function centered at (1/4,1/4,1/4) + atomic-centered d-like WFs
s_at_0.50 : s-like Wannier function centered at (1/2,1/2,1/2) + atomic-centered d-like WFs

In s_at_0.25, we use an additional flag "read_sym = .true." to customize the symmetry operations
to be used.
We exclude the inversion symmetry to create s-like Wannier function centered at (1/4,1/4,1/4).
Information on symmetry operations without inversion symmetry is taken from GaAs calculation.
See more detailed discussion in R. Sakuma, Phys. Rev. B 87, 235109 (2013).
```

The space group of Cu is $Fm\bar{3}m$ (sequential number 225 in the International Tables for Crystallography, Vol. A).

s -like Wannier function centred at the origin

1-5 Compute the symmetry-adapted MLWFs.

In this example both the s -orbital and d -orbitals is placed at the origin, whose Wyckoff letter is a and its multiplicity is 4. The site symmetry group of a is $m\bar{3}m$, which is isomorphous to the full point group of the crystal, known as O_h and it contains 48 symmetry operations. The six MLWFs obtained by placing both the initial s -orbital and the d -orbitals on the Cu atom are shown in Fig. 78.

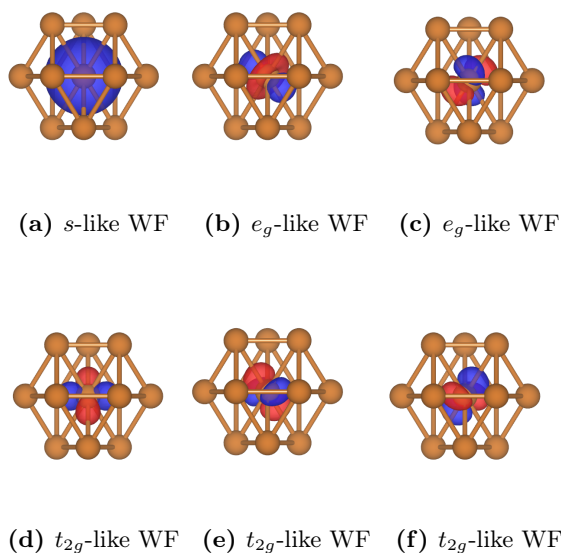


Figure 78: Six symmetry-adapted MLWFs in Cu. The initial s -orbital is placed at the origin.

***s*-like Wannier function centred at (0.25,0.25,0.25)**

1-5 *Compute the symmetry-adapted MLWFs.* In this example the *s*-orbital is placed at (0.25,0.25,0.25), whose Wyckoff letter is *c* and its multiplicity is 8. The site symmetry group of *c* is $-43m$, which is not isomorphous to the full point group of the crystal (O_h). This site symmetry group contains only 24 symmetry operations, i.e. it comes from O_h when inversion is removed. This is the reason why the flag `read_sym = .true.` in the `.pw2wan` file and an additional input is required, namely `Cu.sym`. In fact, this file is not automatically generated by `pw2wannier90.x` but is given as input to be read. The six MLWFs obtained by placing the initial *s*-orbital at (0.25,0.25,0.25) and the *d*-orbitals on the Cu atom are shown in Fig. 79.

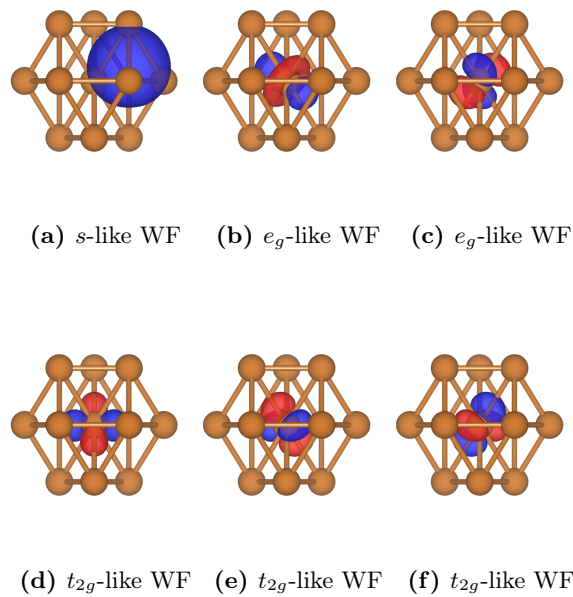


Figure 79: Six symmetry-adapted MLWFs in Cu. The initial *s*-orbital is placed at (0.25,0.25,0/25).

s -like Wannier function centred at $(0.5,0.5,0.5)$

1-5 *Compute the symmetry-adapted MLWFs.* In this example the s orbital is placed at $(0.5,0.5,0.5)$, whose Wyckoff letter is b and its multiplicity is 4. The site symmetry group of c is $m-3m$, which is isomorphous to the full point group of the crystal (O_h). Hence, no additional input file is needed in this case. The six MLWFs obtained by placing the initial s -orbital at $(0.5,0.5,0.5)$ and the d -orbitals on the Cu atom are shown in Fig. 80.

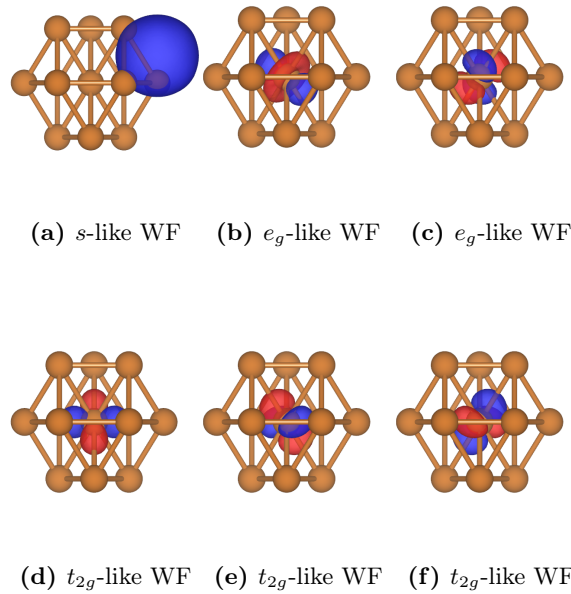


Figure 80: Six symmetry-adapted MLWFs in Cu. The initial s -orbital is placed at $(0.5,0.5,0.5)$.

23: Platinum—Spin Hall conductivity

- Outline: Calculate spin Hall conductivity (SHC) and plot Berry curvature-like term of fcc Pt considering spin-orbit coupling. To gain a better understanding of this example, it is suggested to read Ref. 8 for a detailed description of the theory and Ch. 12.5 of the User Guide.

1-6 Compute the MLWFs, spin Hall conductivity and `kpath`, `kslice` plots.

Spin Hall conductivity

- SHC converges rather slowly with k -point sampling, and a $25 \times 25 \times 25$ `kmesh` does not yield a well-converged value. To get a converged SHC value, increase the density of `kmesh` and then compare the converged result with those obtained in Refs. 8 and 9.

The file `Pt-shc-fermiscan.dat` contains the calculated SHC. The SHC for a $25 \times 25 \times 25$ `kmesh` are shown in the snippet below.

25 × 25 × 25 kmesh		
#No.	Fermi energy(eV)	SHC((hbar/e)*S/cm)
1	6.000000	0.00000000E+00
...		
120	17.900000	0.17230482E+04
121	18.000000	0.17054542E+04
...		
201	26.000000	0.22665760E+03

The calculated Fermi energy obtained from Quantum ESPRESSO is 17.9919 eV. It may vary among different calculations due to the differences between versions of Quantum ESPRESSO or compilers, and these may lead to deviations from the following results. However, the difference should be acceptable and the calculated SHC should be essentially the same.

The SHC at the Fermi energy is 1705 (\hbar/e)S/cm. The converged results reported in Refs. 8 and 9 are around 2200 (\hbar/e)S/cm. Hence, a $25 \times 25 \times 25$ `kmesh` clearly gives an inaccurate value ($\sim 22.5\%$ error).

Since these are quite demanding calculations, we only report the value of the SHC for a $100 \times 100 \times 100$ `kmesh` (see snippet below). The value for the SHC at Fermi energy is 2207 (\hbar/e)S/cm, which is in much closer agreement with the converged result from Refs. 8 and 9.

100 × 100 × 100 kmesh		
#No.	Fermi energy(eV)	SHC((hbar/e)*S/cm)
1	6.000000	0.00000000E+00
...		
120	17.900000	0.21899191E+04
121	18.000000	0.22066678E+04
...		
201	26.000000	0.24919920E+03

- To complete the previous discussions, we also compare the Fermi energy scan plots of the two calculations as shown in the Fig. 81.
- The `seedname.wput` will print the percentage of k -points which have been calculated at the moment, as well as the corresponding calculation time, as shown in the following snippet.

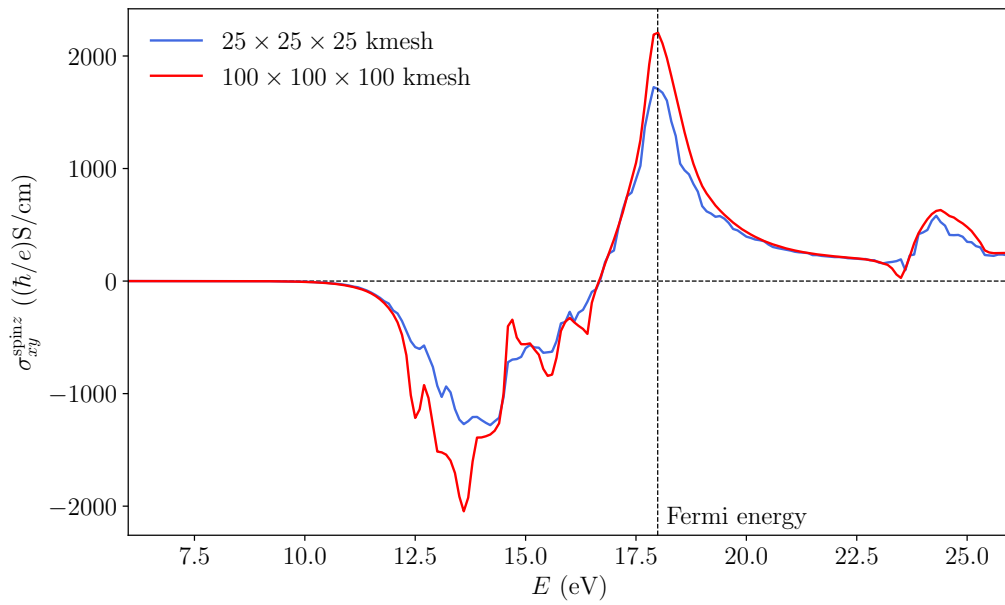


Figure 81: Fermi energy scan plots for calculations with $25 \times 25 \times 25$ kmesh and $100 \times 100 \times 100$ kmesh.

```

Pt.wpout
Properties calculated in module b e r r y
-----

* Spin Hall Conductivity

Fermi energy scan

Calculation started
-----
k-points      wall      diff
calculated    time      time
-----
0%            0.0       0.0
10%           22.7      22.7
20%           36.5      13.8
30%           50.4      14.0
40%           64.4      14.0
50%           78.4      14.0
60%           92.5      14.1
70%          106.5     14.0
80%          120.4     13.9
90%          134.2     13.8
100%         147.9     13.7

Interpolation grid: 25 25 25

Using adaptive smearing
  adaptive smearing prefactor    1.414
  adaptive smearing max width    1.000 eV

```

This might be helpful as you can roughly estimate the total computational time of your calculation, or it might give credence to the code that it is actually functioning :). Note this report is merely based on the “root” computation node. It is accurate if the `postw90` is run in serial, or the load on each node is balanced if running in parallel. However, the estimation is rough if loads are not balanced among nodes. This may happen if the performance of nodes in your cluster are not identical, or adaptive kmesh refinements are triggered so some nodes may compute much more k -points than others. Besides, if you are careful enough, you may find the diff time of 10% is much larger than later ones. This is caused by some done-once-and-for-all computations carried out at the beginning, thus later computations are much faster.

Berry curvature-like term plots

- The band-projected Berry curvature-like term $\Omega_{n,\alpha\beta}^{\text{spin}\gamma}(\mathbf{k})$ is defined as Eq. (12.22) in the User Guide. Plot the band structure of Pt and color it by the magnitude of its band-projected Berry curvature-like term $\Omega_{n,xy}^{\text{spin}z}(\mathbf{k})$, and plot the k -resolved Berry curvature-like term $\Omega_{xy}^{\text{spin}z}(\mathbf{k})$ along the same path in the BZ.

With Fermi energy set as 17.9919 eV we obtain the energy bands colored by the $\Omega_{n,\alpha\beta}^{\text{spin}\gamma}(\mathbf{k})$ and the k -resolved Berry curvature-like term $\Omega_{xy}^{\text{spin}z}(\mathbf{k})$ along high-symmetry lines as shown in Fig. 82, which contains two plots calculated with different fixed smearing width.

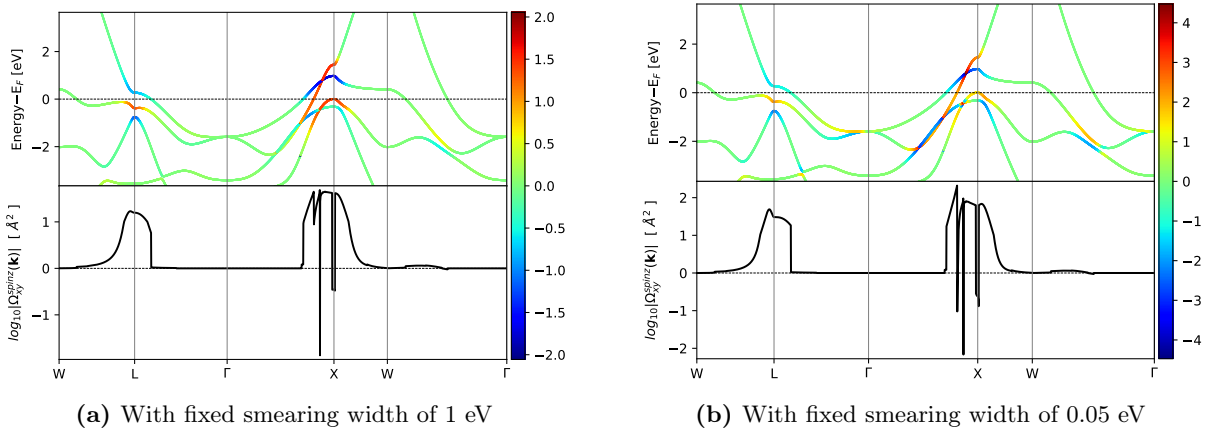


Figure 82: Top panels: Band structure of Pt along symmetry lines W-L- Γ -X-W- Γ , colored by the $\Omega_{n,xy}^{\text{spin}z}(\mathbf{k})$. Bottom panels: k -resolved Berry curvature-like term $\Omega_{xy}^{\text{spin}z}(\mathbf{k})$ along the symmetry lines.

- Combine the plot of the Fermi lines on the (k_x, k_y) plane with a heatmap plot of the Berry curvature-like term of spin Hall conductivity.

The plots of the Fermi lines with a heatmap of $\Omega_{xy}^{\text{spin}z}(k_x, k_y, 0)$ are shown in Fig. 83.

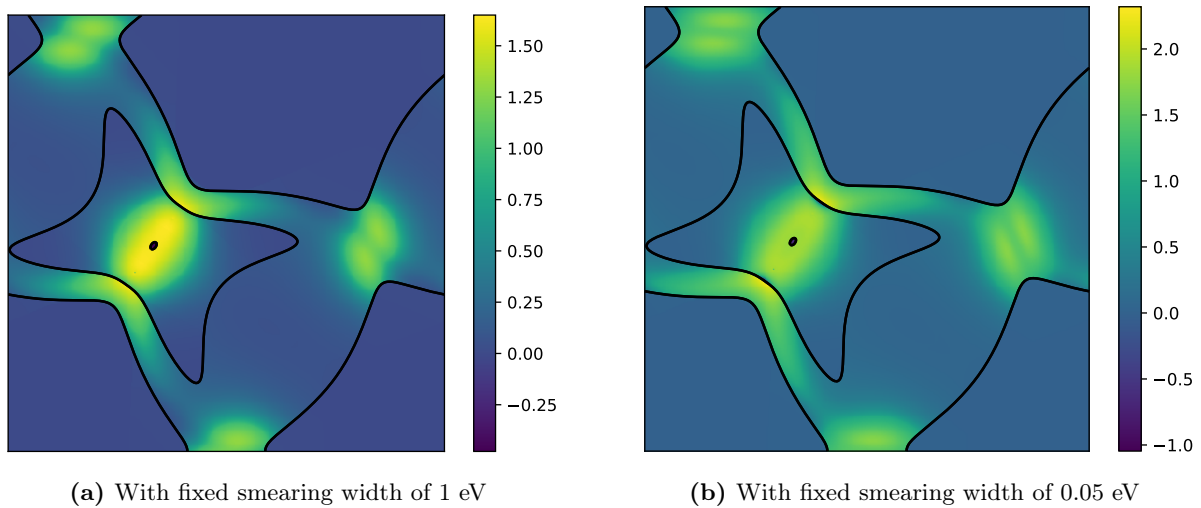


Figure 83: Calculated k -resolved Berry curvature-like term $\Omega_{xy}^{\text{spin}_z}(\mathbf{k})$ in the plane $k_z = 0$ (note the magnitude of $\Omega_{xy}^{\text{spin}_z}(\mathbf{k})$ is in log scale). Intersections of the Fermi surface with this plane are shown as black lines.

24: Gallium Arsenide—Frequency-dependent spin Hall conductivity

- Outline: Calculate the alternating current (ac) spin Hall conductivity of gallium arsenide considering spin-orbit coupling. To gain a better understanding of this example, it is suggested to read Ref. 8 for a detailed description of the theory and Ch. 12.5 of the User Guide.

1-6 Compute the MLWFs and compute the ac spin Hall conductivity.

ac spin Hall conductivity

- The ac SHC of GaAs converges rather slowly with k -point sampling, and a $100 \times 100 \times 100$ k mesh does not yield a well-converged value. To get a converged SHC value, increase the density of k mesh and then compare the converged result with those obtained in Refs. 8.

The file `GaAs-shc-freqscan.dat` contains the calculated ac SHC. The snippet below shows a calculated result with $100 \times 100 \times 100$ k mesh, a fixed smearing width of 0.05 eV and no scissors shift applied.

100 × 100 × 100 kmesh			
#No.	Frequency(eV)	Re(sigma)((hbar/e)*S/cm)	Im(sigma)((hbar/e)*S/cm)
1	0.000000	-0.68114601E+00	0.00000000E+00
...			
801	8.000000	-0.39471936E+01	-0.29928198E+02

The ac SHC is plotted as Fig. 84.

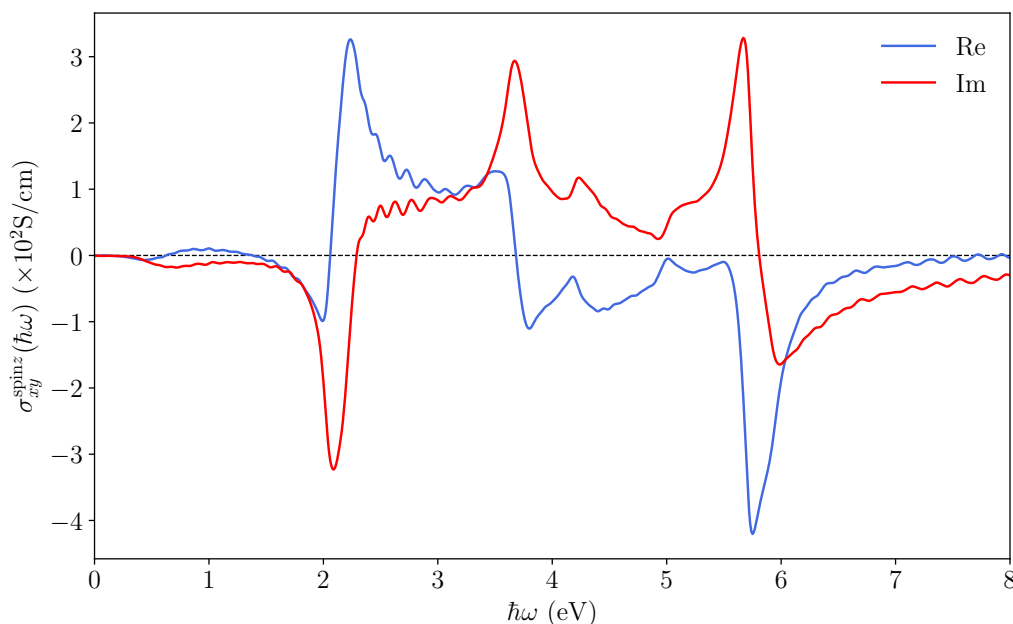


Figure 84: Frequency scan plot for GaAs ac SHC, using a low k mesh of $100 \times 100 \times 100$.

- If further increasing the density of k mesh to $250 \times 250 \times 250$, and using the adaptive smearing, a nice converged plot could be produced as Fig. 85. Note that by using keywords

```

shc_bandshift = true
shc_bandshift_firstband = 9
shc_bandshift_energyshift = 1.117

```

a scissors shift of 1.117 eV is applied. Fig. 85 can be viewed as Fig. 84 translated by ~ 1 eV along the horizontal axis.

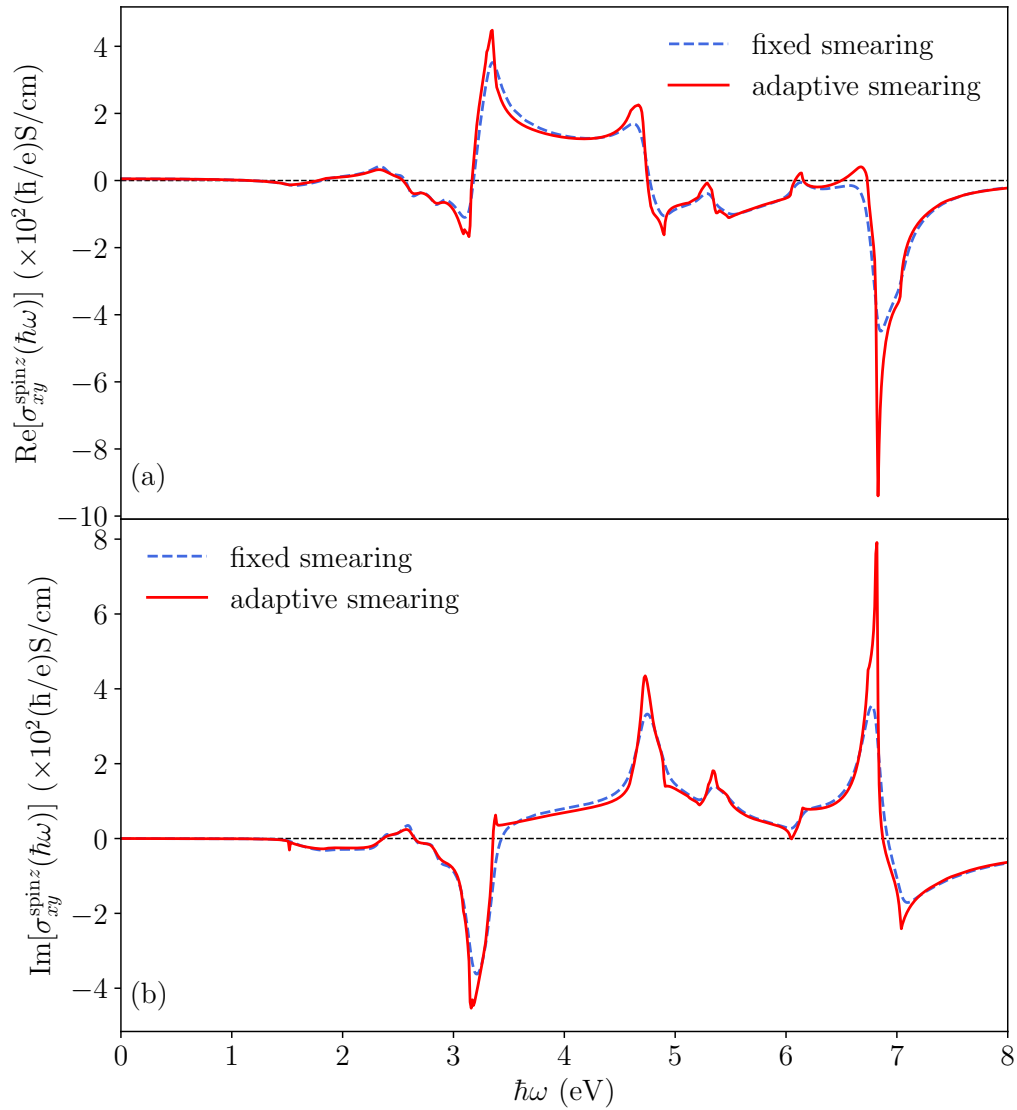


Figure 85: Frequency scan plots for GaAs at SHC, using a dense kmesh of $250 \times 250 \times 250$. Two kinds of smearing are compared.

References

- [1] J. Appl. Crystallogr **44**, 1272 (2011).
- [2] N. Marzari and D. Vanderbilt, Phys. Rev. B **56**, 12847 (1997).
- [3] Y. Yao, L. Kleinman, A. H. MacDonald, J. Sinova, T. Jungwirth, D.-s. Wang, E. Wang, and Q. Niu, Phys. Rev. Lett. **92**, 037204 (2004).
- [4] X. Wang, J. R. Yates, I. Souza, and D. Vanderbilt, Phys. Rev. B **74**, 195118 (2006).
- [5] M. G. Lopez, D. Vanderbilt, T. Thonhauser, and I. Souza, Phys. Rev. B **85**, 014435 (2012).
- [6] M. I. Aroyo, A. Kirov, C. Capillas, J. M. Perez-Mato, and H. Wondratschek, Acta Crystallographica Section A **62**, 115 (2006).
- [7] R. Sakuma, Phys. Rev. B **87**, 235109 (2013).
- [8] J. Qiao, J. Zhou, Z. Yuan, and W. Zhao, Phys. Rev. B **98**, 214402 (2018).
- [9] G. Y. Guo, S. Murakami, T.-W. Chen, and N. Nagaosa, Phys. Rev. Lett. **100**, 096401 (2008).